6-1-2019

Design and Development of Biodegradable Microporous Polymeric Systems with enhanced Characteristics for Food Packaging Applications

Mona Mohamed

THE AMERICAN UNVIVERSITY IN CAIRO

SCHOOL OF SCIENCES AND ENGINEERING

Design and Development of Biodegradable Microporous Polymeric Systems with enhanced Characteristics for Food Packaging Applications

The Thesis Submitted to

The Food Chemistry Master's Program

In partial fulfilment of the requirements for

The degree of Master of Science

By:

Mona Magdi Abd Al-Ghani Mohamed

Under the supervision of

Prof. Tarek Madkour

Spring 2019

Acknowledgment

I would first like to express my special thank of gratitude and my sincere appreciation to my supervisor **Dr. Tarek Madkour** for his support, effort, remarks, guidance and encouragement. This work would not have been achieved without his constrictive recommendations. It has been an honor and pleasure working under his supervision.

I would like also to thank **Dr. Rasha Azzam** for her cooperation, support and advices.

I would like to thank The American University in Cairo for the financial support through the graduate student research grant and the fellowship. I would like also to thank my collogues and friends in the Chemistry Department for their caring, encouragement, love and the friendly working environment.

I would like to express my thanks and appreciation to my mother, sisters, brother and my son for their love and emotional support. I would like to thank them for inspiring and motivating me to continue the long journey. A special thank to my husband for unconditional support and encouragement.

Last but not the least, great appreciation for my late father for making me what I am and believing on my success.

Abstract

The principle of breathable food packaging is providing the optimum number of holes to transfer sufficient amount of oxygen into the packaging headspace. In fact, most of the commercial breathable food packaging are made from non-biodegradable plastic materials. However, these polymers are well known by their negative environmental consequences. Therefore, in this research, polylactic acid (PLA) and polycaprolactone (PCL) were chosen as biodegradable polymers to design permeable food packaging. These bio-renewable polymers were utilized in many biomedical and food packaging applications because of their contribution to the environmental sustainability. In addition, sodium chloride (NaCl) and polyethylene oxide (PEO) were used to develop microporous films by solvent casting/leaching out technique. Thus, it was found through the experimental results that sodium chloride with composition of 50% and PEO with composition of 10% achieved the highest air permeability and oxygen transmission rate (O_2TR) with PLA. Nevertheless, increasing in NaCl percentage showed lower air permeability compared with 50% because of the NaCl agglomeration and formation of larger pores. Indeed, this finding was proved by increasing is PLA crystallinity, which was associated with increasing in NaCl percentage. In addition, the same result was also demonstrated by increasing in the Brunauer-Emmett-Teller (BET) surface area and pores volume that were observed with increasing in NaCl composition. Moreover, incomplete extraction of agglomerated NaCl was another reason in the permeability reduction. Furthermore, the concentration of PEO was increased in order to improve the interconnectivity of the pores within PLA matrices. However, it was found that increasing in PEO percentage above 10% did not improve air permeability because it led to increase pore size polydisparity and it led to increase the tortuosity of the diffusion path within the polymeric matrices. However, increasing in the BET surface area of the porous PLA film was observed at 20 % PEO. According to these results, 50% NaCl and 10% PEO were chosen as optimum concentrations to further development in the properties of the porous films.

Polylactic acid is characterized by stiffness and low elongation at break percentage. Therefore, PCL was added to PLA in order to improve its mechanical properties as a food packaging material. Hence, PLA was blended with different concentrations form PCL. In order to choose the optimum concentration of PCL, the mechanical properties for each blend was investigated.

The result showed that the blend of 80% PCL and 20% PLA was characterized with the best mechanical properties in terms of elongation percentage at break and the maximum energy needed to break. Accordingly, the blend of 80% PCL and 20% PLA was chosen to study the effect of NaCl composition on the developed microporosity in the presence of PCL.

In contrast to porous PLA films, the blend showed increasing in air permeability and O_2TR when NaCl percentage increased. In fact, the highest air permeability and O_2TR showed at 100 % NaCl. Thus, this result indicated high dispersion of NaCl particles within the polymeric matrices. Consequentiality, high composition of NaCl formed large number of small pores due to the lack of agglomerated particles. Moreover, complete leaching out of NaCl due to the hydrophobicity of PCL was another reason in improving high porosity with high NaCl composition. The same result was proved through the observed proportional relationship between NaCl percentage and BET surface area. Nevertheless, low number of small pores was observed in porous PCL-PLA films compared with porous PLA films. This observation was resulted from incomplete extraction of PEO from the blend during leaching out step due high affinity between the two polymers. This result was proved by several characterization methods such as FTIR and TGA analysis.

Porous films were coated by cinnamaldehyde, as a natural antimicrobial ingredient, to eliminate passing of pathogens through the porous food packaging material. Hence, the result showed that cinnamaldehyde concentration, porosity and nature of polymer affected antimicrobial properties. With regard to the porosity, it showed enhancing effect on the antibacterial properties through increasing loading capacity of cinnamladehyade in the films. In addition, the result showed that PCL was more interactive with cinnamaldehyade than PLA because of PCL is more hydrophobic than PLA. Therefore, porous PCL-PLA films showed antibacterial effect at lower concentration of cinnamaldhyade than porous PLA films.

Table of Contents

List of tables

List of Figures

List of abbreviations

MAP	**Modified Atmospheric Food Packaging**
O_2	**Oxygen**
CO_2	**Carbon dioxide**
GTRs	**Gas transmission rates**
O_2TR	**Oxygen transmission rates**
PLA	**Ploylactic acid**
LDPE	**Low density polyethylene**
PP	**Polypropylene**
PVC	**Polyvinyl chloride**
Nacl	**Sodium chloride**
WVTR	**Water vapor transmission rate**
PCL	**Polycaprolactone**
PEO	**Polyethylene oxide**
EO	**Ethylene oxide**
AM	**Antimicrobial**
GRAS	**Generally Recognized As Safe**
Eos	**Essential oils**
CA-MAP	**Controlled modified atmosphere food packaging**
IMAP	**Intelligent modified atmospheric food**
HDPE	**High density polyethylene**
Nd:YAG	**Neodymium-doped yttrium aluminum garnet**

EMAP **Equilibrium modified atmospheric food packaging**

FDA **Food and Drug Administration**

DSC **Differential Scanning Calorimetry**

TGA **Thermogravimetric Analysis**

$CaCl_2$ **Calcium chloride**

BET **Brunauer-Emmett-Teller**

FTIR **Fourier-Transform Infrared Spectroscopy**

SEM **Scanning electron microscope**

α_m **Maximum elongation at break**

f^*_m **Maximum nominal force**

E_m **Maximum energy needed to reach the maximum nominal force**

T_g **Glass transition temperature**

T_{cc} **Crystallinity temperature**

T_m **Melting temperature**

ΔH_{cc} **Enthalpy of crystallinity**

ΔH_m **Enthalpy of melting**

X_c % **Crystallinity degree**

DTG **Derivative thermogravimetric**

T_{onset} **Initial temperature of degradation**

T_{max} **Temperature of the maximum degradation at 50% weight loss**

T_f **Temperature of final degradation**

Staph **Staphylococcus aureus**

E.coli **Escherichia coli**

1. Introduction

1.1. Respiration and transpiration processes in fruits and vegetables

Respiration and transpiration are the most important biochemical processes for the fresh fruits and vegetables. Indeed, horticultural crops keep their metabolic activities after harvest through the respiration and transportation reactions. Therefore, self-life of fresh food is strongly affected by respiration and transpiration reactions rates. With regard to transpiration, it is a transferring of the crop moisture to the surrounded atmosphere through its skin, which leads to crop deterioration. On the other hand, respiration is a reaction between sugar and oxygen and it produces carbon dioxide and water vapor. Although respiration reaction is obtained by the crop after harvesting, it is an essential process because it produces the energy required for crops metabolic activities. Many parameters affect the respiration and transpiration rates such as temperature, the growth conditions and intactness of the crop. For example, high temperature accelerates the respiration and transpiration rates, which leads to reduction in the crops shelf life. Therefore, fresh crops should be stored under low temperature after harvest in order to delay the respiration rate and moisture loss is resulted from transpiration [1].

1.2. Functions of atmospheric gases in food preservation

Atmospheric gases compositions whiten the packaging headspace play a significant role in fresh food preservation. As for carbon dioxide (CO_2), it is characteristic by its bacteriostatic property. Therefore, existence of CO_2 in the headspace of food packaging has a beneficial effect in food preservation because its ability to inhabit the growth of some microorganisms such as aerobic and gram negative bacteria. However, the effect of CO_2 on bacterial growth inhibition is restricted by many factors. For instance, although CO_2 has a high solubility in water (1.57 g/kg at 20 °C) and in lipids, the solubility of carbon dioxide in water increases when temperature decreases [2]. Therefore, the effect of carbon dioxide as a microbial inhibitory reinforces only at low temperature. Additionally, CO_2 solubility is strongly dependent on the moisture and lipid contents in the packed product. On other words, if the product contains low amount of water and fat, its absorption to carbon dioxide decreases. Consequently, inhabitation effect of CO_2 decreases when the product contains low amount of both moisture and fat. Another limitation of using CO_2 in food preservation

is that its ability to inhibit the bacterial growth is restricted only to the lag phase of growth. Indeed, when the bacterial growth transfers to the logarithmic growth, CO_2 functionality as a bacterial inhibiter decreases. Moreover, presence of CO_2 in packaging headspace for the food products that expose to yeast is not recommended. This is due to yeast growth being encouraged by the high CO_2 concentration. Additionally, the growth of some kinds of pathogens such as *clostridium perfrigens* and *clostridium botulinum* is not affected by CO_2 [1, 3].

Moreover, oxygen (O_2) is an essential gas for metabolism of the plant tissues. In spite of the fact that O_2 plays a significant role in the crops enzymatic reactions, high amount of O_2 leads to aerobic spoilage. This is due to the fact that it encourages the micro-organisms metabolic activity [3]. Therefore, oxygen transmission rate for the food packaging is recommended to be as low as possible. Nevertheless, in the case of packed fresh fruits and vegetables, high depletion of the oxygen concentration below a certain level inside the packaging leads to develop anaerobic condition. In fact, respiration under anaerobic condition produces ethanol, acetaldehyde and some organic acids. These components lead to unacceptable odor and flavor for the packed product. In addition, absence of oxygen simulates the growth of several anaerobic pathogens like *Clostridium botulinum*. Although anaerobic pathogens may not lead to a visible spoilage, contamination by these pathogens is responsible for a food poisoning. Hence, oxygen concentration inside the packaging headspace should be kept in an appropriate level [4].

With regard to nitrogen, it has no effect on food preservation due to its inadequate solubility in water (0.018 g/ Kg at 20 °C). Indeed, nitrogen is an uncreative gas and it has neither odor or flavor [3]. Therefore, nitrogen is only used in modified atmospheric food packaging (MAP) to fill the package and to inhibit its collapse. This collapse sometimes occur as a result of carbon dioxide absorption by the food. Finally, the effect of the other atmospheric gases such as ozone, carbon monoxide and nitrogen dioxide is not considerable in MAP applications [5].

1.3. Breathable food packaging

Breathability of fresh products packaging is obtained through two techniques which are mircoperforated modified atmospheric packaging (MAP) and ventilated packaging. Each technique has its unique properties and applications in fresh food preservation.

1.3.1. Microperforated modified atmospheric food packaging

Modified atmospheric food packaging technique has been developed in 1930s. It was used as a preservation method for fruits during transportation by reducing O_2 and increasing CO_2 concentrations inside the packaging headspace. In the end of 1970s, MAP technique became commercial for packed perishable food. Recently, MAP is considered an important technique for increasing the shelf life of perishable products without using high amount of chemical preservatives. In fact, the principle of MAP in food preservation relies on modifying the compositions of the air gases inside the packaging headspace. Thus, compositions of atmospheric gases inside packaging are changed from their original atmospheric ratios to the optimum ratios in order to increase the shelf life of the crops. The optimum gases compositions for different fruits and vegetables are shown in table 1 [2].

Name of Product	O_2 (%)	CO_2 (%)
Fruits		
Apple	1-2	1-3
Grape	2-5	1-3
Kiwi	1-2	3-5
Orange	5-10	0-5
Peach	1-2	3-5
Strawberry	5-10	15-20
Vegetables		
Cabbage	2-3	3-6
Cauliflower	2-5	2-5
Corn	2-4	10-20
Lettuce	1-3	0
Mushrooms	3-21	5-15
Spinach	21	10-20
Tomatoes	2-5	0
Onion	1-2	0

Table 1: Recommended gas compositions for different fruits and vegetables.[6]

Modifying the compositions of atmospheric gases inside the packaging headspace is obtained through manipulating and adjusting the permeability of packaging material [6]. Therefore, gas barrier properties are the most signification parameters in the design of MAP. For this purpose, non-degradable polymers such as low-density polyethylene (LDPEs), polyvinyl chloride (PVC) and polypropylene (PP) are used as MAP due to their moderate O_2 permeability. For example, LDPEs is used for its high O_2TR, which is 7,800 cm^3/m^2.day.atm. In addition, PP is also used in MAP although its relative low O_2TR, which is ranged between 2,000 to 3700 cm^3/m^2.day.atm, because of its characteristic mechanical properties such as its stiffness and durability. Polystyrene also has high O_2TR but it lacks for durability. Thus, by combining different plyometric materials such as LDPE and PP, high O_2TR is achieved. This high O_2TR is used to increase the self-life of some fresh products such as lattice. Nevertheless, the products with high respiration rates require a polymeric martials with O_2TR which is higher than the O_2TRs that are provided by the common used polymers. Hence, the permeability properties of most of the polymeric films do not meet MAP specifications for these kind of products. Therefore, plyometric films are modified using several techniques in order to be suitable for MAP applications [5].

Providing the packaging material with micro or macro perforates is one of the packaging systems that used to regulate the gas transmission rates (GTRs). Accordingly, perforated plyometric films used as MAP are classified size into micro perforated and macro perforated systems based on the pores [5]. With regard to the macro-perforated food packaging, it is designed to contain large holes with a dimeter ranged from 3 to 6 mm. However, the large holes unable to sufficiently modify the atmospheric gases compositions inside the packaging. Furthermore, macro perforated food packaging does not prevent food contaminations as well. On the other hand, microporous films allow controlling of gases compositions inside the packaging and regulate the gases exchange between the headspace and the surrounded atmosphere. Moreover, microperforated MAP has a significant contribution in preventing moisture loss for the fresh products. This is due to its low water vapor transmission rate. However, in spite of the fact that preventing moisture loss reduces weight loss of the product during the storage period, it leads to increase the concentration of water vapor inside the food packaging, which encourages the microbial growth [7]. Therefore, porosity of MAP should be manipulated to adjust the optimum water vapor transmission rate and to prevent the microbial growth. Such growth is resulted from water condensation inside the packaging [5].

1.3.2. Ventilated food packaging

Precooling process after harvest is an influential step in maintenance the quality of fresh products through preventing deleterious effect of high temperature. Indeed, it was reported that enzymatic and microbial activities rates are doubled for each 10 °C increase in temperature. Therefore, precooling technology was applied through several methods such as hydro-cooling, package icing vacuum cooling and forced-air cooling

Forced-air cooling is an essential technique in food preservation. In this technique, shelf life of a horticultural products increases through providing a current cold air flow with high relative humidity. In fact, these conditions help in developing cold chain inside the products and decreasing its thermal stress. Hence, the efficiency of this method is highly dependent on packaging permeability because it is considered a heat transferring medium between the provided cold air flow and the product inside the packaging [7, 8]. To explain, high barrier packaging materials show significant heterogeneity in cooling, which has a negative effect on fruits quality. Heterogeneity is cooling causes damage to the product as a result of over cooling, frizzing or chilling for some crops. Indeed, as a result of the high resistance of the packaging to the forced air flow, fruits are cooled based on their position to the cooling source. Thus, heterogeneity in air flow leads to formation of cooling gradient, which leads to fast cooling for the fruits in front of the cooling source followed by slower cooling rate for the fruits placed on the middle and the back to the cooling source respectively. Therefore, ventilated packaging is one of the innovative and promising techniques that were used to improve the cooling process efficiency during product storage. Hence, the main principle of ventilated packaging is based on providing channels for air flow within the packaging material to facilitate air exchanging between the cooling medium and the product inside the packaging.

Accordingly, ventilated packaging plays a significant role in reducing moisture loss. To clarify, in the first two weeks after postharvest, moisture loss reaches its highest level. This occurs if the product is still not stored under uniform cooling environment. This significant weight loss is stimulated by transpiration and carbon dioxide accumulation. In addition, high water vapor pressure deficit between surrounded air and fruits also leads to increase moisture and weight loss. Therefore, providing environment with high relative humidity and appropriate flow rate reduce water vapor deficit and consequently reduce weight loss.

Moreover, ventilated food packaging has a great influence on preventing fruits decay. Although the effect of high humidity on reducing weight loss, high humidity may lead to develop environment with saturated humidity as a result of water condensation. The phenomenon of water condensation occurs when fruits are transferred from ambient temperature to the cooling temperature. In fact, water condensation becomes obvious when the packaging material has low water vapor transmission rate as a result of accumulation of vapor inside the pack. Thus, this problem leads to fruits decay because of the stimulated microbial growth. Therefore, ventilated packaging is used to limit water condensation because of its high water vapor transmission rate. Accordingly, porosity of the packaging plays a significant role in preventing fruits deterioration through its optimum permeability to water vapor.

Furthermore, permeability of packaging materials helps in removing excess heat is resulted from the respiration reaction. The importance of removing excess heat from the packaging headspace is delaying respiration rate, preventing product deterioration and reducing weight loss.

In addition, using ventilated food packaging has essential contribution in reducing consumed cooling energy. In particular, fan system is most energy consuming operation in forced –air cooling technique. Hence, optimization of energy consumption of cooling process is dependent on many factors such as nature of fruits, cooling time, temperature and packaging design. Certainly, reduction of packaging resistance to air flow significantly reduces time and temperature needed for cooling, which consequentially reduces the energy consumption [9, 10].

With regard to ventilated plastic packaging, it was recommended that the total area of vents should be up to 25 % form the packaging area in order to provide sufficient airflow and to increase the permeability of the homogenous air flow inside the packaging. Therefore, the efficiency of the ventilated packaging is based on the vents size, number and distribution. On the other hand, inefficient ventilated packaging design leads to heterogeneous airflow during the cooling. Hence, uniform air distribution through the packaging area in the major parameter that should be taken in consideration [11]. Therefore, developing pores through casting /leaching out technique improves the pores distribution within the packaging film and consequently provides uniform air flow through the packaging and maintains the mechanical properties of packaging as a result of small pores size.

1.3.3. Gas transferring through permeable food packaging

Gas transferring through the porous food packaging is an interchangeable process governed by the food respiration rate and packaging material permeability. In fact, gases concentrations change inside the food packaging as a result of respiration process for the crop that depends on consuming O_2 and producing CO_2. Thus, the driven force of gases exchanging is the pressure gradient is resulted from the difference of O_2 and CO_2 concentrations inside and outside the packaging. Therefore, packaging material permeability, pore size, temperature and the surrounded pressure are the most important parameters used to vary the inside atmospheric gases compositions according to the optimum conditions required for each crop.

In general, atmospheric gases transfer between the packaging headspace and the surrounding atmosphere through the permeable packaging by diffusion through the polymeric films and transferring through the perforations. With regard to the diffusion phenomenon, it is established by sorption of gases on one surface of packaging film and then the desorption of these gases from the opposite surface. Therefore, if the polymeric material of the packaging has a high gases barrier properties, gases exchange through perforations is more prominent. In this case, diffusion of gases through the polymeric film is neglected. On the other hand, if the polymer film is semi-preamble or the number of holes is relatively low, gases exchange occurs as a result of a transmission through holes and diffusion through the polymeric material. Thus, in this case, diffusion phenomenon should be considered in GTRs determination [12].

1.4. Fabrication of porous polymers by solvent casting/particulate leaching technique

Porous polymers have recently gained more attention due to the influence of porosity on their properties and functionality. In particular, the high surface area generated by the pores is the significant advantage that allows porous polymers to be utilized in many applications such as gas separation, drug controlling and releasing, catalysts, membranes for water treatment applications and breathable food packaging applications.

Porous polymers are distinguished form each other by the porosity structure. In fact, the properties and structure of porous polymers are governed by pore geometry, size and distribution. These parameters are controlled by the synthetic method used to develop the porous membranes. Hence,

according to the IUPAC system, porous materials are categorized into microporous when the pores size is less than 2nm, mesoporous polymer when the pore size is ranged between 2 to 50 nm and macroporous polymer when the pore size is higher than 50 nm. However, microporous polymer also refers sometimes to a porous polymer with a pore size in the microscale. Porous polymer is produced by either direct templating methods or indirect tamplating methods. With regard to direct templating methods, they include infiltration of raw plyometric material into a voided templet followed by solidification of the plyometric material and removing of the templet. On the other hand, indirect methods do not include the formation of prior templet. These methods include solvent casting/particle leaching, electrospinning and thermally induced phase separation techniques [13].

Solvent casting followed by porogen leaching out is one of the simple techniques that are used to develop porous polymer for scaffold and tissue engineering applications. Indeed, this technique relies on adding pore forming agent (porogen) into a homogenous polymeric solution and then leaching out this porogen after the polymer solution casting and solvent evaporation. Thus, removing the porogen is applied by immersion the polymeric film in a solvent that highly dissolves the porogen. Accordingly, size, geometry and amount of the generated pores are easily controlled by manipulating the porogen's amount, size and shape [14].

Porogen selection is controlled by several parameters such as the porogen and polymer interaction, polymer properties, the required surface area and pore volume. Therefore, many types of porogens were used in the literature for different applications. Accordingly, porogens are classified into organic porogens, solvating porogens , non-solvating porogens , polymeric porogens , inorganic porogens and ionic liquid [15].

Inorganic salts such as potassium chloride, sodium bicarbonate and sodium chloride (NaCl) have been used as porogenic agents to obtain highly porous polymer. In particular, the main advantage of inorganic porogens is their ability to be easily extracted by water because to their high solubility. On the other hand, porous polymer prepared by using with inorganic porogens is characterized by a relativly small surface area compared to using solvating porogens. Meanwhile, water soluble polymeric porogens sometimes are combined with the inorganic porogens in order to enhance the pores interconnectivity [14].

1.5. Biodegradable polymers in food packaging

1.5.1. Polylactic acid as a biodegradable polymer

1.5.1.1. Structure and synthesis of polylactic acid

Biodegradable polymers have recently gained a significant attention due to their advantages over the petroleum based polymers, which are known by the undesirable environmental impacts. Therefore, polylactic acid (PLA) has been used in many applications as an alternative for petroleum based polymers. In fact, PLA is an aliphatic thermoplastic biodegradable polyester that is synthesized from renewable resources. Lactic acid is the monomer used in PLA synthesis and it is produced from natural resources such as sugar beet, corn and other starch and rich products. Indeed, lactic acid has two types of isomers, which are called L and D isomers as shown in figure 1. Although both of them are asymmetric active configurations of lactic acid, the ratio between these two isomers significantly affects PLA properties such as the degree of crystallinity and melting point [16].

PLA is synthesized by three consequential steps. The first step is the synthesis of lactic acid isomers by the carbohydrate fermentation of corn dextrose. Then, the second step is the formation the lactide monomer by the prepolymerization of the lactic acid isomers to a low molecular weight polymer followed by depolymerization to form the stereoisomers lactide. Finally, the third step is the ring opening polymerization to produce PLA. Furthermore, direct condensation and azeotropic dehydration condensation are other two methods that produce PLA directly from lactic acid isomers without the intermediate lactide formation as shown in figure1 [16, 17].

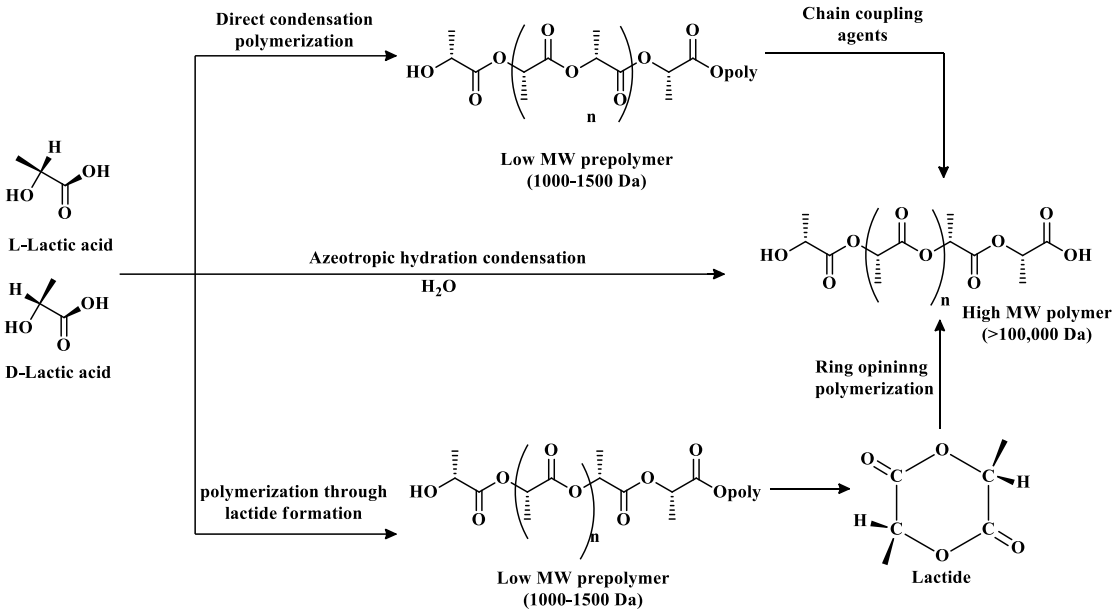

Figure 1: Synthesis of PLA from D, L lactic acid isomers.[17]

1.5.1.2. Properties of polylactic acid

Polylactic acid as a biodegradable polymer is characteristic by its ability to produce recyclable products. Moreover, PLA has thermoforming ability and high mechanical strength. However, it is brittle and its thermal resistance is low. With regard to PLA crystallinity, it is dependent on the ratio between of the L and D lactic acid isomers. In fact, it is semi-crystal when the L- lactic acid percentage is high while it is amorphous when the L – lactic acid percentage is low. In addition, the glass transition temperature has a wide range, which is ranged between 50 -80°C, because it is also dependent on the ratio between the lactic acid isomers.

Barrier properties of PLA are also worth noting. It has a high water vapor transmission rate (WVTR), compared with the other petroleum based polymer [18, 19]. Whit regard to O_2TR of PLA, it is relatively high and its value is ranged between the O_2TRs of terephthalate and polystyrene. In fact, high O_2TR for PLA is resulted from its low glass transition temperature that enhances the mobility of the polymer chains and consequently stimulates the gases diffusivity and permeability [20].

In addition to the production of PLA from renewable sources, its production method includes consuming large amount of carbon dioxide. Furthermore, physical and chemical properties of PLA can be easily modified by controlling its chemical compositions, in term of L, D isomers ratios [21].

1.5.1.3. Applications of polylactic acid

Polylactic acid became an economical alternative biodegradable material for petroleum based plastics, which are associated with undesirable environmental consequences. Therefore, PLA has been used in many applications in biomedical field such as tissue engineering scaffold and drug delivery systems [17].

With regard to using PLA as a food packaging material, safety of PLA as a food packaging material was studied. According to the migration study that carried out by FDA, it was proved that the migration of some components such as lactic acid, lactide and lactoyl lactic acid from PLA does not represent a risk on food because this migration is insignificant. Hence, PLA is categorized as 'Generally Recognized as Safe' for food packaging applications. Therefore, PLA recently is used as food centenaries, lamination films and cups. Moreover, PLA gained high attention as a packaging material for perishable products such as fruits and vegetables [21, 22].

1.5.2. Polycaprolactone as a biodegradable polymer

1.5.2.1. Structure and synthesis of polycaprolactone

Polycaprolctone (PCL) is another biodegradable polymer that has been utilized in many widespread applications because of its characteristic properties. As shown in figure 2, several methods are used to synthesize PCL through different polymerization reactions. Polycondensation of 6-hydroxycaproic acid is one of the methods that are used to synthesize PCL. However, this method is relay reported in the literature. Moreover, PCL is synthesized through radical ring opening polymerization of cyclic ketene acetals in the presence of vinyl monomer. Most importantly, ring opening polymerization (ROP) of cyclic monomer Ɛ-caprolactone by using ionic or metallic catalysts is the most common method used for PCL synthesis. Indeed, Ɛ-caprolactone is a cyclic monomer that is synthesized by Baeyer-Villiger oxidation of cyclohexanonone and hydrogen peroxide in the presence of selected catalysts and initiators.

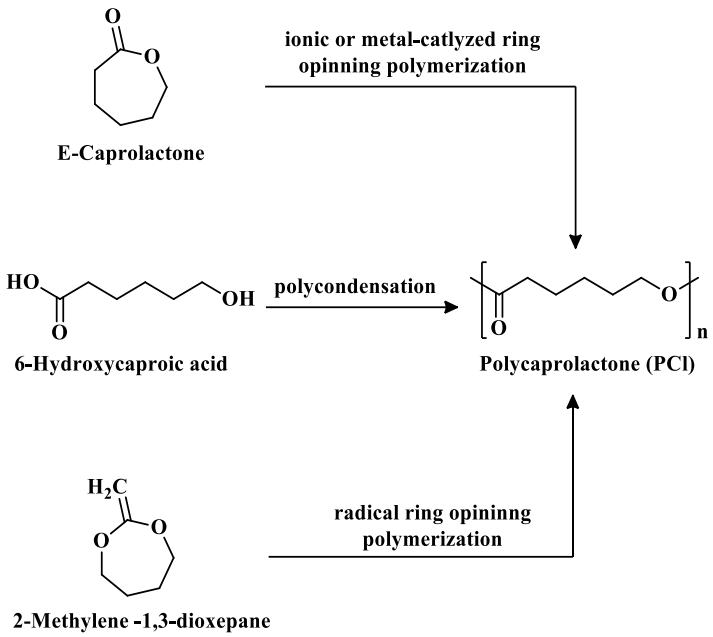

Figure 2: Synthesis methods of polycaprolactone.[24]

Many factors control ROP mechanism such as monomer ratios and concentrations, temperature, reaction time and types of the catalysts and initiators. In fact, ROP of PCL gives a variety of possibilities by using different polyvalent initiators [23]. Therefore, ROP is classified according to the type of initiator into cationic and anionic ROP as shown in figure 3. In the case of cationic ROP, the carbonyl oxygen in Ɛ-caprolactone is attacked by a cation species through nucleophilic substitution (SN_2) mechanism. For instance, ROP is the presence of Lewis acid is an example of cationic ROP. With regard to anionic ROP, the carbonyl group in Ɛ-caprolactone is attacked via anionic species that leads to the opening of the monomer ring followed by alkoixde growth.

Moreover, ROP is obtained by using alkali-metal based initiators through coordination –insertion mechanism [24]. In particular, metal complexes are used in this type of ROP is based on tin and aluminum metals such as Tin (II) octoate and aluminum(III) isopropoxide. With regard to Tin (II) octoate, which is also called stannous (II) ethylhexanoate, it is a commercial and effective catalyst that is used in ROP. Indeed, its function as a catalysis is obtained by association with nucleophilic compound, which are usually alcohols, to act as initiators as shown in figure 3. Although the efficiency of Tin based catalysts, ROP in this case required high temperature, which stimulus intermolecular and intramolecular esterification and consequently leads to high polydisparity for the produced polymer [23].

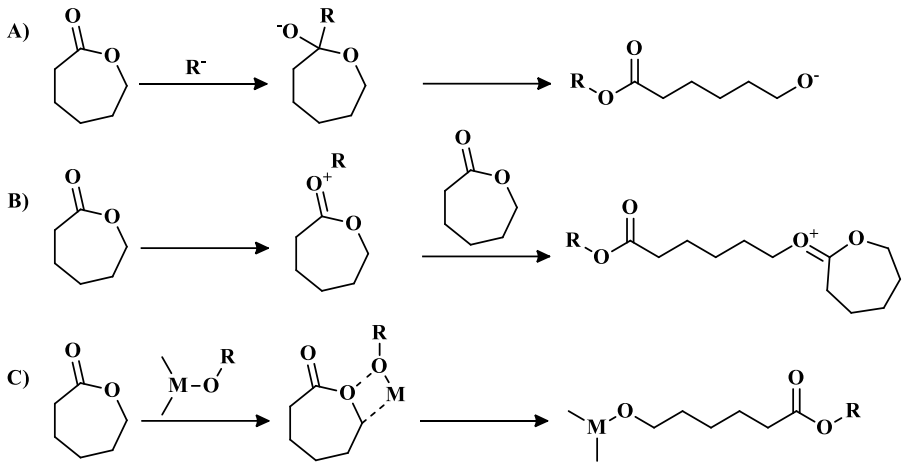

Figure 3: Ring opening polymerization of Ɛ-caprolactone.[24]

1.5.2.2. Properties of polycaprolactone

Polycaprolactone (PCL) is hydrophobic, semi-crystalline aliphatic polyester. Physical, chemical and degradation properties of PCL is varied based on crystallinity degree and the molecular weight, which is varied between 3000-800,000 g/mol. With regard to its biodegradation, PCL is completely degraded under the effect of bacterial, fungal and lipase enzymes. In fact, its degradation is interpreted by the ability of the ester bonds for hydrolysis, which is inversely proportional to the PCL chain length. Furthermore, PCL has relatively low glass transition temperature which is – 60° C and its melting point is 60 °C. Nevertheless, low melting point of PCL is considered a drawback in many applications. Therefore, this disadvantage is usually treated by blending PCL with other polymers. Indeed, PCL is characterized by its compatibility with many polymers and its high solubility in many organic solvents at moderate temperature [23, 24]. Moreover, the chains of PCL are flexible and characterized by high elongation and low modulus of elasticity [25].

1.5.2.3. Applications of polycaprolactone

Polycaprolactone (PCL) is easily fabricated to complicated structure forms as a result of its elastic behavior at room temperature. In fact, the elastic behavior is resulted from its low glass transition temperature. Therefore, PCL exhibits adequate mechanical properties that makes it suitable for many medical applications. With regard to utilizing PCL in medical applications, it is used in wound dressing, medical devices scaffold and engineering tissues applications. PCL is also used

as controlled drug delivery systems because to its high permeability that enhances uniform distribution and releasing for the drug. Accordingly, PCL is approved by FDA and the European Community for using as drug delivery system. In addition, applications of PCL as a biodegradable polymer for food packaging is widespread due to its flexibility [23].

1.6. Synthesis, properties and applications of polyethylene oxide

Polyethylene oxide (PEO) is a hydrophilic, thermoplastic and semi-crystalline polymer [26]. The general formula of PEO is - $(OCH2CH_2)_n$- , since n is the number of oxyethylene group. It is molecular weight is ranged between 100,000 and 7, 000, 000 Da [27]. Indeed, PEO is synthesized by anionic ring opening polymerization of ethylene oxide (EO), which is a three-member epoxide ring. In this synthetic method, hydroxide or alkoxide initiators are used in the anionic polymerization of EO. Hence, the reaction includes opening the EO ring by nucleophilic attack on the EO methylene group and formation of propagating species as shown in figure 4. The advantage of this method that it is characteristic by producing PEO with narrow molecular weight [28].

Figure 4: Anionic ring-opening polymerization of EO initiated by hydroxide.[29]

Furthermore, coordination polymerization for ethylene oxide is used to produce PEO. This technique is characterized by its ability to produce high molecular weight PEO, which is higher than 200, 000 Da. In this method, the molecular weight is controlled by the nature of used initiator and the polymerization conditions. Many types of initiators have been used in this technique such as acetylacetonate and trialkylaluminum-water zinc [29].

PEO is a colorless and odorless powder and it is easily degraded under the presence of oxygen and UV light, which leads to reduction in the molecular weight. In addition, PEO forms a gel by adsorption high amount of water because of its high swelling capacity. In fact, swelling properties of PEO is a significant feature that leads PEO to be an important ingredient in many biomedical and pharmaceutical applications such as swelling controlled devices and drug releasing system. In addition, PEO also has many other applications such as synthesis of hydrogels and fibers. PEO also used as pore forming agent in porous polymer and scaffold design. [28, 29, 30].

1.7. Antimicrobial food packaging

1.7.1. Function of antimicrobial food packaging in food preservation

Antimicrobial (AM) food packaging plays a signification role in protecting food form spoilage by inhibition of microbial growth. In particular, AM food packaging preserves food by incorporation of small amount of an antimicrobial agent into the food packaging material. Accordingly, AM packaging is classified into two types: the non- migratory and migratory AM. In the case of non-migratory AM, the antimicrobial agent is localized in the packaging film. In this case, the microorganism growth inhibition is obtained by the direct contact between the microorganism and antimicrobial agent through the packaging material. On the other hand, in case of migratory AM, the mechanism of inhibiting the microorganism growth relies on controlling the active agent release from the packaging material to the packaging headspace during the food shelf life. Therefore, the migratory AM packaging is categorized according to the nature of the antimicrobial agent into nonvolatile and volatile active agent AM packaging [31].

1.7.2. Natural antimicrobial agent in food packaging

Reducing chemical and synthesized additives in order to limit their health risk potential is a major concern in food applications. Therefore, natural food preservatives are recently used as alternatives to chemical preservatives in food preservations. Hence, it was found that essential oils (Eos) are good candidates to replace many chemical food preservatives because they are characteristic by beneficial antioxidant and antimicrobial properties. Although Eos are categorized as Generally Recognized As Safe (GRAS), their applications as food preservatives are limited because of their undesirable odor and flavor that may affect the sensory properties of food. Thus, Eos are applied as preservatives through incorporation in plyometric material of food packaging [32].

1.7.2.1. Synthesis and properties of cinnamaldehyde

Cinnamaldehyde is a natural antimicrobial active agent in cinnamon and it is extracted form cassia or cinnamon essential oils. It is also called cinnamic aldehyde or 3-phenyl-2-propenal according to its structure as shown in figure 6. In fact, cinnamaldehyde is characteristic by it is antimicrobial and antioxidant properties. Therefore, it is used as food preservative and it is approved as a GRAS

food additive by FDA. In particular, cinnamaldehyde shows antioxidant activity for fresh food by reducing dehydration and delaying browning and shriveling. Moreover, it has an ability to inhibit the growth of mold and mycotoxin. Indeed, inhibition properties of cinnamaldehyde is resulted from penetration of its lipophilic group to the interior cell of the microorganism through the microorganism's membrane, which leads to inhibit the microorganism growth [33, 34].

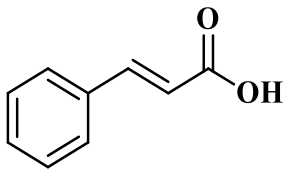

Figure 5: Chemical structure of cinnamaldehyde.[34]

2. Literature Review

2.1. Modified atmospheric food packaging

2.1.1. Applications of microperforated modified atmospheric food packaging in fresh food preservation

Many attempts have been done to extent the shelf life of fresh products and to reduce the weight loss during storage time. Therefore, MAP was designed with different technologies to meet the requirements of fresh food preservation. It is used to preserve the crops which are characterized with high respiration rates. In addition, MAP is combined with other chemical treatments to increase its efficiency as a fresh food preservation method. Accordingly, MAP are classified into five types according to the technology used in the packaging's design and the technique used in food preservation. These five categories are high oxygen modified atmosphere packaging, controlled modified atmosphere food packaging, active modified atmospheric food packaging, intelligent modified atmospheric food packaging and perforated modified atmospheric food packaging [35, 36].

High oxygen modified atmosphere packaging preserves fresh food by providing high oxygen concentration inside the packaging. This technique inhibits the growth of specific kinds of microorganisms and prevents the anaerobic conditions. Effect of high oxygen modified atmosphere packaging on the shelf life of fresh food was studies before by many researchers. Zheng et al. proved that storing mushroom under high oxygen concentration, which is ranged between 80 and 100 % from atmospheric gases in packaging headspace, had significant effect in reducing weight loss and inhibiting of enzymatic browning [35]. High oxygen food packaging is also combined with other preservation methods to improve the fresh products shelf life. For example, Li et al. found that high oxygen MAP associated with ascorbic acid as a preservative improved the shelf life of fresh cut eggplant. Furthermore, it was found that using of this system showed reducing in enzymatic browning through inhibition of oxidase and peroxidase activates [37].

Controlled modified atmosphere food packaging (CA-MAP) is developed by modified the gases atmospheric ratios into the optimum ratios that is desired for the product preservation as shown in table 1. In this case, the optimization is developed by injecting the desired gases compositions

inside the packaging at the beginning of the storage period. The influence of CA-MAP as a food preservation method was investigated through several studies. Sukhvinder et al. studeid the effect of controlled atmospheric food packaging (1-2.5 % O_2 and 3 % CO_2) on the chilling injury inhabitation. It has been shown that CA-MAP reduced the chilling injury and improved the flesh firmness and the titratable acidity retention [38].

Active modified atmospheric food packaging is dependent on incorporation of an active ingredient inside the packaging material in order to improve the food sensory properties and extent its shelf life. Thus, active ingredients release from the packaging material into the packaging headspace and play their role in food preservation. Antimicrobial food packaging is an example of this kind of MAP [39]. Furthermore, other active ingredients play their role in food preservation without being release from the packaging materials. Indeed, these ingredients adsorb some undesirable components from the food packaging headspace. For instance, oxygen scavengers are added as an active ingredient to remove oxygen from the packaging and to delay the oxidation process for the products that are sensitive to oxygen. Moreover, carbon dioxide absorbers and emitters have been used to remove or add carbon dioxide to packaging in order to inhibit the microbial growth for some kinds of food such as poultry, fish and cheese. Certainly, carbon dioxide absorbers and emitters are used in fresh fruits food packaging to delay the respiration rate and extent the shelf life [40]. In fact, effect of optimizing gases concentrations in active packaging on food preservation was demonstrated in literature. Mehmet et al. investigated the effect of active packaging incorporated with both O_2 and CO_2 scavengers on the stored strawberry at 4°C. It was found that gases concentrations inside the packaging headspace reached the optimum level during the storage period. Moreover, CO_2 scavenger helped in maintaining the total soluble solid content and the color of strawberry [41].

Intelligent modified atmospheric food packaging (IMAP) has been designed to observe the food safety through quality indicators such as time-temperature indicators, security tags and radio frequency identification tags. Therefore, IMAP is a low cost, accurate and rapid technique to observe the product's quality. Indeed, it is used to insure the quality of see food and several types of fruits and vegetables. However, IMAP is not used to improve the product shelf life because it only acts as an indicator for the food freshness [42, 43].

Furthermore, micro-perforated MAP is one of the MAP techniques that gained high attention due to its low cost and high performance as a food preservation method. In fact, it was proven that micro-perforated film could achieve equilibrium concentrations of O_2 and CO_2 inside the food packaging, which strongly affect several quality aspects in fresh food [42]. This effect was demonstrated through several studies on different products. Lucera et al. studied the effect of micro-perforated food packaging on fresh cut cauliflower crops quality. In this study, polypropylene with different numbers of micro-perforations was used. The result showed an increasing in CO2 concentration and a decreasing in O_2 concentration without observed anaerobic condition in the packaging headspace. Additionally, the equilibrium concentrations of both gases was reached inside the packaging as result of mass transportation through the perforated film. Thus, concentrations of CO_2 and O_2 were optimized for cauliflowers preservation through the developed perforation. Therefore, flavor off and undesirable odor were not observed [43].

Moreover, Li et al. also investigated the effect of micro-perforated MAP with a 0.5 to 2 mm pore dimeter on the CO_2TR, O_2TR and WVTRs at different temperatures. In this study, micro-perforations showed a desirable effect on increasing GTRs. The effectiveness of micro-perforated MAP also has been tested on tomato as fresh product. Hence, the result proved the ability of the micro-perforated MAP to modify the atmospheric gases concentrations inside the packaging headspace for 5 days has been proven [44].

2.1.2. Applications of ventilated food packaging in fresh food preservation

Wood boxes and corrugated cartons were used early in fruits storage and transportation. However, using wood has several disadvantages that might be harmful to fruits. For example, the irregularity of wood structure leads to non-uniformity of pack permeability. In addition, wood highly absorbs moisture from the surrounding atmosphere and fruits, which encourages microbial growth. Furthermore, abrasive between wood and fruits is also possible during transportation and this fraction may affect fruits integrity. Therefore, the usage of ventilated corrugated fiberboard is more widespread in fruit storage and transportation. However, it was shown that corrugated fiberboard is not suitable for storage under cooling. This is due to its absorption of high amount of water under humid environment, which affects its mechanical strength [10].

Thus, plastic was highly recommended in ventilated food packaging applications. In fact, it was found that storage peach in ventilated polyethylene bags with 2.5 % total ventilated area reduced the its weight loss [45]. Furthermore, the effect of opening size on the performance of precooling process was also investigated. For example, Vigneault et al. studied the effect of opening width of the pressure drop during the forced air precooling process by using acrylic plates with different opening width, which was ranged between 3.2 and 12.7 mm. In this study, it was found that opening width did not show difference on pressure loss relative to each other. However, the study proved that the total area of the openings should represent 25 % form the packaging area in order to show significant effect on the pressure drop [46]. Moreover, effect of perforated plastic films as packaging materials on the moisture loss for several fruits has been investigated in many studies. Robert studied the effect of perforated high density polyethylene (HDPE) film in the quality of pomegranate fruit. In this study, effect of perforations on packaging resistance to air flow was investigated. Indeed, significant reduction in weight loss has been observed for the fruit stored in perforated packaging compared with non-perforated packaging. Furthermore, by using perforated packaging, short cooling time was needed during forced air cooling process, which enhanced energy consumption [47]. Furthermore, Ngcobo et al. investigated the moisture loss rate of grapes stored in non-perforated and perforated LDPE and HDPE films. In this study, it was found that although all the samples were stored under low temperature, grapes stored in non-perforated films showed significant weight loss after three days, which was around 49%. On the other hand, the weight loss for grapes stored in the perforated packs was less the 10 % [48].

2.1.3. Methods of developing breathable and microperforated food packaging

The principle of using porous polymer to adjust the atmospheric gases compositions inside the food packaging has been investigated through several techniques. Physical drilling, inorganic filler and nonwoven web are the three common technique that are used to develop breathable membranes for food packaging applications [36].

Physical drilling includes four methods which are tube perforation, cold and hot needle, electrical discharge and Laser technique. Tube peroration is the attachment of a macro-tube to a tight controlled gas packaging. This method was investigated thoroughly by Montanez et al. through studying the effect of attaching PVC tube to glass containers on gases concentrations. In this study, it was found that the tube with small dimeter had a positive effect on the transfer of gases masses

values with the applied hydrodynamic conditions [49]. Furthermore, P.V. Mahajan et al. studied the effect of tube perforation on the water vapor transmission rate (WVTR). Accordingly, it was shown that the WVTR was enhanced as a result of the presence of tube perforation. Moreover, the packaging was shown its suitability to fresh product such as mushroom [50]. In general, in spite of the fact that tube perforation showed desirable impact on controlling gas compositions in several studies, its applications are not widespread because of its practical difficulty [46].

The second method of physical drilling is cold and hot needle perforations, which is also known as pin perforation. It is a mechanical method to develop perforations in packaging material by using manual or semi-automatic tools. In fact, the difference between cold and hot needle perforations is the type of the applied mechanical method. To clarify, cold needle produces holes by punching the plyometric film while hot needle produces holes by melting the plastic material. On the other and, cold and hot needle perforations are similar in some characteristics such as producing large pores, which are larger than 1 mm in diameter. Mechanical perforation has been used in MAP applications to preserve many several kinds of fruits and vegetable such as spinach, tomato, capsicum and parsley. For instance, Shafafi, used a punched polyethylene film with 6 mm hole dimeter as MAP for fresh spinach and parsley. During this study, it was found that MAP decreased the weight loss of parsley, increased its chlorophyll retention, maintained vitamin C content and prevented anaerobic conditions [51]. Although pin micro-perforation is distinguished by its cost efficiency and the practical easiness, Larsen et al. found that formation of holes with regular shape is hindered by using the puncturing equipment. Hence, calculation of TRs using the developed mathematical models is inaccurate in this case because of the difficulty of determination the specific hole area [45, 52].

Electrical discharge is one of the mechanical drilling technique used to develop micro-perforated membrane. The technique's principle is based on developing pores by either melting or vaporizing the plyometric material through applying heat energy by electrical discharge machine. This machine is composed of two electrodes, which are separated by water or oil in order to generate electrical discharge [36]. Thus, the type of electrodes with other operating conditions control the size and the shape of the developed perforations. This method was used to develop micro-perforated membranes for MAP applications in several studies. For example, Allan et al. used electrical charge technique to produce micro-perforated polyester film with 30-100 µm hole

dimeter. In this study, it was found that micro-perforations with small diameter significantly increased the GTRs of polyester. However, it was observed that accurate measurement of the whole area was also hindered because of the difficulty of specify the hole edge [53].

Laser technique is one of the promising techniques that has been recently used in designing micro-perforation MAP. This technique is characterized by its ability to produce a well determined hole surrounded by specific edges. Laser system is composed of laser beam, power source for energy generation after excitation with the laser beam and optical activity for the emitted beam stimulation. Despite the cost efficiency of laser techniques, controlling the pore size is also difficult because it is dependent on the heat conductivity of the plyometric material. Therefore, laser technique was developed by using effective kinds of laser beams such as Co_2, ultraviolet, Nd:YAG (neodymium-doped yttrium aluminum garnet) and Nd:YLF (neodymium-doped yttrium lithium fluoride). Indeed, laser gas perforation using CO_2 at 10640 nm is a widespread technique that was recently developed to obtain micro- perforated food packaging. Moreover, Laser using Nd:YAG , which are a crystal laser in a solid state, was used in many studies. In fact, because Nd:YAG is used at 1064 – 532 nm wavelength, it is able to perforate many types of plyometric materials as a result of its high energy [36, 54]. Therefore, applying laser theology by using Nd:YAG laser beam is widespread in MAP applications. For instance, Charinee et al. studied the effect of Nd-YAG laser beam on perforations of polypropylene, polyethylene and terephthalate. Furthermore, the study investigated the effect of perforations size on GTRs. Hence, it was found during the study that Nd-YAG beam developed pores with an average size of 100 micrometers. Indeed, the accurate size was dependent on the beam intensity and the polymer thermal conductivity. Moreover, it was proved that the pores developed by this method was able to increase O_2TR and to modify the β ratio to 0.9 [54].

Inorganic composite membrane is one of the techniques used to develop microporous membrane for MAP applications. The basic principle of this technique is based on developing micro voids at the interface area between the polymer and the inorganic particles through applying uniaxial and biaxial mechanical stretching. Indeed, micro voids are producing during stretching as a result of the poor interaction between the plyometric material and inorganic filler. Thus, these micro voids enhance the gases transmission rates of the plyometric film [42]. Many inorganic fillers were used in the literature for this purpose such as calcium carbonate, barium sulfate and zeolite. For

example, Wu et al. investigated the porosity of polyethylene and polypropylene through using $CaCo_3$ as an inorganic filler. In this study, it was found that the amount of $CaCo_3$, its particle size and polymer nature had a significant influence of the developed porosity. Furthermore, the moisture vapor transmission rate was investigated for the produced porous membranes. Accordingly, it was demonstrated that WVTR significantly increased when the membranes starched as a result of porosity improvement [55]. Moreover, Kim et al. used zeolite as an inorganic filler to produce breathable membrane from low density polyethylene (LDPE), linear low density polyethylene (LLDPE) and high density polyethylene (HDPE). Hence, the study showed a formation of air holes after stretching as a result of the interfacial interaction between zeolite and the plyometric matrixes. In addition, it was shown that the number of air holes was higher with HDPE as result of its high crystallinity [56].

Nanofibers has been used as breathable food packaging because of its high gas permeability. In fact, nanofibers are characterized by a random distribution and entangled structure. Thus, these properties enhance the fibers toughness and water resistance. Therefore, a suitability of nanofiber as food packaging was proved through several studies [42]. For instance, Shao et al. investigated the effect of using electrospun nanofibers loaded with polyphenols as a packaging material on fruit preservation. In addition, the parameters that affect the nanofibers structure such as polymer solution, feeding rate and applied voltage were also investigated. In this study, it was proved that the packaging had a desirable effect on the quality of the stored strawberry in terms of weight loss and firmness maintenance [57].

Although the several advantages of microperforated MAP as discussed previously, its cost is high due of the technologies used to develop pores. Moreover, from the prospective of food safety, microorganisms are able to transfer through the micro holes from the surrounded environment into the food substrate inside the packaging. However, it was decided by food producers that contamination by the microorganism transferred through the packaging holes does not threaten the food safety compared to the pathogens growth as a result of the anaerobic atmosphere or carbon dioxide injuries in the conventional packaging [42].

2.2. Sodium chloride as a porognic agent

2.2.1. Recrystallization of sodium chloride by salting –out precipitation

Recrystallization of sodium chloride is one of the essential techniques that are used to improve its quality for many applications. The main purposes of recrystallization are purification and size reduction. In fact, sodium chloride in submicron size has several advantages over sodium chloride with its original size. In other words, the crystals with a small size are characterized by high surface area and consequently high surface activity. Therefore, recrystallized sodium chloride is required for many applications such as food, electronics and pharmaceutical applications [58].

Recrystallization is a phase transition for material from the soluble state into solid state. To clarify, this transition occurs as a result of a reduction in the free energy of liquid system. This reduction leads to molecules clusters. Consequently, these clusters are converted to nuclei followed by a formation of crystal lattice through growth mechanism and precipitation after reaching a critical size [59]. Precipitation of sodium chloride from a diluted solution induces by super saturation condition, which leads to reduction in the total free energy of the system. Thus, inducing super saturation condition is obtained through three methods, which are evaporation, cooling and anti-solvent techniques. In fact, using evaporation and cooling techniques are characterized by developing polydispersed crystal size, high energy consumption and needing of high supersaturation level. On the other hand, anti-solvent technique is obtained under ambient temperature and therefore it is considered a cost efficient method for recrystallization (60). In this method, supersaturation state is obtained by adding non-solvent to sodium chloride solution in order to reduce its solubility in water. Consequently, sodium chloride is precipitated in a form of fine powder crystal [61]. Thus, Anti-solvent precipitation could be obtained under low super saturation level. This is considered an advantage because high super saturation level required by the other techniques may lead to particles agglomeration [62].

2.2.2. Recrystallization of sodium chloride by ultrasonic technique and salting –out precipitation

Despite the advantages of anti-solvent precipitation, it produces asymmetric crystals with a broad size. Therefore, anti-solvent precipitation was combined with sonocrystallization technique in order to control the nucleation and consequently to narrow the produced size. Indeed,

sonocrystallization has several advantages over the conventional crystallization. To explain, by using ultrasonic technique, particles agglomeration is prevented during the nucleation and growth. This is due to the crystal growth and the reproducible nucleation are well controlled under a low supersaturation condition by sonocrystallization parameters. Thus, the precipitated particles are characterized by a narrow size distribution [59, 60, 63].

Many researchers explained and studied the effect of sonocrystallization principle and the effect of its parameters on the produced crystal size. For instance, Abbasa et al. explained the principle of sonocrystallization of sodium chloride used for inhalation. In this study, the sonocrystallizations was interpreted based on cavitation phenomenon. In fact, ultrasonic waves develop voids in the anti-solvent as a result of the pressure fluctuation. The main function of these voids is holding the nuclei, which are formed under a supersaturation level after the addition of diluted salt solution. These voids are short lived cavities and therefore these cavities easily go under catastrophic collapse and produce high amount of energy. Accordingly, these collapse leads to a generation of large number of nuclei, which are characteristic with high surface area. Consequently, these nuclei are further converted to crystals through the consumption of the solute through growth mechanism. Moreover, parameters affect NaCl crystallization by ultrasonic technique were investigated through this research. It was shown that increasing in the sonication power leads to broadness in the crystal size because of the reduction in the cavitation intensity threshold. In addition, the influence of temperature also was a critical factor because it affected the grown crystals properties. Indeed, it was found that low temperature has a positive effect in narrowing the size distribution and decreasing the average mean size because of enhancing the supersaturation conditions. On the other hand, lowing temperature at a certain limit may lead to the opposite effect. To clarify, at a temperature of 5 °C, the viscosity of both solvent and anti-solvent increase. Hence, the probability of natural cohesive force also increases and thus reduces the cavitation intensity and decreases the nucleation [63]. In another study, Judy et al. also studied the effect of stirring, time and ultrasonic frequency on anti-solvent recrystallization of NaCl. According to this study, it was found that stirring enhances the mixing between anti-solvent and NaCl solution and also inhabits the formation of two phases between the solvent and anti-solvent. On the other hand, extending the contact time between the solvent and anti-solvent showed negative effect on the produced crystals because it leads to formation of thick zone of crystals. Therefore, the nucleation rate

decreases because of the difficulty of NaCl diffusion. Finally, investigation of the influence of ultrasonic frequency showed that it has no effect of NaCl recrystallization [60].

2.2.3. Applications of porous polymer by using sodium chloride as a pore forming agent

Sodium chloride was used as a pore forming agent in many applications by using salt-leaching out technique. Furthermore, NaCl was recrystallized using several techniques in order to develop pores in the submicron size. For example, Tran et al. prepared porous cross-linked urethane doped polyester for tissue engineering applications using NaCl as a porogenic agent. In this study, NaCl was re-crystalized through inducing the supersaturation condition by using temperature gradient. Recrystallization was obtained through heating NaCl solution to certain temperature followed by cooling. Thus, lowering temperature stimulated nucleation and growth processes to start. Therefore, the developed pores were characterized by narrow size distribution. Furthermore, it was shown that the generated scaffold is characterized by lack of dead pores and the high interconnectivity between the produced pores [58].

Furthermore, producing porous polymer by NaCl as a pore forming agent through salt-leaching out technique was combined with other techniques to improve the developed porosity. For example, Rossella et al. used sieved NaCl as a pore forming agent to prepare porous scaffold from D, L-lactic-glycolic-copolymer by using solvent casting/particulate leaching technique followed by freezing technique. According to this study, it was shown that increasing the scaffold viscosity was observed as a result of the NaCl residuals reminded in the membrane. Although the positive effect of freezing on the ruddy texture of scaffold, broad size of pores was noticed, which is ranged between few microns to 300 µm. In fact, the broad size appeared as a result of solid-liquid phase separation, which was produced from solvent crystallization when the mixture was cooled under the solvent's freezing point [64].

Moreover, many attempts were done in order to improve the pores interconnectivity by combined a second pore forming agent with NaCl. For instance, Aydin et al. used naphthalene as a second porogen with NaCl to improve the pores interconnection within the prepared scaffold. Hence, it was found that Naphthalene produced small pores that played a significant function in the interconnectivity of large pores, which were produced form NaCl. In addition, it was found that

when NaCl used as a single porogen, formation of few amount of small pores was observed. On the other hand, when naphthalene was used as a second porogen with NaCl, the number of small pores significantly increased, which consequently improves the pores interconnectivity [65].

2.3. Biodegradable polymers in food packaging applications

2.3.1. Polylactic acid in food packaging applications

Polylactic acid (PLA) was used as food packaging due its desirable features. However, some properties of PLA were needed to be modified in order to improve its suitability as a food packaging material. Indeed, some of the properties that hinder using of PLA in food packaging application are high modulus of elasticity and low elongation percentage at break. Therefore, mechanical properties of PLA were improved in several studies either by adding plasticizers or by blending with another elastic polymer. For instance, Wang et al. investigated the effect of blending polybutylene adipate-co-terephalate with PLA in order to improve its properties for food packaging application. In this study, the blend showed higher flexibility compared with the pure PLA. In addition, barrier properties of the blend were acceptable for some products such as potatoes and green onion. The blended film also provided antifogging behavior that helped in maintaining food quality [66]. In another study, Bhatia et al. also studied the properties of PLA and polybutylene succinate (PBS) blend for food packaging applications. According to this study, significant improvement was observed in the PLA mechanical properties after blended with PBS within the compatibility limits [67].

2.3.1.1. Applications of polylactic acid in modified atmospheric food packaging

PLA was used as MAP by applying laser perforation to enhance its gases transmission rates. Despite the low values of O_2 TR and CO_2 TR for PLA, these values are adjacent from each other. Therefore, non-vented PLA could regulate the gases compositions inside the packaging headspace of the fresh products until reaching the steady state conditions. Thus, this unique property of PLA was utilized in design MAP by many researchers. For example, Almenar et al. studied the effect of using PLA trays on the shelf life of stored blueberry. In this study, it was shown that equilibrium modified atmosphere has been reached inside PLA containers as result of blueberries respiration reaction and the permeability of PLA packaging. Indeed, the steady state conditions were reached

after three days from the blueberry storage under 10° C, which extended the shelf life and reduced the weight loss [68].

Moreover, several authors investigated the influence of micro-perforated PLA on improving the shelf life of fresh products. For instance, Mistriotis et al. prepared a biodegradable equilibrium MAP (EMAP) by using micro-perforated PLA. In this study, the suitability of three-layer PLA film and micro-perforated PLA film as EMAP has been investigated. Accordingly, it was shown that the multilayers PLA film is characterized by high WVTR compared with other conventional polymers that enhanced its ability to apply as EMAP. Furthermore, using multiple perforated PLA showed higher TRs than using single hole with an equivalent total area. In addition, O_2TR and Co_2TR became more adjacent by the micro-perforation feature. Thus, the designed packaging showed its ability to develop steady state modified atmospheric conditions for cherry tomato and peach by adjusting the number of holes [18].

2.3.2. Polycaprolactone in food packaging applications

Polycaprolactone (PCL) was approved by FDA as a biodegradable and biocompatible polymer for medical devices and food packaging applications. However, it should be blended with other polymers and additives due to its low elastic modulus and high degradation rate. Therefore, PCL was blended with many polymers such as PLA, chitosan and low density polyethylene in order to improve its properties in severl studies. For instance, Joseph et al. blended chitosan with PCL with different percentages. Accroding to this study, it was shown that the blend contains 20 % PCL exhibited increase in elongation by 20.5% compared with pure chitosan membrane, which was suitable food packaging applications. The blend also showed high miscibility between the two polymers [69]. Moreover, PCL is also blended non-biodegradable polymers such as polyolefin, LDPE and polypropylene. Although the low enzymatic degradations of these polymers, it was shown the enzymatic degradation of the blends may occur if the preparation parameters are well controlled [25].

2.3.2.1. Applications of polylactic acid/polycaprolactone blends

The properties of PCL and PLA blend as well as copolymer was investigated by several authors due to their characteristic attributes in mnay applications. For example, Plackett et al. prepared PLA-PCL copolymer as a packaging for cheese. Moreover, antimicrobial agent was added to the

copolymer to delay the microbial growth in the packed product. The copolymer also was enhanced by nanoclay in order to improve its barrier properties. In addition, the copolymer was provided by cyclodextrin complexes to slow the release of the encapsulated antimicrobial. According to the study, the prepared packaging showed complete degradation in addition to the high thermal stability and low permeability for water and oxygen. However, the copolymer showed decrease in molecular weight as a result of high water absorption at room temperature [70].

Furthermore, PLA/PCL blend also exhibited interesting advantages due to its physical and biodegradable properties. These characteristic properties were investigated in the literature by many authors. For example, Rao et al. investigated the mechanical properties of PLA and PCL at different compositions. According to this study, PLA/PCL (80/20) blend showed increase in elongation and decrease in tensile strength compared with neat PLA. This result was explained by the effect of the high elasticity and viscosity of PCL that increased the viscosity of the blend. Furthermore, PLA has a Newtonian region which is longer than PCL. Thus, blending PCL with PLA reduced the Newtonian region of the whole blend compared with pure PLA [71].

Moreover, PCL/PLA blends were used in preparing porous membranes for scaffold applications in many studies. For instance, Scffaro et al. prepared multi-phasic porous laminate from PLA core and PCL shall. According to the study, the porous multi plastic laminates exhibited high interconnect porosity with narrow pore size. In addition, the mechanical properties of the laminates showed high tensile stress, which indicted high adhesion force between the laminates. Hence, it was shown that this adhesion strength is stronger than the ultimate resistance of PLA layer, which led to high tensile stress [72].

However, the miscibility of PCL with PLC is low due to their incompatibility. Therefore, several attempts were obtained to further improvement in the miscibility of PLA-PCL blends. For example, Chavalitpanya et al. added block copolymer of polyethylene glycol and polypropylene glycol as a compatibilizer to the PLA/PCL blend and studied its effect on the blend properties. According to this study, it was found that addition of a compatibilizer to PLA-PCL blend showed significant improvement on its thermal and mechanical properties and morphology. Additionally, it was found that the tensile strain of the compatibilized blend increased while the tensile stress decreased [73].

2.4. Applications of polyethylene oxide in development of porous polymers

One of the successful attempts that was done to obtain interconnected structure in the scaffold applications is adding hydrophilic polymer, such as PEO, with the porogenic agent to the plyometric blend. Indeed, the added hydrophilic polymer should be immiscible with the polymer, which is used to develop the scaffold. Thus, as a result of the continuous morphology of the blend, interconnected porous structure is formed after extraction of the porogen and the hydrophilic polymer. Therefore, it was proved that continuity of the immiscible phases is depended on their concentrations in the blend. Hence, the ratio between the two immiscible polymers should be far from the phase inversion point.

In fact, many authors investigated several methods to develop membranes with interconnected porous structure by using inorganic pore forming agent and hydrophilic polymer. For example, Reignier investigated the development of three dimensional network scaffold by using leaching out technique. In this study, NaCl is used as a porogen with polycaprolactone (PCL) the presence of PEO as a hydrophilic polymer because of its immiscibility with PCL. According to the study, it was found that as a result of the immiscibility of the PCL and PEO, PEO was easily extracted with NaCl by immersing the formed polymeric membrane in water and highly interconnected porous scaffold was obtained. Thus, it was noticed that by using this technique, the morphology of the produced scaffold is characterized by fully interconnected porous structure [74].

2.5. Cinnamaldehyde as an antibacterial agent in food packaging applications

Cinnamaldehyde was incorporated in the polymeric membranes in order to increase antimicrobial properties for many applications in several studies. For instance, Makwana et al. incorporated cinnamaldehyde as an antimicrobial ingredient into PLA to design active food packaging. Furthermore, in this study, coating PLA with cinnamaldehyde nanoliposome and casting PLA with incorporated cinnamaldhyde were investigated as two methods for adding antimicorbal agent to the packaging film. According to the study, the observations showed that PLA film that casted with cinnamaldehyde is characterized by higher antimicrobial activity compared with PLA film

that coated with cinnamaldehyde nanoliposome [75]. In another study, Qin et al. also has investigated the effect of incorporation cinnamaldehyde with a blend of PLA and polytrimethylene by using solvent casting technique. According to the study, it was found that cinnamaldehyde incorporation led to produce rough surface for the casted film as a result of the developed porosity. Furthermore, the mechanical properties of the blend were improved as a result of the plasticizing effect of cinnamaldehyde on decreasing the intermolecular force between the plyometric chains. Therefore, the study showed that water vapor permeability also increased for films contain cinnamaldehyde. Hence, although the improvement of the antibacterial properties of the blend, it is application as a food packaging was not acceptable as result of its insufficient barrier properties [76]. Qin et al. also studied the properties of the active food packaging designed by incorporating cinnamaldehyde as an antimicrobial agent into PLA/PCL blend. In addition, the designed packaging efficiency was investigated on mushroom as a fresh product. According to the study, it was observed that PLA/PCL packaging with incorporated cinnamaldehyde played a significant role in reducing weight loss of the tested mushroom during the storage time. Moreover, the active food packaging reduced the microbial count and maintained the mushroom color compared with mushroom stored under the control film. The study also showed that the high water vapor permeability was an advantage to preserve the mushroom quality and to improve its shelf life [77].

2.6. The Scope of thesis

The aim of this work is to develop breathable polymeric films from polylactic acid and polycaprolactone as biodegradable polymers for food packaging applications. Accordingly, microporosity will be developed by solvent casting/leaching out technique to enhance the permeability of the polymeric films. Hence, in order to develop microporosity, sodium chloride will be used as a poroginc agent after reducing its size by using ultrasonic-antisolvent technique. Moreover, polyethylene oxide will be incorporated within the polymeric matrices as a hydrophilic polymer to facilitate the extraction of sodium chloride and to improve the interconnectivity of the developed porous structure. In addition, effect of the amount of the porognic agent on the films porosity, permeability and mechanical properties will be demonstrated. Furthermore, characterization methods such as BET, DSC and FTIR are applied to investigate the physical and chemical properties for the developed microporous films. Finally, microporous films will be coated with cinnamaldehyde to develop the antimicrobial properties of the food packaging against food pathogens.

3. Materials and Methods

3.1. Materials

Poly (lactic acid) (PLA) pellets with a commercial name “Ingeo” grade 4043D was purchased from NatureWorks LLC, Minnetonka, USA. The purchased grade has a relative solution viscosity (RV) of 4.0 ± 0.10, and a level of D-isomer of 4.25 ± 0.55%. Polycaprolactone (PCL) pellets was purchased from Sigma-Aldrich, Saint Louis, USA. The purchased grade has an average molecular weight of 80 ,000 Da. Polyethylene oxide was purchased from Alfa Aesar, Karlusruhe , Germany with molecular weight 100, 000 Da. Sodium chloride, absolute ethanol and dichloromethane (DCM) (≤99%) were purchased from Fisher Scientific, Hampton, USA. Trans-cinnamaldehyde was purchased from Scharlau, China.

3.2. Preparation methods

3.2.1. Sodium chloride recrystallization

Sodium chloride were recrystallized by using anti-solvent and ultra-sonication techniques. 15 ml of sodium chloride solution (20% weight per water volume) was added to 150 g (192 ml) of absolute ethanol after sonication for 5 min by using ultrasonic probe sonication (Athena Technology, Maharashtra, India) to remove air bubbles. The mixture was exposed to ultra-sonication for 5 min at 132 V under the presence of magnetic stirring to avoid particle agglomeration. The mixture was filtrated under vacuum and the recrystallized particles were obtained.

3.2.2. PLA and PCL-PLA films preparation method

Samples were prepared form PLA with different concentrations of NaCl, PEO, PCL as shown in table 2 to study their effects on the porosity and physical properties of the film. For all the samples, DCM was used as a solvent and it was added according to the total polymer weight to keep the w/v % of polymer in solvent 10 %. PEO and NaCl were also calculated according to the total polymer weight and added to the 100 % polymer base.

Solvent was measured and added to the glass laboratory bottles than recrystallized NaCl was added to the solvent. The suspended solution was sonicated for 1 min 220 V to ensure complete

dispersion for the salt particles. PLA or PCL-PLA and PEO were then added to the NaCl/solvent suspended solution and the mixtures were left under magnetic stirring for 2 hours at the room temperature. The films were casted over glass plates by using automatic film applicator (JR400D, Shanghai, China) and left for 24 h in the room temperature to ensure solvent evaporation. Then, the glass plates were immersed in water to facilitate removing of the films without cutting or stretching. The films then were immersed in distilled water for 48 days with changing the water every 24 h to remove the PEO and NaCl. The films then were dried on vacuum oven at 40° C and 600 mbar for 24 h to ensure complete solvent evaporation and water residuals before characterizations.

Sample Name	Polymer base compositions		Porogenic agents compositions (porogenic agent weight / polymer base weight %)	
	PLA %	PCL %	PEO %	NaCl %
Neat PLA	100	_	_	_
PL-PO	100	_	10	_
PL-N	100	_	_	50
PL-N10	100	_	10	10
PL-N30	100	_	10	10
PL-N50	100	_	10	50
PL-N70	100	_	10	70
PL-100	100	_	10	100
PL-PO1-N50	100	_	15	50
PL-PO2-N50	100	_	20	50
PL-PC1-N50	80	20	10	50
PL-PC2-N50	60	40	10	50
PL-PC3-N50	40	60	10	50
PL-PC4-N50	20	80	10	50
Neat PCL-PLA	20	80	_	_
PL-PC4-N70	20	80	10	70
PL-PC4-N100	20	80	10	100

Table2: Compositions of polymers and porogenic agents for the porous films.

3.3. Characterizations methods

3.3.1. Sodium chloride and membranes morphologies

Recrystallized NaCl particles size and size distribution and membranes morphology were investigated using Scanning electron microscope (Supra 5S LEQ, Zeiss) in The American University in Cairo. NaCl particles and membranes were gold spattered for 1min at 15 mA before scanning to avid the effect of electrical charge on the scanned images.

3.3.2. Air permeability

Air permeability was measured according to the ASTM D 737 standard method by using air permeability tester in National Institute of Standards. The tested sample was placed on the sample holder and air was drawn under 2125 Pa through an area of 5 cm^2 from the film. The measurement was replicated three times on different areas from the films and air permeability was taken as an average number in $cm^3/cm^2/s$.

3.3.3. Mechanical properties measurement

Maximum elongation at break, maximum nominal force and energy required to reach maximum elongation were obtained from stress-strain isotherms according to the ASTM D822. Samples with dimensions of 1.5 cm* 9 cm*0.0007 cm were cut from the films to study the effect of NaCl and blend compositions of the mechanical behavior. Tow distinguished lines were drawn on the sample before hanging to determine the elongation verses the stress. The sample was fixed between two clamps and exposed to the tensile force. The upper clamp is fixed while the lower one is connected to strain gauge. The date was recorded through digital oscilloscope which is connected to a transducer supplied by a constant voltage DC power supply. The upper clamp was constantly strained and the length between the remarked lines was determined by using cathetometer to calculate the elongation. Readings from the oscilloscope were recorded for each strain after 15 min in order to be stable and the potential was calibrated in Newton (N) from the stress gauge. The elastic force (f) was determined versus elongation and the equilibrium elastic force (f *) was calculated according to following equation

$f^* = f/ A^*$

Where f is the elastic force in (N) and A* is the cross-sectional area. The stress-strain graph was plotted. The maximum energy needed to break (E_m) was determined by calculated the area under the curve of stress-strain.

3.3.4. Thermal properties

3.3.4.1. Differential scanning calorimetry (DSC)

Differential scanning calorimetry DSC131 evo (SETARAM Inc., France) in National Research Centre was used to perform the differential scanning calorimeter analysis. The samples were weighted in aluminum crucible 100 µl and introduced to the DSC. Nitrogen and Helium were used as the purging gases. The test was programed including two zones, the cooling zone -20°C to 25°C and the heating zone from 25°C to 200°C with a heating rate 10 °C / min. The thermogram results were processed using (CALISTO Data processing software v.149).

3.3.4.2. Thermogravimetric analysis (TGA)

TA Instrument TGA Q50 (Lukens Drive, New Castle, USA) in National Research Centre was used to study the thermal stability of the prepared porous PLA and PLA-PCL films. The samples were cut into small pieces and each sample was weighed to 6-10mg in aluminum crucible. During the test, another empty aluminum crucible was used as reference. The measurement was conducted under nitrogen atmosphere with a follow rate of 50 ml/min. The samples were heated from room temperature until 600 °C with a heating rate of 10 °C/min. Changing in the samples weights verses temperature was illustrated on the plotted TGA graphs. DTG curves were also plotted based on the obtained TGA graphs.

3.3.5. Barrier proprieties

3.3.5.1. Oxygen transmission rate (O_2TR)

Oxygen transmission rate was measured according to the ASTM D3985 using GDP- Gas Permeability tester (Brugger FeinmechaniK Gmbh, Munich, Germany) in Plastic Technology Center. The Sample was fixed between two chambers at ambient atmospheric pressure. The upper chamber was filled with oxygen while the lower chamber was purged by nitrogen, as a carrier gas. Concentration of oxygen permeated through the sample was measured by cuolometric detector. The detector produces electrical current with a magnitude that is corresponded to the concertation of the permeated oxygen in the carrier gas. The test was run until steady state conditions was obtained. Oxygen transmission rate value was measured in

cm^3/m^2.d.atm and it expressed amount of oxygen permeated through the sample per unit time and area under the steady state conditions.

3.3.5.2. Water vapor transmission rate (WVTR)

Water vapor transmission rates for the PLA and PLA-PCL porous membranes were measured according to ASTM E96/E96M-12. The test was run by using desiccant method. The desiccant used was calcium chloride $CaCl_2$ that was pre-dried at 200 °C for 24 hr. The dried $CaCl_2$ was placed on autoclaves with leaving enough space to allow shaking. Samples free form pinholes or air bubbles were cut from the casted film with an area of 12.56 cm^2 and sealed on the open mouths of the autoclaves by using wax. The autoclave filled with $CaCl_2$ were weighed after sealing with the tested samples with an accuracy of 0.0001 and the initial weights were recorded (M_0). The assemblies then were placed in the dry keeper under controlled atmosphere and relative humidity. The relative humidity was kept constant by using NaCl saturated solution. The autoclaves were weighed every day (M_t) for 7 days followed by shaken horizontally before returning to the keeper. WVTR is calculated at the end of the test by plotting changing in weights versus time according to the following equation:

$$WVTR= (M_t- M_0)/ \Delta t *A$$

Where M_0 is the initial weight (gm), M_t is the weight at time t (gm), t is time (day) and A is the tested area of the film (m^2). WVTR was calculated in g/day·m^2 by multiplying $(M_t- M_0)/ \Delta t$ (slope of the straight line) and the tested area.

3.3.6. Water absorption test

Water absorption was measured according to water absorption ASTM D570. Samples were cut 76 mm * 25 mm form the whole membranes. The samples were dried in vacuum oven at 40° C and 600 mbar for 24 h and then accurately weighed (W_c). The dried samples were completely immersed in distilled water at 23 °C for 24 h. The samples then were weighed again (W_i) after removing form distilled water and wiped off using tissue papers to remove any excess water from the surface. Percentage the weight gained after immersion in water (W_g %) was calculated form different between W_c and W_i. In order to determine the percentage of weight loss ($W_{L\ \%}$), the samples were re-dried again by using the same previous conditions and then were weighed again (W_f). Water absorption percentage was determined by calculated the sum of the weight gained

percentage after immersion in water (W_g %) and the weight loss percentage after the re-drying (W_L%) according to the following equations:

W_g % =((W_i-W_c)/W_c)*100,

W_L%= ((W_c-W_f)/W_c)*100,

Water absorption % =Wg% + W_L %

3.3.7. Brunauer-Emmett-Teller (BET) surface area

Surface area and porosity were determined by nitrogen gas sorption analysis using an ASAP 2020 analyzer (Micromeritics Instrument Corporation, Norcross, GA,USA) in the American University in Cairo . The samples first were pretreated by using vacuum at 40°C for 4 hours. 48-point pressure tables with 20-s equilibration intervals were used to record the adsorption and desorption isotherms .The surface area was calculated using the method of Brunauer, Emmett, and Teller (BET) by applying a model of adsorption involving multilayer coverage filling. The deBoer t-plot method was carried out to determine the surface area and the micropore volume.

3.3.8. Fourier-transform infrared spectroscopy (FTIR)

FT-IR spectra of neat and porous PLA and porous PCL-PLA films were investigated to study the interaction between the polymers and the porogen. The spectra were obtained by Thermo Scientifc Nicolet 380 FT-IR, Waltham, MA, USA in The American University in Cairo. The samples were cut into 2 cm * 2cm and measured under a wavelength ranged between 500 and 400 cm^{-1}.

3.3.9. Preparation and characterization of antibacterial food packaging

3.3.9.1. Antibacterial coating method

Two samples from each film were cut into 1cm*1cm and immersed in 20ml ethanol/water mixtures with different concentrations of trans-cinnamaldehyde. The ratio of ethanol to water in the mixture was 1:4, molar ratio. The samples were kept immersed in the solutions for 24 h and then were sterilized under UV lamp to remove any contamination before measuring the antimicrobial activity.

3.3.9.2. Antibacterial activity measurement

Antimicrobial activity test was carried out in Biochemistry Central Lab, Cairo University. The sterilized media was poured onto the sterilized Petri dishes (20-25 ml, each petri dish) and left for solidification at room temperature. Microbial suspension was prepared in sterilized saline equivalent to McFarland 0.5 standard solution (1.5x 105 CFU mL-1). Then, the turbidity of the microbial suspension was optimized to be OD= 0.13 using spectrophotometer at 625 nm. A sterile cotton swab was immersed into the adjusted suspension within 15 minutes after optimizing the turbidity of the inoculum suspension. Then, it was flooded on the dried agar surface and left to dry for 15 minutes with lid in place. Wells of 6 mm diameter was made in the solidified media by using sterile borer.1*1 cm^2 of tested films was put to each well. The plates were incubated at 37°C for 24 hrs and zones of inhibition was measured in mm. The experiment was done in triplicate to ensure the accuracy.

4. Results and discussion

4.1. Porogen and membranes morphologies

4.1.1. Morphology of re-crystalized porogen (sodium chloride)

The particle size distribution of the porogen has a great effect on the morphology of the developed porous films. Therefore, in order to reduce the crystal size and narrow the particle size distribution of sodium chloride (NaCl), it was recrystallized by anti-solvent and ultra-sonication techniques.

[A]

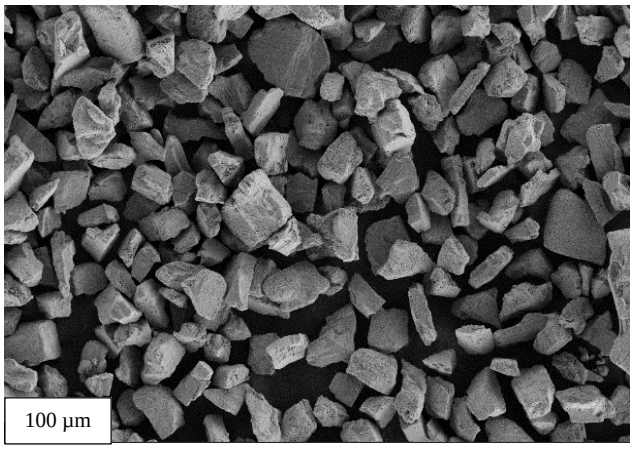

[B]

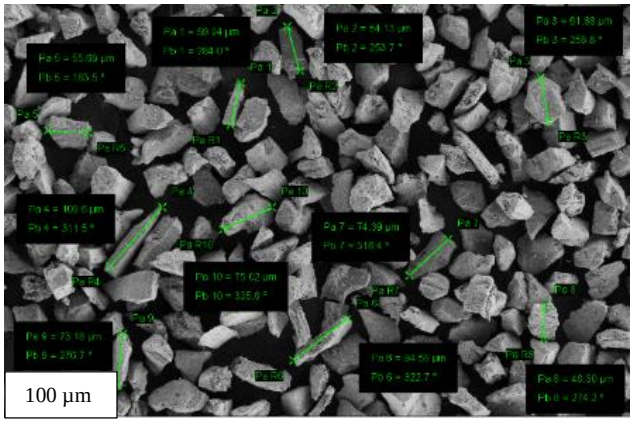

Figure 6: [A] SEM morphology of the initial NaCl crystals, [B] SEM morphology of re-crystalized NaCl crystals

As shown in Figure 6, the initial size of (NaCl) before recrystallization was ranged from 250 to 500 µm. After recrystallization using ultrasonic and anti-solvent techniques, the crystal size was narrowed to be ranged from 40 to 120 µm.

4.1.2 Influence of porogen concentration on the morphology of porous PLA films

Membranes morphologies, pores sizes and distribution in porous PLA films with different NaCl compositions were investigated by scanning electron microscope (SEM). The samples were scanned with two different magnifications to show the distribution, number and size of small and large pores.

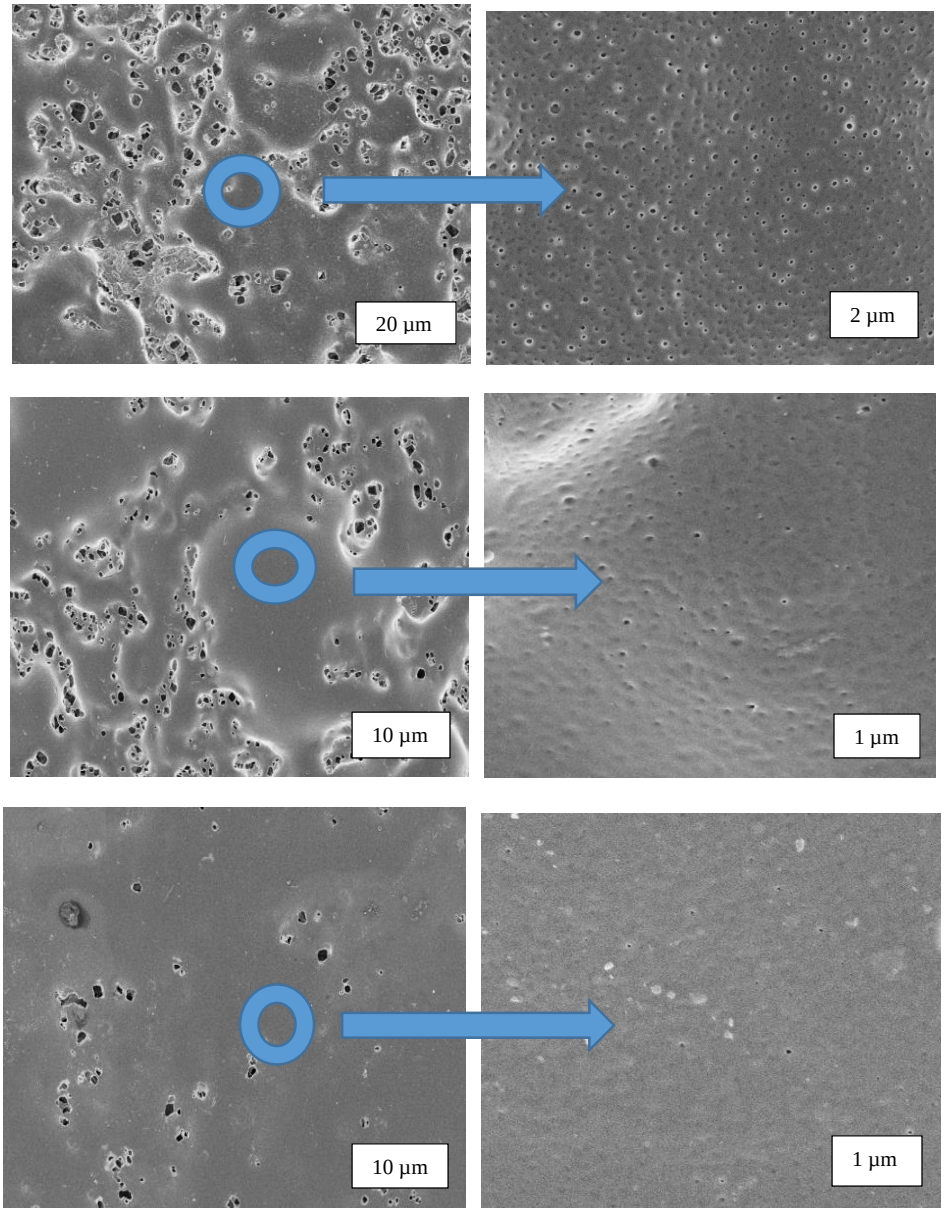

Figure 7: SEM of the macro and micro pores in porous PLA films with 10 % PEO and different NaCl percentages. [A] PL-N50, [B] PL-N70 and [C] PL-N100.

Neat PLA film (not shown) without addition of NaCl and PEO were characterized by denies morphology. As shown in figure 7, 8 &9, after addition of NaCl and PEO, porous structure was developed with different morphologies. The morphology was highly dependent on polymers ratios and NaCl and PEO compositions. In fact, all the porous films showed bimodal distribution of macro and micro pores size because of the extraction of NaCl and PEO respectively. To explain, PEO extraction formed microspores with a size ranged from 200 to 300 nm while NaCl extraction formed macrospores with a size ranged from 2 to 8 µm. Thus, small pores act as interconnected channels between the large pores. Thus, morphologies of all the porous films represent networks composed of large cavities interconnected by small channels. The same result was proved by Reignier et al. and Cui et al. during studying of the effect of PEO and NaCl on the porosity of PCL scaffold [74, 78]. Indeed, this structure was resulted from the cooperative effect of both NaCl and PEO on the developed porosity. This result proved through studying the separated effects of NaCl and PEO on the developed porosity in separated polymeric films as discussed in the next section. In general, the observed interconnectivity of the porous films is an essential property in enhancing gases transmission rates through the packaging materials.

Moreover, contradiction between crystals size of NaCl before mixing and the size of the formed macrospores was worth noting. In other words, the crystals size of NaCl particles before mixing was ranged between 40 and 120 µm. Nevertheless, it was observed that these particles formed cubic and cylindrical macropores with a smaller pore size, which is ranged between 0.2 µm and 8 µm. Hence, this unexpected observation indicated that NaCl particles were exposed to cleavage and erosion during the mixing process. In fact, this phenomenon become more significant at high NaCl percentage. To explain, at high composition of NaCl, the particles started to strongly contact each other, which affected their size and shape. This result was confirmed by the obvious increase in the un-uniformity of the pores size and shape when NaCl compositions increased in samples PL-N70 and PL-N100. Furthermore, NaCl particles before mixing were also characterized by their irregular shape because of the effect of ultrasonic recrystallization process. Thus, the formed pores were characterized by irregular shape because the influence of sonication process on NaCl crystals shape.

The porosity should theoretically increase with increasing in the NaCl percentage. However, porosity showed inversely proportional relationship with NaCl compositions. In fact, this result

was obvious through the high number of interconnected pores observed in the SEM for sample PL-N50 compared with the small number of pores that was observed in samples PL-N70 & PL-N100. This result indicated the agglomeration of NaCl that led to formation of lower number of pores with relatively larger size, which is proved by BET analysis. Another possible explanation is that when NaCl percentage was above 50%, the added PEO percentage was not sufficient to completely extract NaCl crystals during leaching out step. Therefore, lower number of micropores were formed. In addtion, existence of NaCl residuals within the polymeric matrices blocked the small pores, which is resulted from PEO extraction. Thus, blocking of the small pores led also to formation of lower number of interconnected channels. This explanation was proved through the observed sub-nucleus within the morphologies of samples PL-N70 & PL-N100, which indicated the presence of un-extracted NaCl particles.

4.1.3. Difference between the influence of PEO and porogen on the porosity and morphology of porous PLA films

In this study, NaCl was used as a pore forming agent to improve the permeability of PLA. Furthermore, PEO was added as a hydrophilic polymer to facilitate the extraction of NaCl by water during the leaching out step. Moreover, according to several studies in the literature, PEO plays a significant role in improving the interconnectivity of the developed porous structure. However, investigation of the individual effects of PEO and NaCl on the porosity was an essential step in order to interpret the structure of the developed porous membranes. Accordingly, scanning electron microscope (SEM) was carried out for samples PL-PO and PL-N, which were prepared by adding 10% PEO and 50% NaCl respectively to PLA. The samples were also scanned with two different magnifications to show the distribution, number and size of small and large pores.

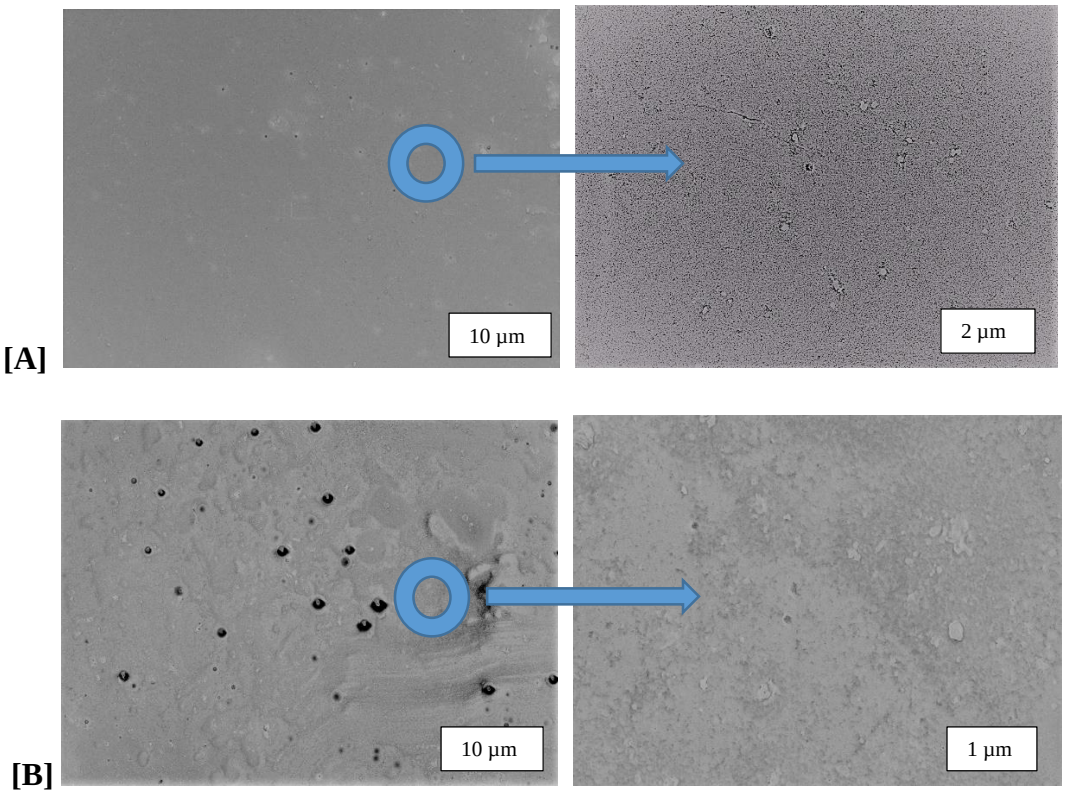

Figure 8: SEM morphology for porous PLA with PEO and NaCl. [A]: Sample PL-PO with 10% PEO. [B] Sample PL-N with 50% NaCl

As shown in figure 8, extraction of 10% PEO in sample PL-PO led to form a few amount of micropores. However, this amount is extremely lower than the amount of micropores that formed with the same percentage of PEO in the presence of NaCl as shown is figure 7 [A]. Furthermore, 50 % NaCl in sample PL-N formed small number of macropores compared with the number of macropores that formed with the same composition of NaCl in the presence of PEO. Indeed, this reduction was resulted because significant amount of NaCl was not extracted from the polymeric matrix. Moreover, the macropores in sample PL-N were not interconnected because of the absence of the small channels, which were formed in the presence of PEO in sample PL-N50 as discussed previously. Accordingly, this observation indicated that the interconnected porous structure, which is formed by extraction of PEO and NaCl, in porous PLA films with different NaCl compositions, is resulted from the synergistic effect of both NaCl and PEO.

4.1.4. Influence of PCL composition on the morphology of porous PLA films

Polycaprolactone (PCL) was added to improve the mechanical properties of porous PLA film. Different compositions of PCL were added to porous PLA film with 50 % NaCl to determine the optimum concentration that able to improve the mechanical properties. The morphology of porous PLA-PCL blends was also investigated by SEM at two different magnifications.

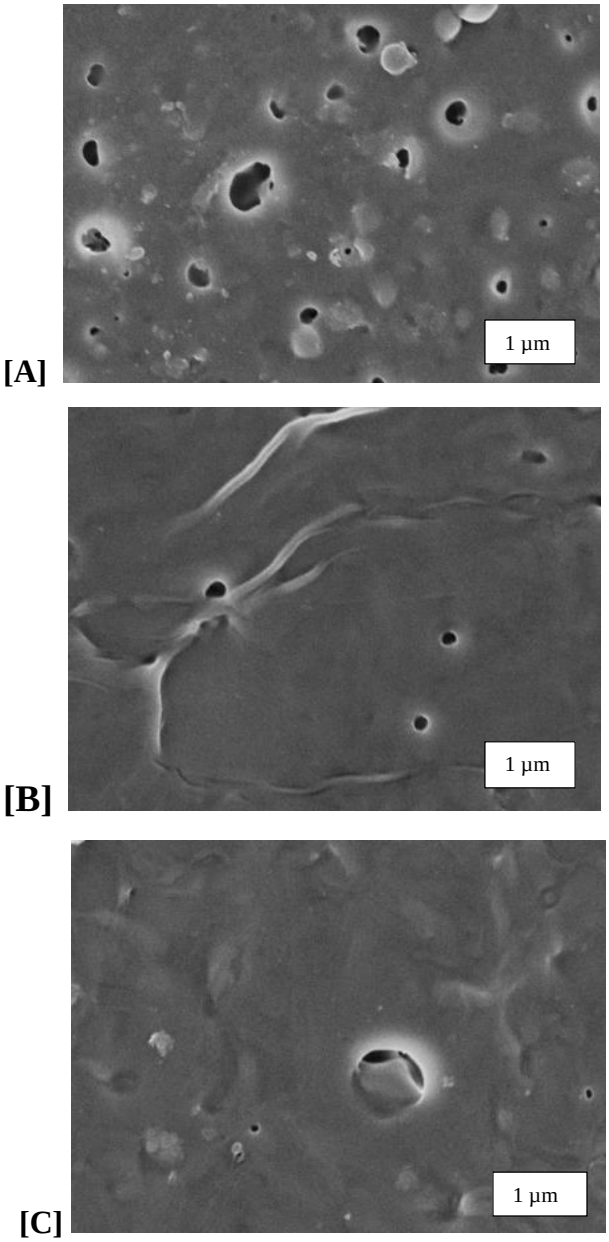

Figure 9: SEM morphology of porous PLA/PCL films with different PCL percentages, 50% NaCl and 10% PEO. [A] PL-PC2-N50, [B] PL-PC3 -N50 and [C] PL-PC4-N50.

As shown in figure 9, introducing of PCL into the blend showed significant effect on the membranes morphologies in terms of homogeneity, pores number and distribution. To clarify, when PCL was blended with PLA with different percentages, some droplets were observed as a result of coalescence phenomenon, which is a merging between the particles of the dispersed phase within the matrix of continuous phase. Indeed, depending of the PLA and PCL compositions in each bland, the minor ratio represented the dispersed phase while the major ratio represented the continuous phase. Accordingly, this phenomenon indicated phase separation of the system as result of immiscibility between PLA and PCL. Furthermore, sample PL-PC4-N50 showed the lowest number of small pores compared with simple PL-PC3-N50 and PL-PC2-N50. This observation indicated that the number of small pores decreased when PCL percentage increased. In fact, this result was expected because PEO was not fully extracted from the blends. To explain, high affinity between PCL and PEO hindered its full extraction form the polymeric matrices during leaching out step. Therefore, this effect became more significant when PCL percentage increased, which decreased the number of small pores [74].

4.1.5. Influence of porogen concentration on the morphology of porous PCL-PLA films

PCL-PLA blend that is composed of 80% PCL & 20 % PLA was chosen to study the effect of NaCl compositions on the blend porosity. Hence, the morphology of the blend with different NaCl percentages was investigated by SEM.

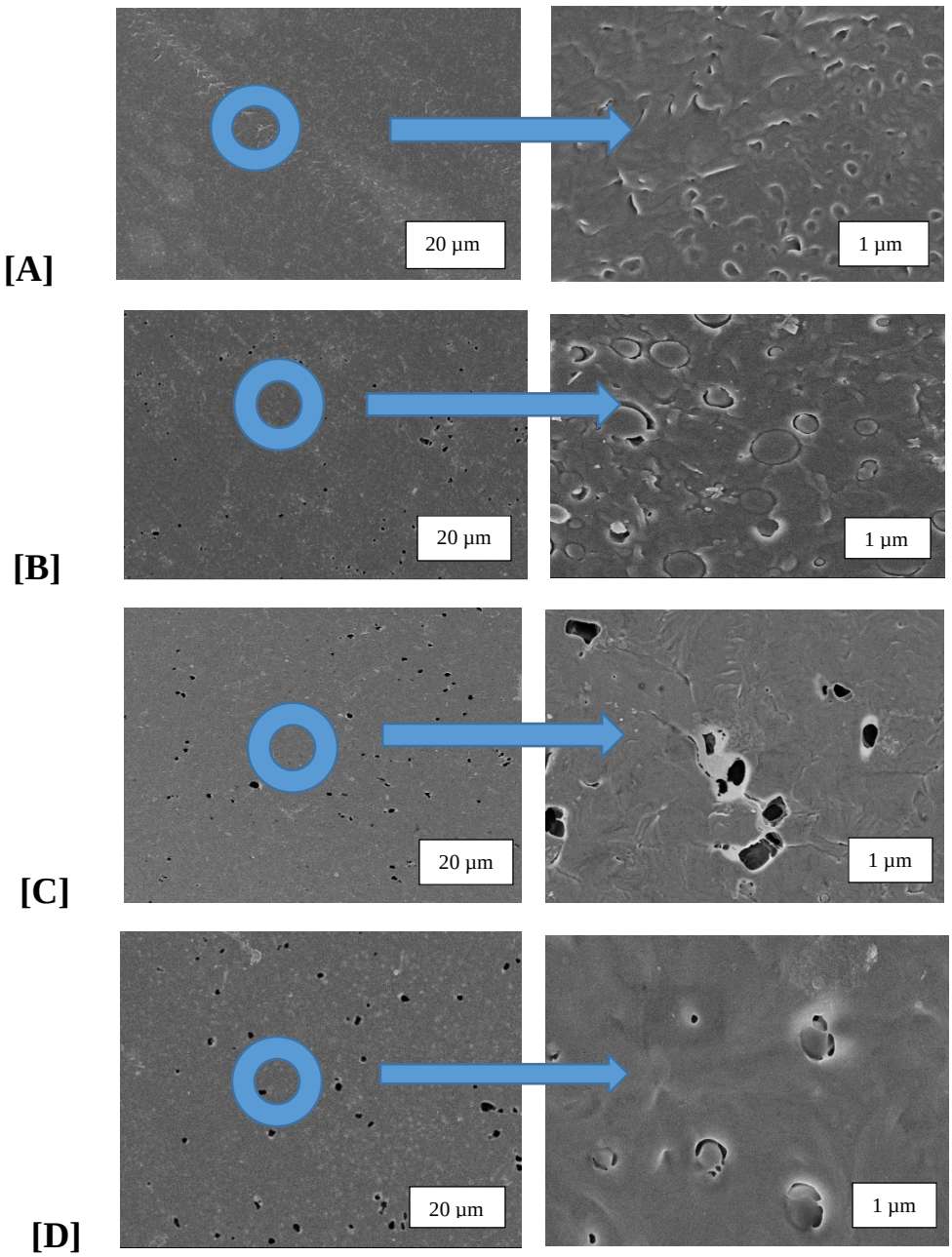

Figure10: SEM morphology of neat and porous 80% PCL/20 % PLA films with 10%PEO and different NaCl percentages. [A] Neat PCL-PLA (4:1) [B] PL-PC4-N50, [C] PL-PC4-N70 and [D] PL-PC4-N100.

As shown in Figure 10, numbers of macroporous, resulted from NaCl extortion, increased with increasing in NaCl percentages that indicated the extraction of the majority of NaCl particles. Indeed, high hydrophobicity of PCL, compared with PLA, enhanced leaching out of NaCl particles even at high composition. On the other hand, numbers of microporous, resulted from PEO

extraction, is low compared with porous PLA films. This reduction resulted from the high affinity between PCL and PEO, which led to incomplete extraction of PEO [79].

4.2. Air permeability

The main purpose of developing porosity within PLA and PLA-PCL films was to improve air permeability. Therefore, air permeability measurement was used as a main indicator in determining the optimum NaCl percentage and PEO percentage that achieved the highest porosity. Moreover, the effect of adding different compositions of PCL on air permeability was also investigated.

4.2.1. Influence of porogen concentration on the air permeability of porous PLA films

In order to study the effect NaCl composition on porosity, different NaCl percentages were added to PLA at constant PEO percentage, which is 10%, and air permeability was measured. Furthermore, distribution of NaCl within the polymeric matrices and the homogeneity of the films morphology were investigated through measuring air permeability at different areas among each sample.

Sample name	Air permeability ($cm^3/cm^2/s$)					Air permeability increase (%)
	Reading 1	Reading 2	Reading 3	Average reading	Standard deviation	
Neat PLA	2.06	2.06	2.05	2.06	0.005	_
PL-N10	2.06	2.06	2.06	2.06	0	0.16
PL-N30	2.1	2.1	2.1	2.1	0	2.1
PL-N50	5.29	5.3	5.6	5.40	0.17	162.4
PL-N70	4.64	4.7	4.8	4.71	0.08	129.2
PL -N100	3	2.9	3.2	3.03	0.15	47.5

Table 3: Air permeability for PLA with different NaCl percentages

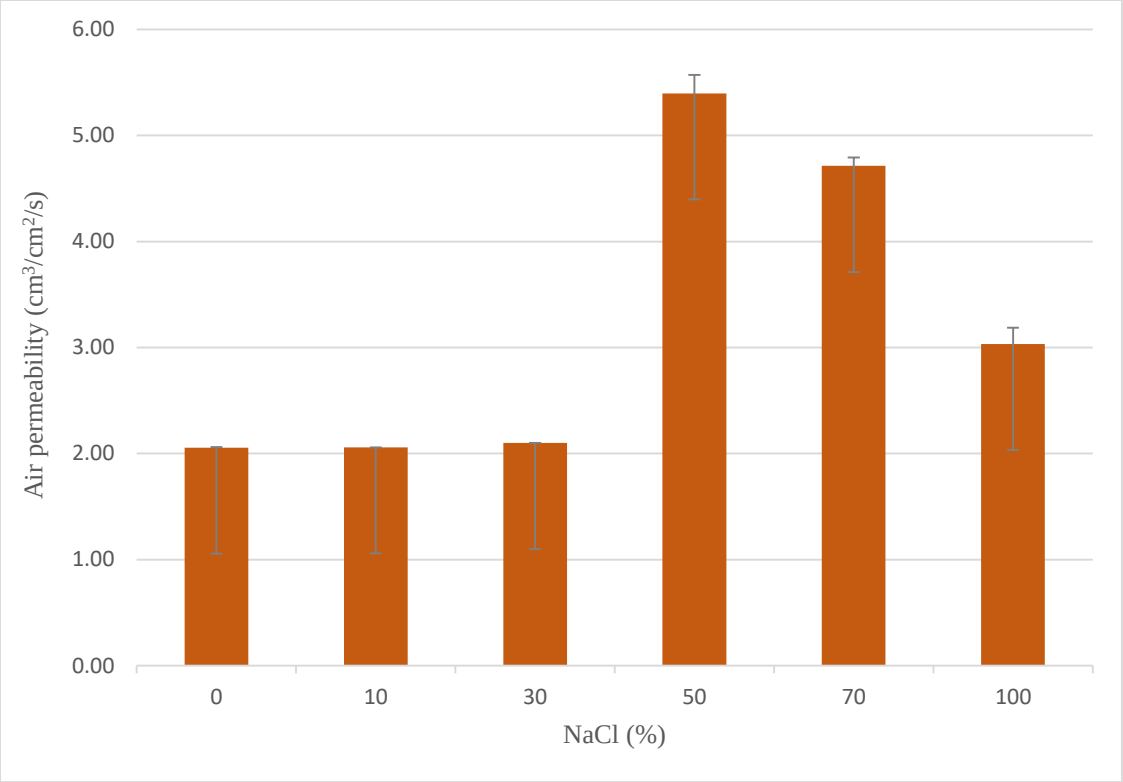

Figure 11: The relationship between air permeability and NaCl percentage in porous PLA films

As shown in table 3, adding 10 % NaCl in sample PL-N10 did not showed any improvement on the air permeability of the film compared with neat PLA while sample PL-N30 with 30 % NaCl showed slight increase in the air permeability. Thus, this result indicated that NaCl at these concentrations did not achieve the sufficient porosity needed to enhance air permeability of PLA. However, samples PL-N 10 & PL-N30 were characterized by constant air permeability values at different areas through the films. Fluctuation of air permeability values between the different areas of the films indicated high homogeneity of the mixtures. On the other hand, sample PL -N50 showed significant increase in air permeability by 162 % compared with neat PLA. This increasing was associated with slight variation in the air permeability values through different areas of the film. Indeed, this variation was resulted from the reduction of the salt distribution homogeneity because of its higher composition compared with samples PL-N10 & PL-N30. The same observation was noticed for samples PL-N70 & PL-N100 which showed increasing in air permeability by only 129.2% and 47.5% respectively compared with neat PLA.

In fact, reduction in permeability when NaCl percentage increased from 50 % to 100 % was resulted from agglomeration of salt particles. Probability of agglomeration during the mixing period increased when salt concentration increased. This phenomenon was explained by the effect of NaCl maximum pack concentration on membranes morphologies. To clarify, monodisperse dense spheres, such as salt, is known by theoretical maximum pack concentration around 68%. Thus, when particles concentration exceeded this percentage, the mixtures lost their ability to flow and the particles started to contact each other due to the lack of liquid phase that should facilitate the mixtures motion. Therefore, NaCl particles agglomerated in samples PL-N70 and PL-N100. Indeed, this result was expected when increasing in suspension viscosity was observed during preparation of sample PL-N70 & PL-N100, which indicated the effect of NaCl composition on the solutions fluidity [74].

Accordingly, leaching out of agglomerated NaCl particles from the plyometric mercies of samples PL-N70 and PL-N100 led to formation of small number of large pores compared with the pores number and size formed form leaching out of dispersed NaCl particles in sample PL-N50. This result is demonstrated by BET analysis through the observed increasing in the pores volume when NaCl percentage increased. Thus, pores structure of samples PL-N70 and PL-N100, which characterized by low number of large pores, allowed a permeation of lower volume of air compared with sample PL-N50. This result is in a good agreement with previous investigation for the effect of pores size on gas permeability in literature. Lin et al. demonstrated significant reduction on permeability after modification of microfiltration alumina membrane by chemical vapor disposition. In this study, it was explained that the reduction in permeability was resulted from the effect of modification on broadening the pore size distribution in addition to formation of small amount of large pores [80].

Moreover, another possible explanation for the air permeability reduction is that salt agglomeration phenomenon resulted in incorporation of some salt particles within the plyometric matrices. Indeed, minor amount of the agglomerated particles did not release during the leaching out step due to their large size and the consequent extraction difficulty. Accordingly, the presence of agglomerated NaCl in the samples PL-N70 and PL-N100 led to formation of spheres in submicron sizes that hindered the air diffusivity through the films.

On the other hand, in sample PL N50, when NaCl concentration was lower than the maximum pack concentration, the particles were isolated from the plyometric matrix. This isolation facilitated their dispersion and prevented their agglomeration. Therefore, despaired distribution and absence of agglomeration of NaCl particles within the plyometric matrix of sample PL-N50 led to complete leaching out of NaCl particles and formation of large number of small pores, which allowed a permeation of high volume of air. Accordingly, 50 % NaCl was chosen to be the optimum porogen percentage to study the effect of PEO and PCL on the air permeability.

4.2.2. Influence of PEO concentration on the air permeability of porous PLA films

In attempt to increase air permeability through improving the interconnectivity of pore structure, PEO percentage was increased. Hence, effect of adding higher concentration of PEO with 50 % NaCl to PLA on air permeability was investigated.

Sample name	Air permeability ($cm^3/cm^2/s$)				
	Reading 1	Reading 2	Reading 3	Average reading	Standard deviation
PL-N50	5.29	5.3	5.6	5.40	0.18
PL-PO1-N50	2.15	2.18	2.12	2.15	0.03
PL-PO2-N50	2.04	2.08	2.09	2.07	0.026

Table 4: Air permeability of porous PLA films with different PEO percentages.

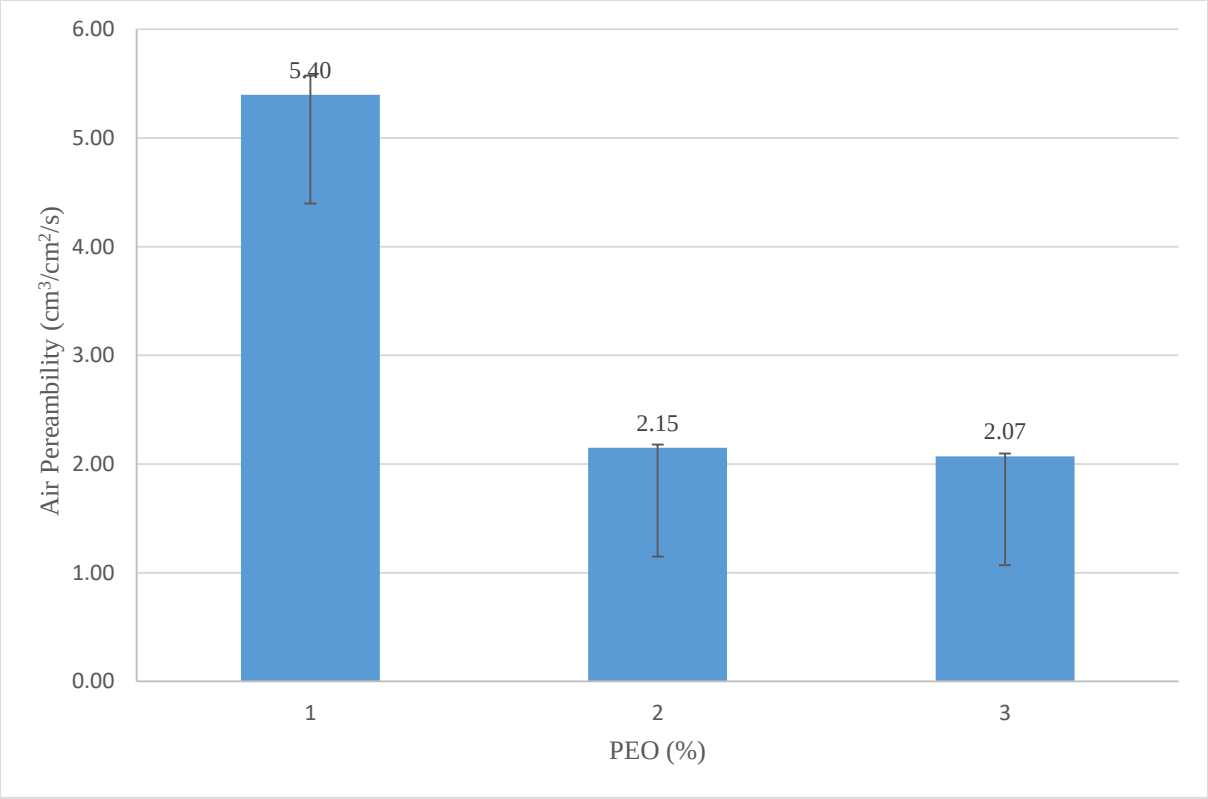

Figure 12: The relationship between air permeability and PEO percentage for porous PLA films.

PEO percentage increased for 10 % in to 15 % and 20 % in samples PL-PO1-N50 and PL-PO2-N50 respectively at constant NaCl percentage, which is 50%. As shown in table 4, in spite of the fact that increasing in PEO percentage improved NaCl extraction, it led to reduction in air permeability. This result was expected because the effect of the polydispersed pore size distribution on gas permeability. To explain, as discussed previously, pores resulted from NaCl and PEO extractions are highly different in size. Therefore, increasing PEO compositions led to increase the polydispersity of the pores size and the irregularity of the pore shape through the membranes. Consequentially, the channels that interconnect the large pores are characterized by high tortuosity, which led to increase the airflow resistance during permeability. In fact, increasing in tortuosity indicated increasing in the diffusion path length of air, which reduced permeability. Therefore, the morphologies of the films with high PEO percentages did not enhance gas permeability even with increasing in the surface area of sample PL-PO2-N50 as demonstrated by BET analysis. Effect of diffusion path tortuosity in reducing permeability was reported in several

studies. Ahmed et al. observed the same inversely proportional relationship between tortuosity factor and permeability during studying the pores structure of concrete [81]. Accordingly, 10% PEO in sample PL-N50 was chosen to be the optimum concentration to study the effect introducing PCL on air permeability.

4.2.3. Influence of PCL concentration on the air permeability of porous PLA films

Although the high permeability achieved by adding 50 % NaCl and 10 % PEO to PLA in the sample PL-N50, the mechanical strength of the sample suffered from low elongation at break as shown in sec 4.3.1. Therefore, PCL was blended with PLA to improve the mechanical properties of porous PLA films.

Sample name	Air permeability ($cm^3/cm^2/s$)					Reduction in air permeability (%)
	Reading 1	Reading 2	Reading 3	Average reading	Standard deviation	
PL N50	5.29	5.3	5.6	5.40	0.18	
PL-PC1-N50	4.2	4.15	4.18	4.18	0.025	22.5
PL-PC2-N50	2.7	2.67	2.83	2.73	0.085	49.44
PL-PC3-N50	2.78	2.74	2.7	2.74	0.04	49.25
PL-PC4-N50	3.08	3.08	3.04	3.07	0.023	43.15

Table 5: Air permeability of porous PLA-PCL blends with different PCL percentages.

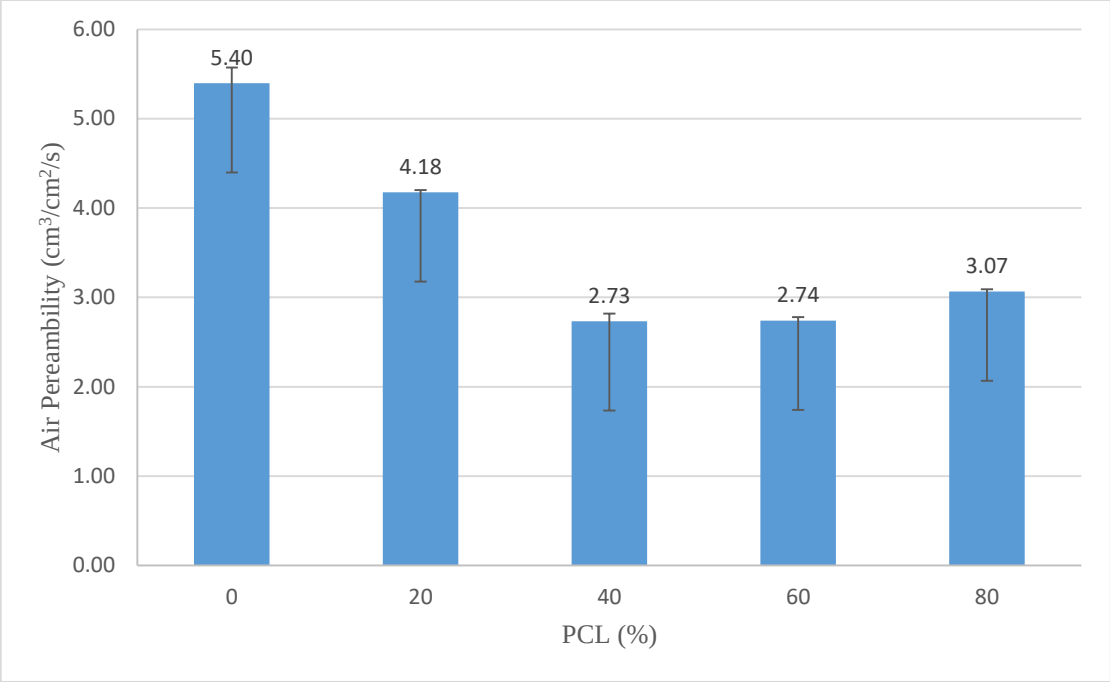

Figure 13: The relationship between air permeability and PCL percentage for porous PCL-PLA films

As shown in table 5, the porous PLA-PCL films showed reduction in air permeability compared with porous PLA films. To clarify, samples PL-PC2-N50 & PL-PC3-N50 showed reduction in air permeability by 49.44 % and 49.22% respectively compared with porous PLA with the same NaCl percentage. In fact, this result was expected because of the heterogeneous nature of the blends. This heterogeneity was resulted from immiscibility of the two polymers which consequentiality led to formation a phase separated system. Therefore, because of the polymers immiscibility, PCL formed small globules surrounded by disguised boundaries within the PLA matrix in sample PL-PC2-N50 & PL-PC3-N50. Thus, existence of PCL spherulites on the PLA matrices decreased the free volume available for gas diffusion.

On the other hand, influence of blending immiscibility was low in samples PL-PC1-N50 and PL-PC4-N50 because the concentration of one of the polymers was predominant while the another one represented a minor ratio. Thus, reduction on air permeability in sample PL-PC1-N50 & PL-PC4-N50 was lower compared with samples PL-PC2-N50 & PL-PC3-N50 because the effect of phase separation in this case was not strong enough to show its significant influence.

Indeed, decreasing in permeability for an immiscible polymers blend as a result of the phase separation was demonstrated before in several studies. De Sales et al. investigated the effect of phase- separation on the permeability of polyurethane and polymethacrylate blend. In this study, it was shown that when polymethacrylate percentage increased, the permeability decreased as a result of formation of phase separated system. Hence, it was demonstrated that phase separation led to reduction in the free volume available for gas diffusion [82]. In another study, it was proved that addition of small amount of thermotropic liquid crystal phosphorus to polyethylene terephthalate (PET) led to significant reduction on the gas permeability compared with pure PET. This result was also explained based on the incompatibility of the system. It was demonstrated in this study that liquid crystal phosphorus mesospheres , which were resulted from phase separation, formed impenetrable barriers. Thus, these impenetrable barriers represented impermeable regions that allowed the steady state permeation to only pass through tortuous path. Therefore, mesospheres formed in the phase-separated system reduce the overall gas permeability [83].

4.2.4. Influence of porogen concentration on the air permeability of porous PCL-PAL films

Incorporation of PCL whiten the polymeric matrices of PLA with 50 % NaCl showed significant improving in mechanical properties when PCL concentration reached 80%, as shown in sec 4.3. However, blending PCL with PLA also showed a change in the air permeability and films morphology because of the effect of polymers immiscibility. Hence, it was expected that added different compositions of NaCl in PCL-PLA blend would show change in the proportional relationship with air permeability compared with porous PLA films. Therefore, 10 % PEO and NaCl was added with different compositions to PCL-PLA blend, which composed of 80% PCL and 20 % PLA. Porosity, distribution of NaCl and the homogeneity of the films morphology were investigated through air permeability measurement.

Sample name	Air permeability ($cm^3/cm^2/s$)				
	Reading 1	Reading 2	Reading 3	Average reading	Standard deviation
PL-PC4-N50	3.08	3.08	3.04	3.07	0.02
PL-PC4-N70	3	3.4	3.3	3.23	0.2
PL-PC4-N100	4.55	4.55	4.58	4.56	0.017

Table 6: Air permeability of porous PCL/PLA (80%/20%) films with different NaCl percentages.

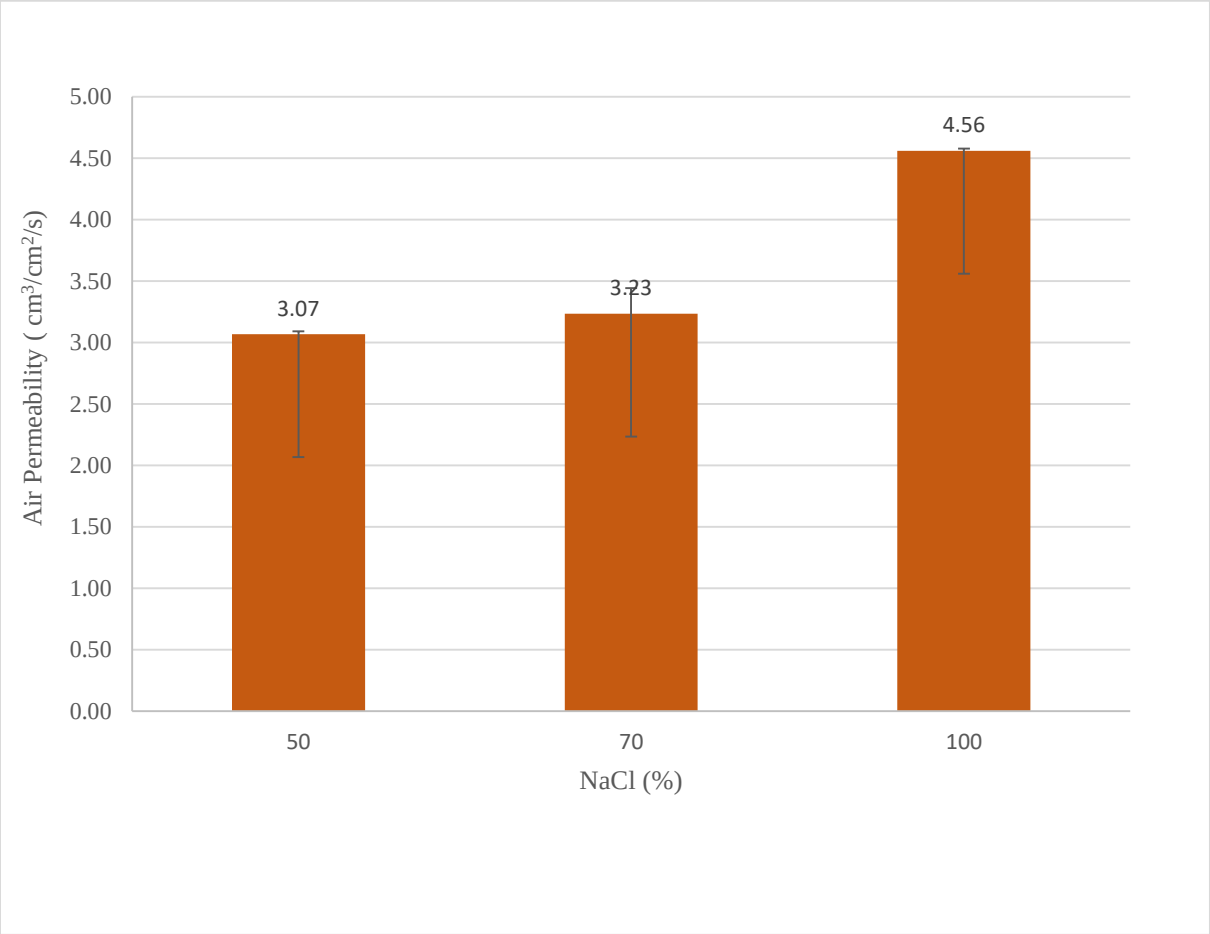

Figure 14: The relationship between air permeability of porous PCL-PLA membranes and NaCl percentages.

As shown in table 6, air permeability of porous PLA-PCL films increased when NaCl concentrations increased in contrast to porous PLA films behavior. In fact, the direct proportional relationship between the porosity and NaCl percentage in PLA-PCL blend indicated complete extraction of well dispersed NaCl particles form polymer matrices and absence of agglomerated particles. Therefore, when NaCl percentage increased, number of macro-pores increased, which enhanced air permeability. Thus, the results showed that the highest air permeability in porous PCL-PLA films achieved by adding 100 % NaCl in sample PL-PC4-N100, which indicated that this sample achieved the highest porosity. Indeed, well dispersion of NaCl in the blend matrices was resulted from the high affinity of PEO to PCL. This result is in a good agreement with previous studies for the same blend. Ezzati et al. reported that the maximum porosity of PLA, PCL and PEO (10: 50: 40) achieved when concentration of NaCl was 80% [79].

In addition to the dispersion of NaCl within the blend matrices, complete leaching out of NaCl form PCL-PLA films was resulted from the heterogeneous nature of the blend. This heterogeneity is resulted from the immiscibility between PLA and PCL, which led to formation of a phase separated system. In fact, phase separation between the polymers facilitated high water absorption and consequently enhanced NaCl solubility and extraction. The same explanation was concluded by Cai et al. during the interpreting the high efficiency of PCL-PLA blend as a drug delivery system compared with the two homopolymers. In this study, it was proved that releasing of the hydrophilic substance from the blend is more influential by bland morphology, which controls water absorption, rather than the drug hydrophilicity [84]. Furthermore, the hydrophobic nature of PCL facilitated water removing and the soluble NaCl from the polymeric matrices.

4.2.5. Comparison between air permeability in porous PLA films and porous PCL-PLA films

Influence of NaCl composition on the porosity of PCL-PLA films was different form its influence on the porosity of PLA films. Therefore, comparison between the effect of NaCl percentage on the air permeability of PLA films and PCL-PLA films was investigated.

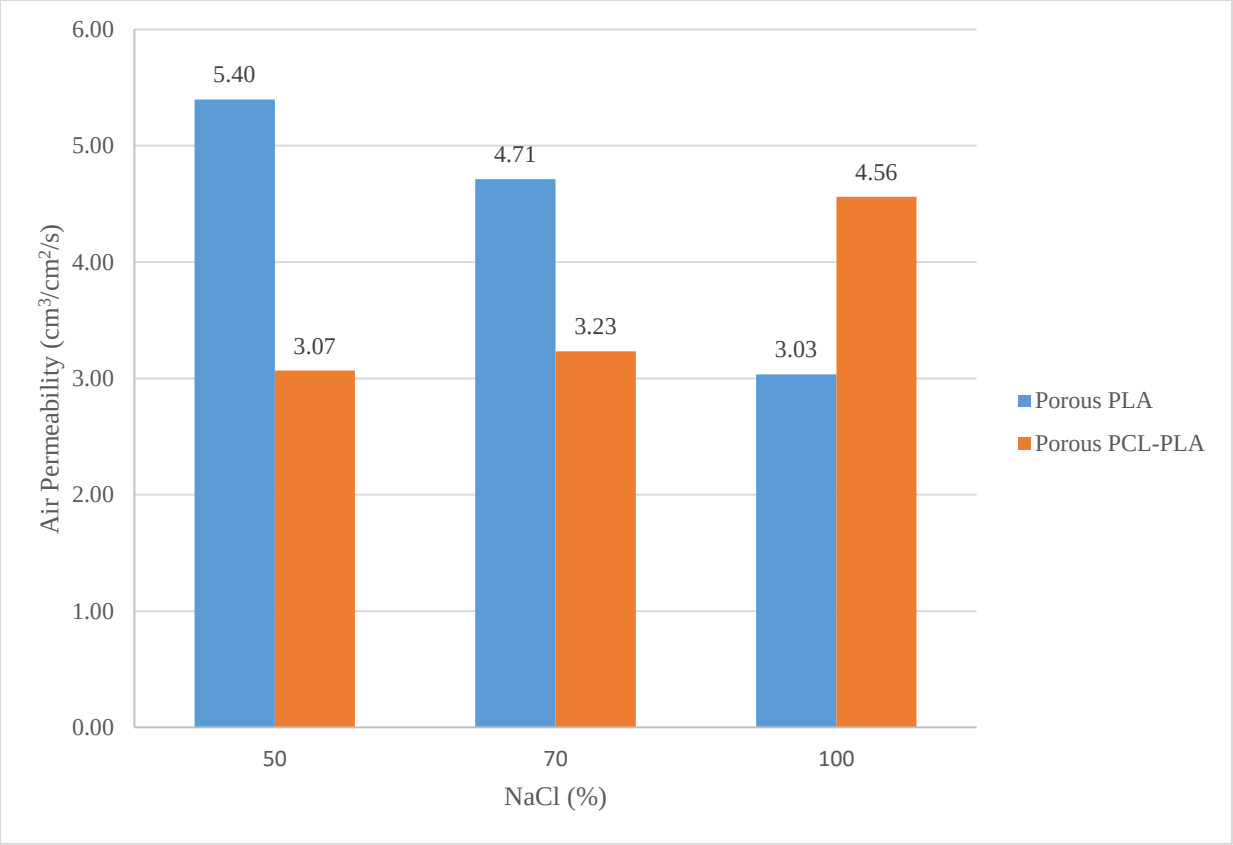

Figure 15: Comparison between the effect of NaCl percentage on air permeability of porous PLA and PCL-PLA films

As shown in Figure 15, porous PCL-PLA films showed slight reduction in air permeability compared with the porous PLA films at the same PEO and NaCl concentrations. This reduction was observed in the air permeability of samples PL-PC-N50 and PL-PC-N70 compared with samples PL-N50 and PL-N70. Indeed, this reduction appeared because PCL-PLA films contain lower number of the small pores, which resulted from PEO extraction, compared with porous PLA films. Number of small pores decreased in the blend because the affinity of PEO to PCL is higher than its affinity to PLA. This result is in a good agreement with literature since it was reported that the surface and interfacial tensions between PLA and PEO are lower than the surface and interfacial tensions between PCL and PEO. According to a previous work, surface tension for PCL /PEO and PLA/PEO blends at 25 °C are 10.14 and 1.16 mN/m respectively [79]. To explain, interfacial and surface tensions are essential parameters in controlling the segregation scale between the two polymers, which is a measurement of the space between clamped particles [85]. Therefore, high surface tensions between PCL and PEO enhanced their affinity and hindered its

complete extraction from PCL-PLA films. This result was proved by DSC, FTIR and TGA analysis. Accordingly, relatively small number of micropores were formed in the blend, which led to low interconnectivity in the porous film and consequently low air permeability. On the other hand, as a result of low surface tension between PLA and PEO, PEO was fully extracted form PLA matrices and led to formation of interconnected porous membranes due to large number of microspores.

However, this relationship changed at a high concentration of NaCl. On other words, sample PL-PC-N100 showed higher air permeability than sample PL-N100. In fact, this change resulted from the effect of the high number of macroproes, which are formed form complete extraction of NaCl particles, on enhancing air permeability with regardless to pores interconnectivity. To emphasize, sample PL-N100 contains low number of large pores, which were resulted from extraction of agglomerated NaCl particles. On the other hand, sample PL-PC-N100 contains large number of small pores, which were resulted from extraction of well dispersed NaCl particles. Thus, non-extracted PEO did not affect air permeability at high NaCl percentage.

4.3. Mechanical properties

Mechanical properties measurement was the second major factor after air permeability in evaluating the suitability of the films for food packaging applications. Therefore, studying the effect of NaCl percentage on the mechanical properties of porous PLA and PLA-PCL films was mandatory. In addition, determination of the optimum PCL percentage was based on the mechanical properties measurement for porous films with different PLA and PCL compositions.

4.3.1. Influence of porogen concentration on the mechanical properties of porous PLA films

The effect of NaCl percentage on the mechanical parameters of porous PLA films was investigated. Mechanical properties were discussed based on plotting the stress –strain for each sample. It was found that maximum elongation (α_m), maximum nominal force (f^*_m) and maximum energy needed to reach the maximum nominal force and maximum elongation (E_m) were significantly affected by the developed porosity and the remaining NaCl residuals in PLA matrices.

Sample name	α_m	f_m^* (Nmm^{-2})	E_m (J mm^{-1})
Neat PLA	1.13	27.54	3.1
PL-N50	1.08	4.1	1.08
PL-N70	1.09	5.35	1.1
PL-N100	1.15	7.18	1.15

Table 7: Mechanical properties of porous PLA membranes with different NaCl percentages.

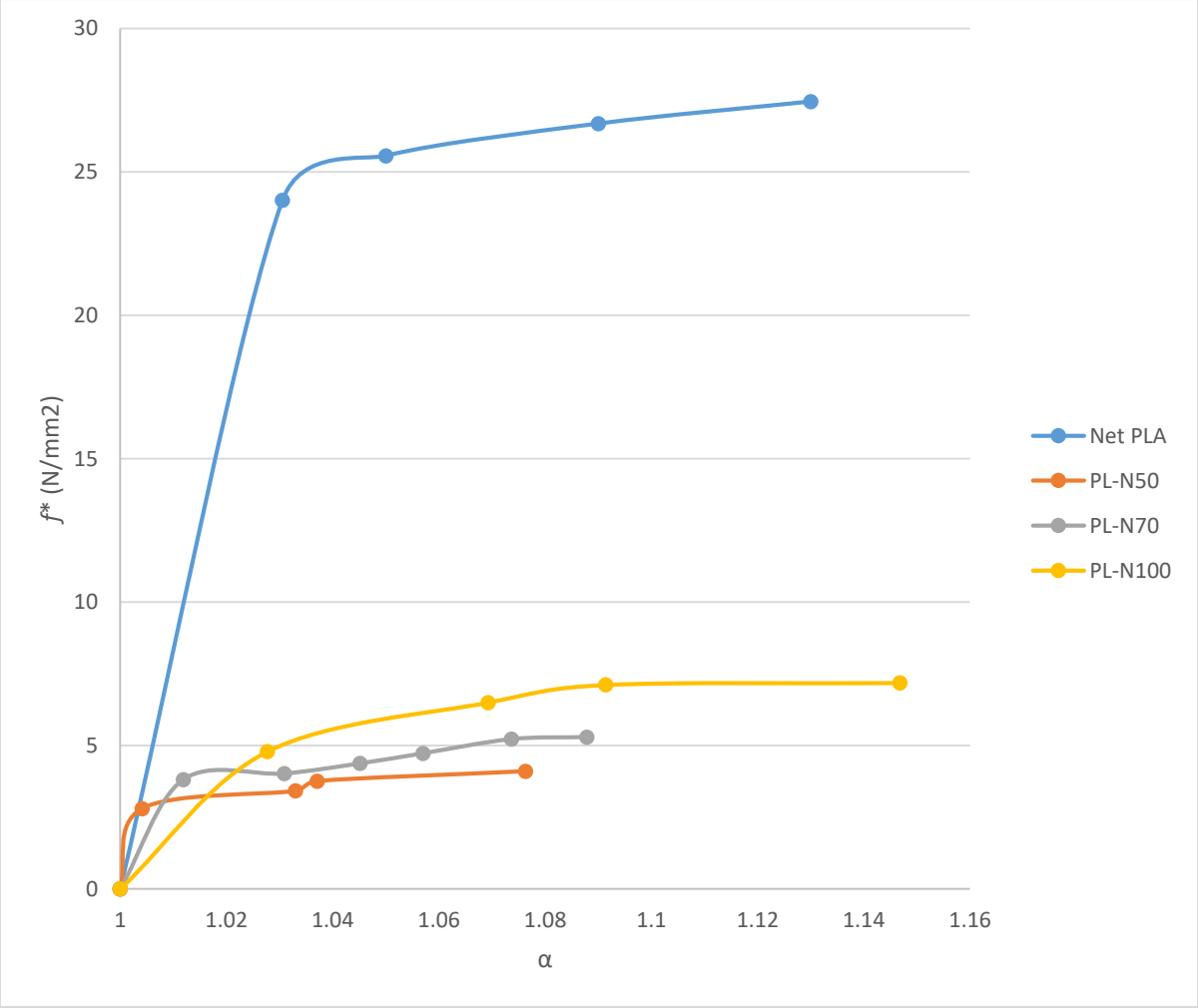

Figure16: Stress-strain graph for porous PLA films with different NaCl percentages

As shown in table 7, developed porosity by leaching out PEO and NaCl affected the mechanical properties of PLA. In fact, α_m, f^*_m and E_m decreased for all the porous samples compared with neat PLA. However, this reduction was inversely proportional with NaCl percentage. To clarify,

f^*_m decreased by 85.11 %, 80.75 % and 73.92% for samples PL-N50, PL-N70 and PL-N100 respectively compared with neat PLA while E_m decreased for all the samples with no significant difference. In addition, α_m slightly decreased for sample PL-N50 and PL-N70 while no change was observed for sample PL-N100 compared with neat PLA.

Slight reducing in f^*_m , E_m and α_m for sample PL-N50 resulted from the effect of porosity on the mechanical strength of the film. Indeed, pores structure and interconnectivity enhanced the microcracks growth during scratching as a result of localized concentration of the stress. Thus, stress localization resulted in porous films because pores represent week point within the film structure. Furthermore, reduction in the mechanical strength was observed for porous PLA films because of the effect of irregular porous morphology on enhancing the films fragmentation. The same result was demonstrated before by Sawalhe et al., and Riddle et al. who investigated the relationship between porosity and mechanical properties of porous PLA [86, 87].

On the other hand, the result showed that f^*_m, E_m and α_m slightly increased when the NaCl percentage increased and led to formation of larger pores due to its agglomeration. This result was expected because porous material with high pores volumes, as shown by the BET results, can withstand high micro-deformation during stretching compared with porous material with low pore volume. In fact, increasing in the cracking at high pore volume is resulted from withstanding further deformation in the material after the cracking reaches the pores terminals. This result is proved by increasing in the crystallinity degree when NaCl percentage increased, as shown by DSC results. Therefore, samples PL-N70 and PL-N100 showed higher f^*_m, E_m and α_m than PL-N50. The same result was demonstrated by Buzimov et al. during studying the effect of zirconia on the mechanical properties of ceramic [88].

Additionally, direct proportional relationship between NaCl percentage and the mechanical parameters may indicate the presence of some minor NaCl residuals within PLA matrices. To explain, after leaching out NaCl from the plyometric matrix, the remaining particles formed robust bonds with the plyometric matrix. Thus, the formed bonds between NaCl and PLA led to increase the maximum elongation at break. The observed effect of NaCl on PLA elongation in a good agreement with literature. In fact, interaction between PLA and NaCl and its effect on PLA elongation were demonstrated before by Roberson et al. during studying the effect of adding NaCl, as an inorganic filler, on PLA matrix [89].

4.3.2. Influence of PCL concentration on the mechanical properties of porous PLA films

PLA is characterized by high modulus of elasticity and high stiffness. Therefore, in order to overcome this limitation, PCL was blended with PLA to reduce its brittleness and to improve its overall mechanical performance as a food packaging. Indeed, PCL is well known by its high elasticity, which results from its low glass temperature. Hence, in order to investigate the effect of PCL on the mechanical properties of porous membranes, PCL was blended with different percentages with PLA while NaCl percentage and PEO percentages remained constants at 50 % and 10 % respectively for all the blends.

Sample name	α_m	f_m^* (N/mm^{-2})	E $_m$ (J mm^{-1})
PL-N50	1.08	4.1	1.08
PL-PC1-N50	1.03	7.67	0.13
PL-PC2-N50	1.03	8.45	0.24
PL-PC3-N50	1.09	6.89	0.33
PL-PC4-N50	1.22	6.78	1.31

Table 8: Mechanical properties of PLA-PCL blends at different PCL percentages.

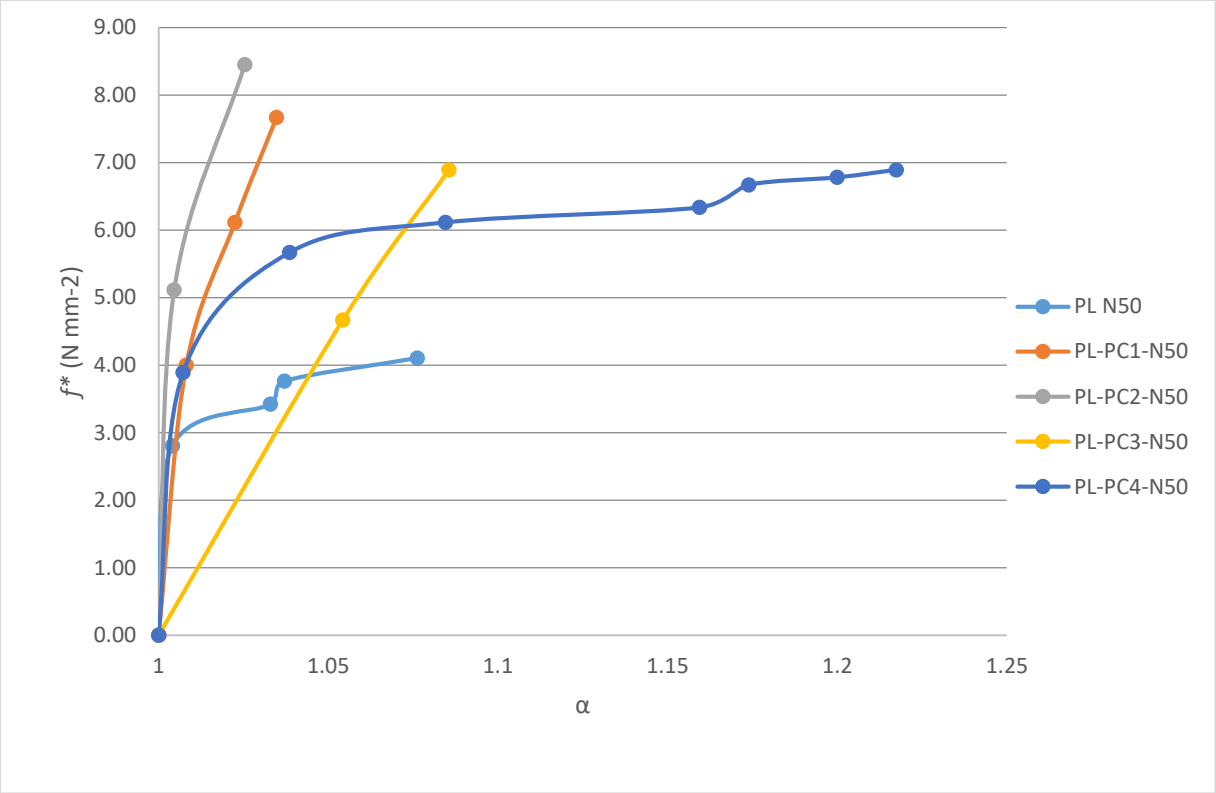

Figure 17: Stress –Strain graphs of porous PLA and PCL-PLA films with different PCL percentages.

As shown in table 8, samples PL-PC1-N50, PL-PC2-N50 & PL-PC3-N50 did not show improvement on the mechanical properties compared with sample PL-N50. In contrast, reduction in α_m was observed by 4.8 % for sample PL-PC1-N50 & PL-PC2-N50 while sample PL-PC3-N50 showed no change on α_m compared with sample PL-N50. In addition, f_m increased by 87.1%, 98.7 % and 68% for samples PL-PC1-N50, PL-PC2-N50 and PL-PC3-N50 respectively compared with sample PL-N50 while the corresponded E_m showed reduction by 87.96%, 77.78 % and 69.44% for the same samples respectively.

On the other hand, PL-PC4-N50 showed increasing in α_m by 18.46 % In addition, E_m and f_m increased by 21.3% , 65.4% respectively for the same sample. Accordingly, it is obvious that addition of PCL had negative effect on mechanical parameters of PLA until its percentage reached 80%. Indeed, deteriorative effect of PCL at these concentrations on the mechanical properties of PLA was resulted from immiscibility of PCL and PLA, which led to formation of phase separated systems. As shown in Figure 9, phase separation is obvious in membranes morphology through

observing PCL spherulitrs, which are distributed whiten PLA matrix. These large PCL spherulites led to local stress concentration that enhanced fast fracture as demonstrated by Takayama et al. [90]. This result also is in good agreement with the previous studies for the same blend in literature. In fact, the same result was observed by Wachirahuttapong, et al. during studying the mechanical properties of PCL-PLA [91].

Improvement impact of PCL on the mechanical properties of PLA appeared at percentage of 80 %. Thus, this result indicated that the influence of phase separation on this blend was insignificant because PCL ratio was predominant. Accordingly, increasing of α_m and E_m indicated the flexible elastomer nature and the high strength of PCL in the film. The same result observed by Semba et al., who proved that 70% PCL with 30 % PLA showed considerable increasing in elongation at break [92]. Furthermore, increasing of f_m indicated the low porosity of the blend compared with the porosity of PLA with same NaCl percentage. Accordingly, blend of 80% PCL and 20% PLA was chosen to study the effect of NaCl compositions on porosity and air permeability.

4.3.3. Influence of porogen concentration on the mechanical properties of porous PCL-PLA films

The blend contains 80% PLC and 20% PLA was chosen to study the effect of NaCl percentage on porosity and permeability due to its improved mechanical properties compared with the other blends with low PCL percentage. Therefore, the effect of NaCl percentage on the mechanical properties also was also investigated.

Sample name	α_m	f_m (N mm^{-2})	E m (J mm^{-1})
PL-PC4 -N50	1.22	6.78	1.3
PL-PC4-N70	1.17	3.36	0.61
PL-PC4-N100	1.14	2.35	0.33

Table 9: Mechanical properties of porous PCL-PLA with different NaCl percentages

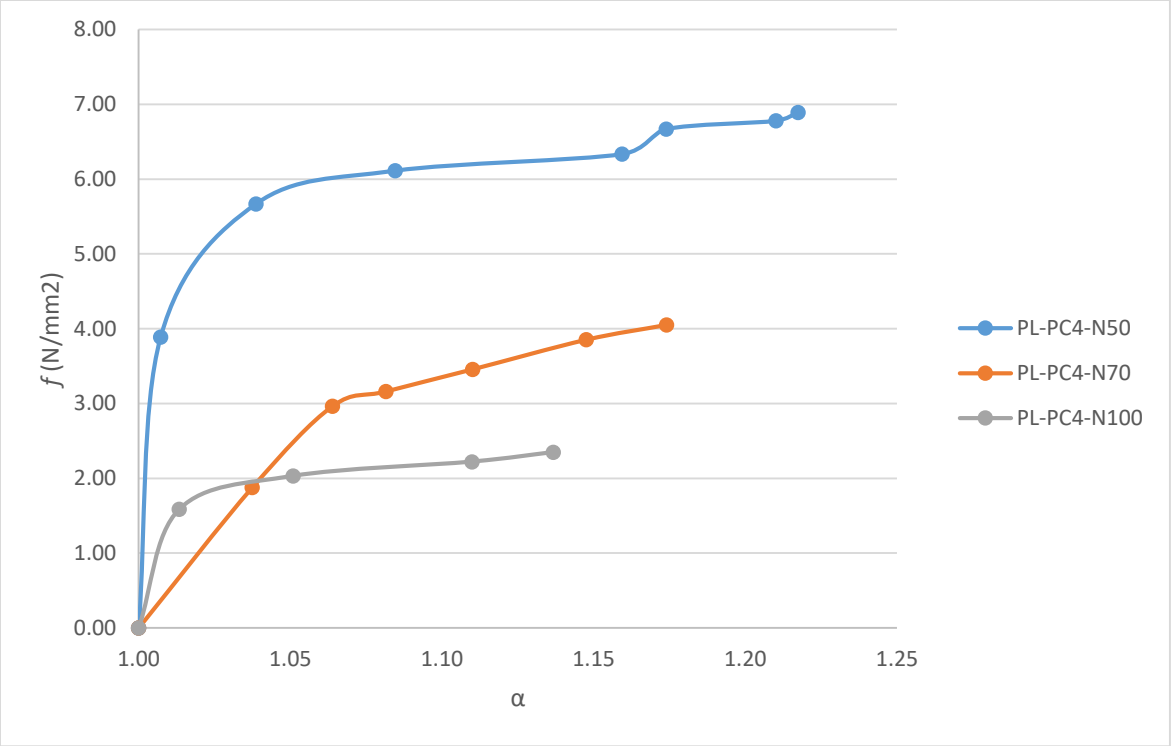

Figure 18: Stress-Strain Curves for porous PCL-PLA films with different NaCl percentages

In contract to the porous PLA membrane, increasing on NaCl % led to increase the porosity of PCL-PLA blend, which indicated complete leaching out of NaCl. Hence, α_m, f_m, and the corresponded E_m decreased with increasing on NaCl percentage. In fact, Gupta et al. demonstrated the same result for porous PCL scaffold [93]. Furthermore, Sun et al. also proved that tensile strength of porous PLA-PCL blend decreased compared with pure PCL [94]. This result was explained by effect of porosity on the continuity of the plyometric structure. To clarify, it was shown that the high porosity led to brittle structure because pores form weak points within the membrane morphology. Therefore, when the membrane exposed to the tension force, pores stretched easily and reduced the tensile strength. This phenomenon strongly affects the films mechanical properties when NaCl percentage increased and consequentiality the porosity increased.

4.4. Thermal properties

4.4.1. Differential scanning calorimetry analysis (DSC)

4.4.1.1. Influence of porogen concentration on the DSC analysis of porous PLA films

Thermal behavior is an essential factor in evaluate food packaging quality. Furthermore, effect of porosity of crystallinity degree on the porous films was a key factor in explaining the relationship between porosity, permeability and mechanical properties. Therefore, DSC were carried out to investigate the effect of porosity on the thermal behavior of the porous films at different NaCl percentages

Sample name	T_g °C	T_{cc} °C	T_m °C	ΔH_m PLA (J/g)	X_c (%) PLA
Neat PLA	67.45	NA	151.55	17.73	19.06
PL-N50	68.83	96.55	152.91	9.83	10.57
PL-N70	68	94.48	152.41	14.44	15.53
PL-N100	67.55	96.43	152.7	18.21	19.58

Table 10: Thermal properties of neat and porous PLA films with different NaCl percentage

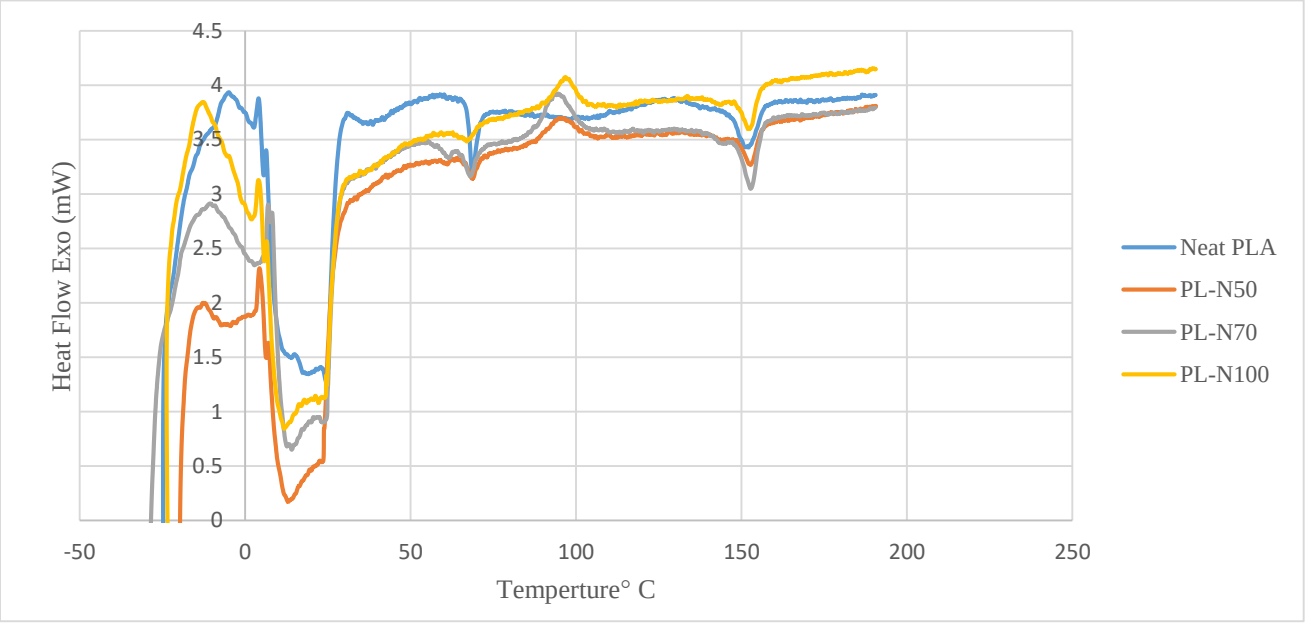

Figure19: DSC graphs for neat and porous PLA films

As illustrated in the DSC curves in figure 19, glass transition temperature (T_g) of neat PLA showed at 67.45° C while T_g for porous PLA films showed at 68.6, 68 and 67.55° C for samples PL-N50, PL-N70 and PL-N100 respectively. Hence, it is obvious that there is no significant difference was shown between the T_g of neat PLA and the porous samples. This result indicated that the porosity did not affect the glass transition behavior of the PLA.

On the other hand, it was observed that the developed porosity shown significant effect on the crystallinity degree. The crystallinity degree (X_c %) of neat PLA was 19.06% while X_c (%) for samples PN-N50, PL-N70 and PL-N100 were 10.57 %, 15.35 % and 19. 58% respectively. Thus, reduction in crystallinity for sample PL-N50 was resulted from the effect of porosity in the hindering the crystallization kinetic. In fact, this effect was resulted from confined geometry of pores, which is formed by the developed porosity within the polymeric structure. Thus, the highly distributed large number of small pores hindered and interrupted the re-arrangement of the plyometric chains during crystallinity due to the high confinement degree. On other words, existence of pores within the polymeric matrix led to interfere between the pore confinement and the crystal growth during crystallinity. The same result was proved by Huang et al., who demonstrated the effect of porosity, which is developed by salting out –casting technique, on PLA crystallinity [95].

However, increasing in X_c % was observed for sample PL-N70 followed by sample PL-N100 compared with sample PL-50. Indeed, sample PL-N100 showed the same X_c percentage of neat PLA. The direct proportional relationship between X_c % and NaCl percentage was resulted from the effect of agglomerated particles in the pores size. To clarify, increasing in the pores size reduced the influence of confinement effect and provided larger space for polymeric chains to re-arrange in thermodynamically favorable order, which increased crystallinity degree. The similar result was found before by Shin et al. during studying the effect of cylindrical nano-pores on the crystallinity of polyethylene [96]. In this study, it was demonstrated that increasing in cylindrical pores size led to comparable increase crystallinity. For the same reason, reduction in enthalpy of melting (ΔH_m) was observed for sample PL-N50 followed by slight increasing for sample PL-N70 and PL-N100 respectively.

Furthermore, existence of non-leached agglomerated NaCl within the plyometric matrices of samples PL-N70 and PL-N100 is another possible explanation of the observed increasing in

crystallinity degree compared with sample PL-N50 in spite of the developed porosity. This result is in a good agreement with literature with regard to the investigation of the effect of inorganic filler on the crystallinity degree. In fact, Yu et al. demonstrated the same result through studying the effect of adding talc, as an inorganic filler, on increasing crystallinity degree percentage of PLA [97]. Moreover, formation of lactic acid oligomers as a result of PLA degradation during hydrolysis also contributed to increasing in the polymer crystallinity [98].

4.4.1.2. Influence of porogen concertation on the DSC analysis of PCL-PLA films

As discussed previously, blend of 80% PCL and 20% was chosen to study the effect of NaCl percentage on the porosity. It was expected that the effect of porosity on the thermal properties of the porous PCL-PLA films will be different from its effect on porous PLA films. The difference was expected to result from the lack of agglomerated NaCl particles whiten the blend matrix and high affinity between PCL and PEO. Therefore, studying the effect on NaCl percentages on the thermal properties of PCL-PLA blend was carried out by DSC analysis.

Sample name	T_m °C	ΔH_m PLA (J/g)	X_c (%) PCL
Neat PCL-PLA	61.78	68.85	61.69
PL-PC4-N50	61.67	41.36	37.06
PL-PC4-N70	64.02	73.68	66.02
PL-PC4-N100	65.1	52.49	47.03

Table 11: Thermal properties of neat and porous PCL-PLA films. with different NaCl percentages

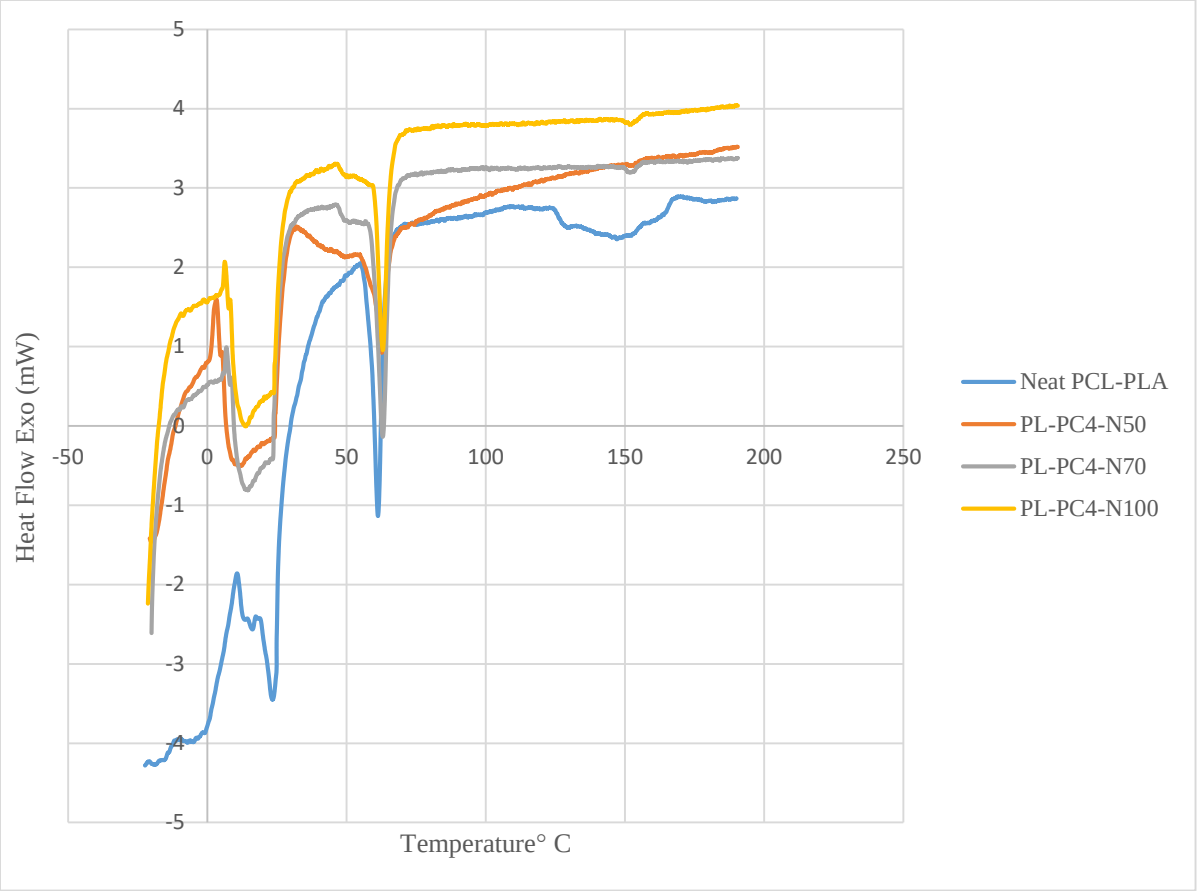

Figure 20: DCS graphs for neat and porous PCL-PLA films

As shown in DSC curves in figure 20, T_g of PLA in the blend was not observed in the DSC curves of all PCL-PLA films due to its overlapping with T_m of PCL. In fact, T_m of PCL is 57.32 °C and it is closed to the T_g of PLA as showed on the DSC of neat PLA film. T_m for samples PL-PC-N50, PL-PC4-N70 and PL-PC4-N100 were 61.67°C, 64.02°C and 65.1°C respectively. Thus, no significant difference was observed in T_m between the neat PCL-PLA and the porous samples. In addition, T_g of PCL is -61.5 °C, as reported in the literature, and therefore, it was not observed under the used conditions [91].

Porous and neat PCL-PLA membranes were characterized with high crystallinity compared with neat and porous PLA membranes with regardless to the NaCl percentage and porosity. This result was expected because PCL is a semi-crystalline polymer and it represented the major percentage in the blend, which enhanced the overall crystallinity [91]. Neat PCL-PLA, which is composed of 80% PCL and 20 %PLA, showed a crystallinity degree of 61.69 %, while PL-PC40-N50, PL-

PC40-N70 and PL-PC-N100 showed crystallinity degrees of 37.06 %, 66.02% and 47.03& respectively.

The DSC curves of porous PCL/PLA indicated the immiscibility of PEO with PCL and also indicated incomplete extraction of PEO from the membranes. Two crystallization peaks were observed in the DSC curves of porous PCL-PLA samples. The first peak appeared with low intensity at 50 °C and it represented PEO crystallization peak. Meanwhile, the second broad peak appeared at 60º C and it represented PCL crystallization peak. The same result was observed before by Huang et al. during studying the effect of using PEO as a porogenic agent on PCL crystallinity [99]. Sample PL-PC4-N50 showed reduction in crystallinity compared with neat PCL-PAL as a result of the effect of porosity in restricting the chains movement. The same result was demonstrated by Yin et al., who proved the effect of porosity on reducing crystallinity [100]. However, degree of crystallinity of PCL showed significant increasing form 37.06 % in sample PL-PC4-N50 to 66.02 % in sample PL-PC4-N70 in spite of increasing in porosity. This result indicated that increasing of NaCl composition led to increase the affinity PEO to PCL [74]. In fact, high affinity between PEO and PCL resulted in increasing the stability of the co-continuous PCL/PEO binary system that enhanced chain re-arrangement. Moreover, PEO during its partial extraction and before dissolution enhanced the rearrangement of PCL chains in thermodynamically favorable order [101]. Therefore, significant increasing in the crystallinity of sample PL-PC4-N70 was observed compared with sample PL-PC4 N50. For the same reason, crystallinity degree of sample PL-PC4-N100 was higher than sample PL-PC4-N50. However, PL-PC4-N100 showed crystallinity degree of 44.03 %, which is lower than sample PL-PC4-N70 although the higher NaCl percentage. This result indicated that the effect of porosity in reducing crystallinity was more influential than the effect of PEO in enhancing chain mobility.

However, due to the complexity of the investigated system, which is resulted from the presence of three different polymers, and their ability to interact with each other distantly, other interpretations maybe exhibited and additional characterization methods such as x-ray diffraction maybe required. Unfortunately, this further investigation is beyond the scope of this research.

4.4.2. Thermogravimetric analysis (TGA)

4.4.2.1. Influence of porogen concentration on TGA of porous PLA films

In order to study the effect of porosity on the thermal stability of the porous films, TGA analysis was carried out for porous PLA films at different NaCl percentages.

Sample name	T_{onset}(°C)	T_{max} (°C)	T_f (°C)
Neat PLA	319.39	351.64	387.5
PL-N50	307.60	341.71	380.61
PL-N70	297.74	339.91	393.75
PL-N100	310.06	341.93	406

Table 12: Characteristic temperatures for neat PLA and porous PLA films with different NaCl percentages

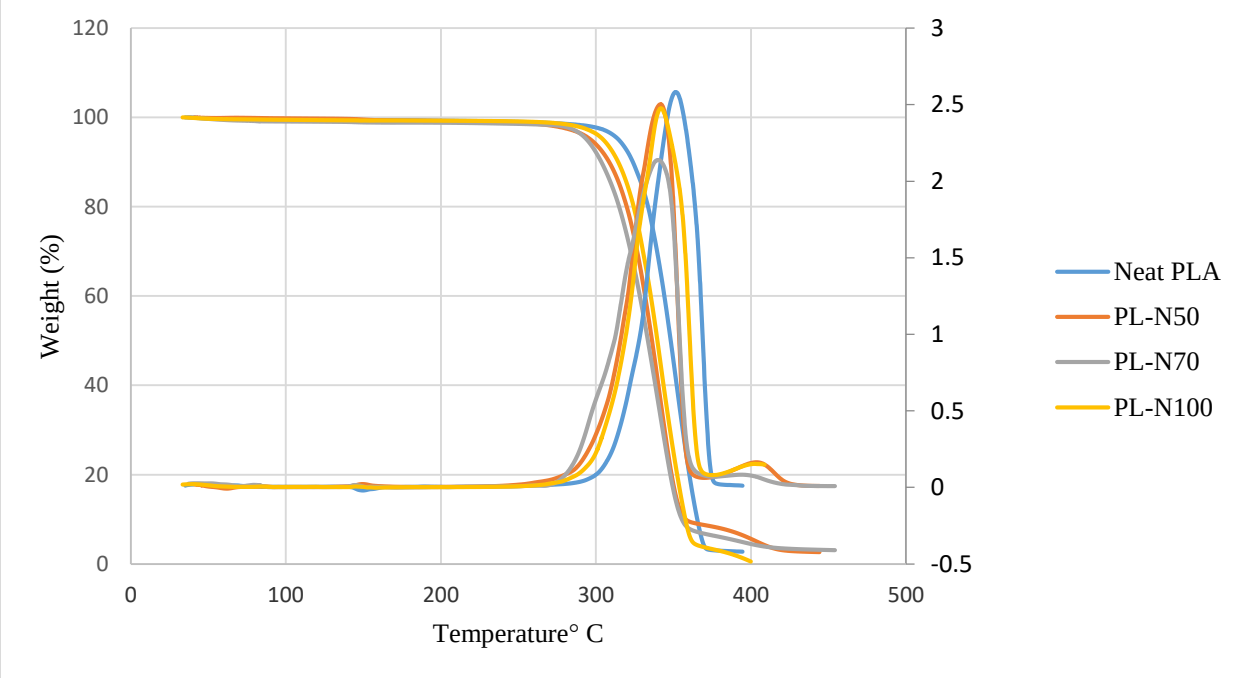

Figure 21: TGA-DTG thermogram for neat PLA and porous PLA films

The initial temperature of degradation (T_{onset}), the temperature of the maximum degradation at 50% weight loss (T_{max}) and temperature of final degradation (T_f) were obtained from TGA and derivative thermogravimetric (DTG) graphs for porous PLA and porous PCL-PLA films. As shown in table 12, T_{onset} and T_{max} for all the samples showed lower values compared with neat PLA. Decreasing in T_{onset} and T_{max} indicated reduction in thermal stability of the porous films, which resulted from the developed porosity.

Sample PL-N50 showed reduction in T_f compared with neat PLA while sample PL-N70 and PL-N100 showed T_f with relatively higher values. In fact, reduction on T_f of sample PL-N50 resulted from its high porosity that enhanced the final degradation to occur at relatively lower temperature compared with neat PLA. On the other hand, NaCl particles hindered chains mobility during degradation of samples PL-N70 and PL-N100, as discussed previously. To clarify, hindering chains mobility by non-agglomerated NaCl particles increased the thermal resistance of the samples and allowed final degradation to occur at relatively higher temperature compared with neat PLA. The same result observed before Kiziltay et al., who demonstrated that the interaction between the non-leached out NaCl and poly(ester-urethane) scaffold improved it thermal stability [102].

However, no chemical shifting or new peaks were observed in the DTG graphs of porous PLA films compared with neat PLA film. This result indicated that the developed porosity did not affect the degradation rate of PLA.

4.4.2.2. Influence of porogen concentration on TGA of porous PCL-PLA films

Thermal stability of porous PCL-PLA films was determined by using TGA analysis. However, it this case, the results express the thermal degradation of PCL, PLA and PEO separately because these polymers are immiscible.

Sample name	T_{onset} (°C)			T_{max} (°C)			T_f (°C)		
	PCL	PLA	PEO	PCL	PLA	PEO	PCL	PLA	PEO
Neat PCL-PLA	372.70	328.76	NA	409.34	345.52	NA	447	362.5	NA
PL-PC4-N50	378.56	324.66	309.47	413.95	330.87	316.49	491.67	352	324.66
PL-PC-N100	374.16	323	301.57	412.10	325.59	315	493.7	337	323

Table 13: Characteristic temperatures for neat and porous PCL-PLA films with different NaCl percentages

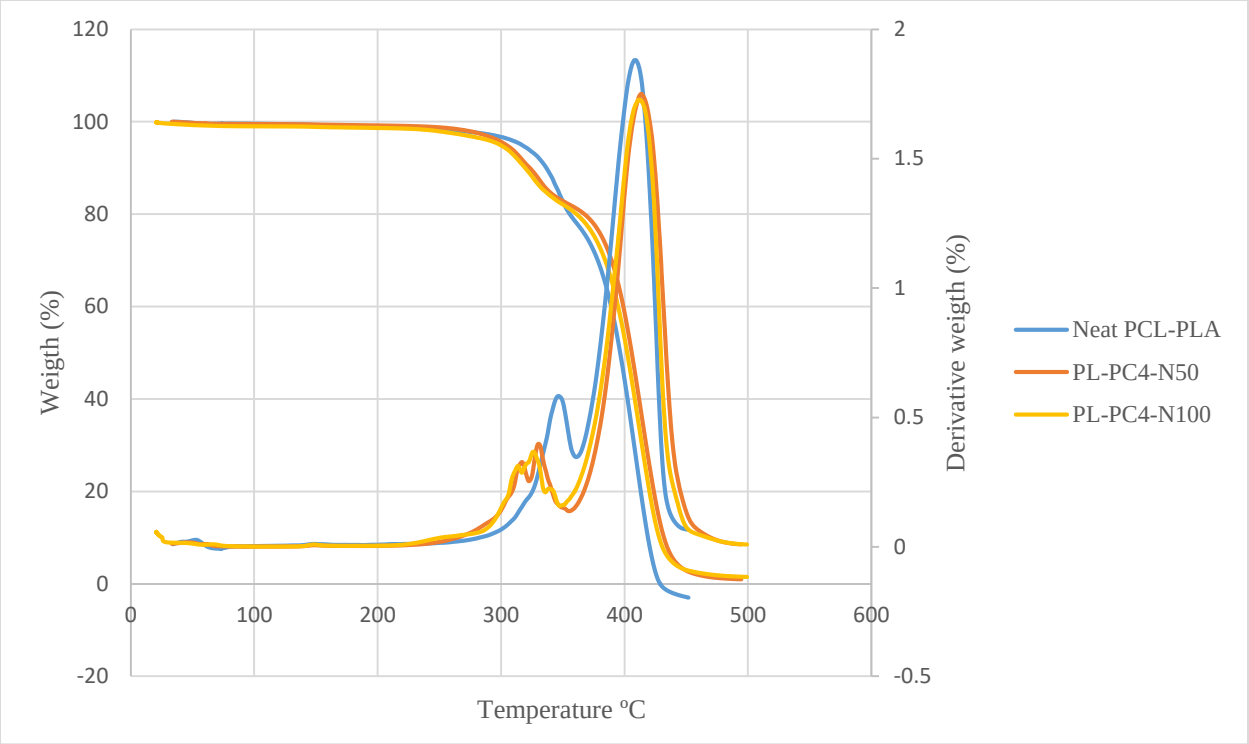

Figure 22: TGA- DTG thermogram for neat PCL-PLA and porous PCL-PLA films

As shown in figure 22, two peaks were observed in DTG of neat PCL-PLA sample, which indicated the immiscibility between the polymers. Moreover, three peaks appeared in DTG graphs of porous PCL-PLA films, which confirmed the incomplete leaching out of PEO. This observation also indicated immiscibility between PEO and both PLA and PCL. In addition, reduction of T_{onset}, T_{max} and T_{f} of PLA when NaCl increased was observed because of the effect of porosity on reducing thermal stability. On the other hand, T_{onest}, T_{max} and T_{f} of PCL increased with NaCl increased, which confirmed the effect of NaCl on enhancement the affinity of PEO and PCL and the consequent plasticization effect as discussed previously. Therefore, reinforcement of thermal stability for PCL was observed for the porous samples compared with PCL in neat PCL-PLA sample. In fact, thermal stability enhancement of the plasticized PCL was demonstrated before by Parra et al [103].

4.5. Barrier properties

4.5.1. Oxygen transmission rate (O_2TR) of porous PLA and PCL-PLA films

Oxygen transmission rate is an important factor is design of fresh food packaging. Therefore, O_2TR was measuring for all the porous films to investigate the effect of the developed porosity on enhancing the films breathability.

Sample composition	O_2TR (c.c/m^2.d.atm)	Increasing in O_2TR (%)
Neat PLA	950	_
PL-N50	4540	377.89
PL-N70	3920	312.63
PL-N100	3040	220.00
PL-PC4-N50	3210	237.89
PL-PC4-N70	4040	325.26
PL-PC4-N100	4540	377.89

Table 14: Oxygen transmission rates for neat PLA film and porous PLA and PCL-PLA films

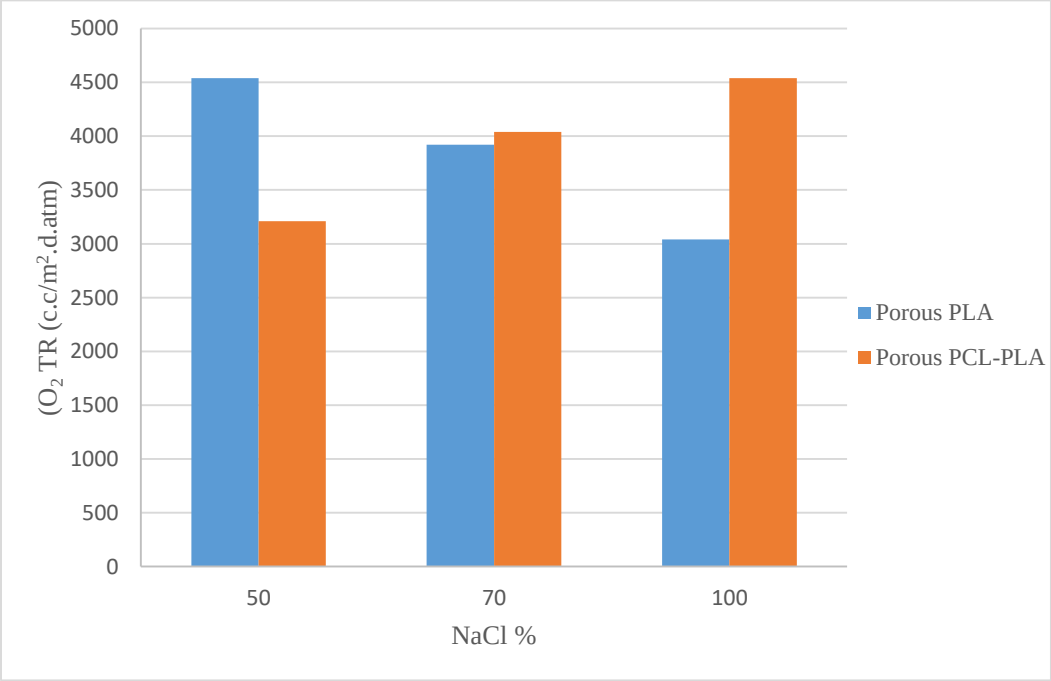

Figure 23: Effect of NaCl percentage on oxygen transmission rates for porous PLA and PCL-PLA films

Gas exchanges through permeable membrane by diffusion mechanism. Indeed, partial pressure gradient across the membrane acts as a driven force for gas transportation from one side to another. Hence, gas transportation starts by sorption of the gas on the surface which is exposed to medium that contains high gas concentration followed by desorption of the gas from the opposite surface, which is exposed to the medium contains lower gas concentration. This process lasts until reaching steady state condition.

In fact, gas exchange through a porous polymeric film is governed by two parameters, which are the permeability of polymer material and the developed porosity. However, according to the nature of polymeric material and the pores number, one parameter might be more predominant in controlling gas transfer than the anther one. To clarify, when the polymer is characterized by high barrier properties and it is modified with high number of pores, gas permeability is only governed by transferring through the pores. Thus, gas permeability through the polymer matrix in this case is neglected. On the other hand, when the polymer's barrier properties are moderate or its porosity is low, gas permeation is governed by both permeability within the polymer matrix and the pores. With regard to PLA, it is characterized by moderate O_2TR that is intermediate between polyethylene terephthalate and polystyrene. Therefore, in order to evaluate the total gas permeability for the porous PLA membranes, both gas diffusion through proses and plyometric matrix should be taken in consideration [12, 104].

Diffusion of gases through the pores is depended on the distribution, shape, number and interconnectivity of pores. Therefore, as expected form the air permeability, sample PL-N50 showed the highest O_2TR due to high number of interconnected pores. Indeed, sample PL-N50 showed increasing by 377.89 % in O_2TR compared with O_2TR of neat PLA followed by samples PL-N70 and PL-N100, which showed increasing by 312.26 % and 220 % respectively. As expected from the previous tests, reduction in convective gas flow in samples PL-N70 and PL-N100 compared with sample PL-N50 was resulted from the decreasing in number of pores and increasing in their volume.

Furthermore, reducing in diffusivity through PLA matrices in samples PL-N70 and PL-N100 also was resulted from the existence of NaCl residuals and the the related high crystallinity as proved by DSC analysis. In fact, decreasing in oxygen permeability because of the effect of inorganic filler in the polymeric films was reported before in several studies. For example, Huang et al.

observed significant reduction in oxygen permeability of PLA after loading with low percentage graphene oxide [105]. Moreover, it was found that increasing in PLA crystallinity reduced oxygen permeability because it hinders diffusion of the gas molecules within the crystalline domain. The similar result was proved by Cougneau et al. who demonstrated reduction in diffusivity and solubility coefficients of oxygen with increasing in PLA crystallinity [106]. Therefore, diffusivity of O_2 in PLA decreased when NaCl percentage increased.

On the other hand, O_2TR of porous PCL-PLA membranes increased when NaCl percentage increased. Indeed, the highest O_2TR value showed in sample PL-PC4 N100, which increased by 377.89 % compared with neat PLA while samples PL-PC4 N70 and PL-PC4 N50 showed increasing in O_2TR by 325.26% and 237.87% respectively. Hence, high O_2TR that showed with highest NaCl percentage indicated high porosity, which is developed form the high dispersion of NaCl particles within the plyometric matrices. In contrast to porous PLA samples, increasing in crystallinity in sample PL-PC4-N70 did not affect the permeability. This observation showed because of the existence of large number of pores, which were resulted from complete leaching out of the dispersed NaCl particles. Consequentiality, increasing of crystallinity degree, which is resulted from the presence of PEO, did not affect O_2TR.

All the samples showed O_2TRs that are within the acceptable range of O_2TR for breathable packaging material for several fruits and vegetables. For instance, Lucera et al. proved that micro-perforated polypropylene film with O_2 TR of 2076 cm^3/m^2.day was a suitable to preserve cauliflower [107]. Moreover, Pan et. al demonstrated increasing in the shelf life of fresh –cut bok choy after stored under polyethylene film with O_2TR of 3200 cm^3/m^2/day in 5 ºC. In this study, the packaging showed improvement in the weight loss, chlorophyll content and color of the product because of the film ability to modify the atmospheric composition inside the packaging [108].

4.5.2. Water vapor transmission rate (WVTR)

4.5.2.1. Water vapor transmission rate of porous PLA films

Water vapor transmission rate is another important parameter in food packaging development because water vapor is a major product form fresh food respiration reaction. Therefore, if the food packaging film does not permeable for water vapor, food deterioration and microbial growth will occur as a result of water vapor accumulation inside the packaging headspace. Hence, WVTR was measured for all the porous samples with different NaCl percentages.

Sample name	WVTR (g/d.m^2)
Neat PLA	78.93
PL-N50	327.73
PL-N70	324.13
PL-N100	315.73

Table 15: Water vapor transmission rate for neat and porous PLA films with different NaCl percentages

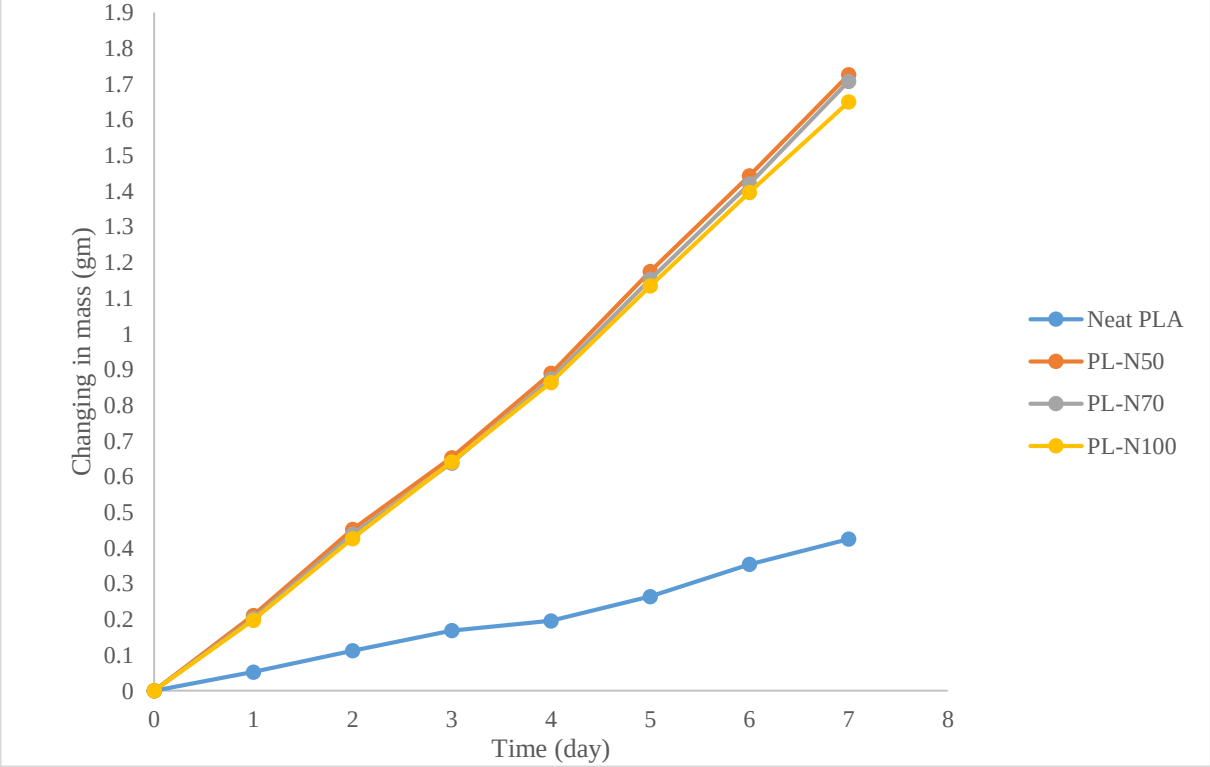

Figure 24: Water vapor transmission rate for neat and porous PLA films

As shown in table 15, water vapor transmission rate (WVTR) for sample PL-N50 showed the highest value compared with samples PL-N70 and PL-N100 as a result of high distribution of small pores within the polymeric matrix. In fact, WVTR for sample PL-N50 increased by 315.22 % compared with neat PLA followed by samples PL-N70 and PL-N100 , which showed increasing by 310. 65 % and 300 % respectively.

As discussed previously, water vapor permeability decreased for samples PL-N70 and PL-N100 compared with sample PL-N50 because of lower number of pores resulted from the agglomerated NaCl particles. Consequentially, decreasing of number and distribution of pores reduced the cross section available for diffusion and increased the diffusion path length, which reduced WVRT. Additionally, water solubility within the polymer matrix also reduced when crystallinity increased because water solubility in the crystal region is lower than its solubility in the amorphous region [109]. Thus, increasing in crystallinity associated with increasing in NaCl percentage enhanced WVTR reduction.

4.5.2.2. Water vapor transmission rate of porous PCL-PLA films

As a result of the observed difference between the effect of NaCl percentage on the porosity of PLA and PCL-PLA films, WVTR was investigated for porous PCL-PLA films

Sample name	WVTR (gm/d.m^2)
Neat PCL-PAL	73.73
PL-PC4 N50	304.53
PL-PC4 N70	318.52
PL-PC4 N100	334.93

Table 16: Water vapor transmission rate for neat and porous PCL-PLA films with different NaCl percentages

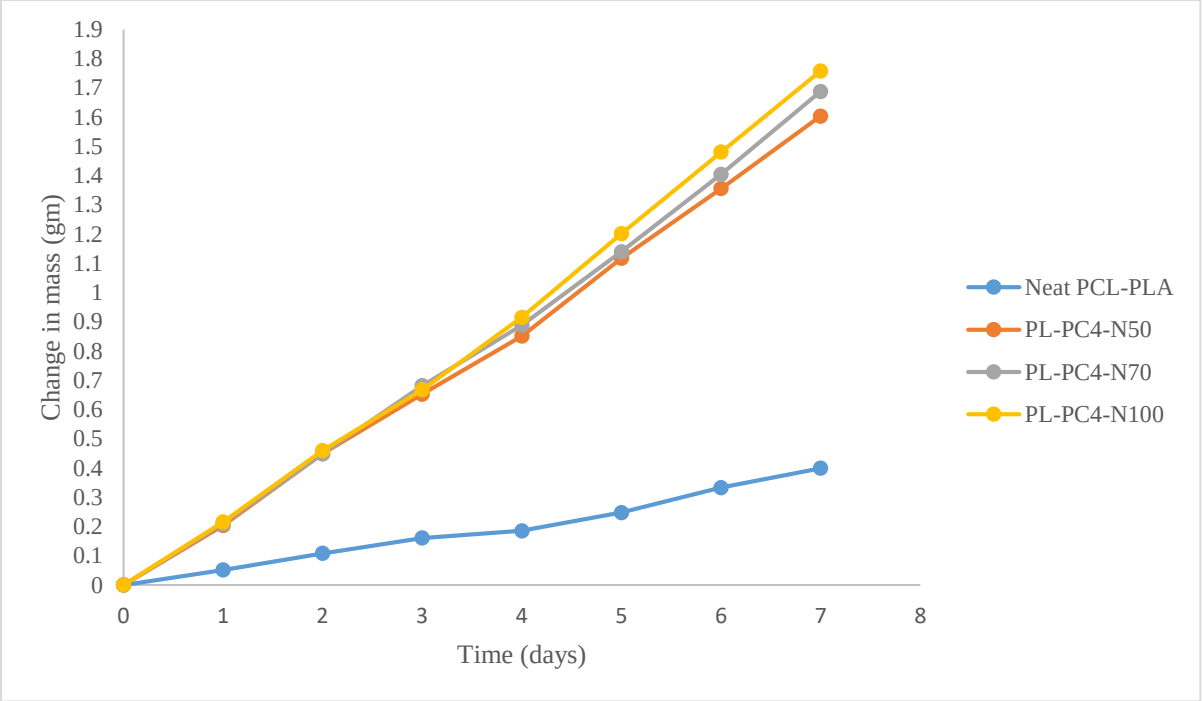

Figure 25: Water vapor transmission rate result for neat and porous PCL-PLA films

Slight reduction in WVTR was observed for neat PCL-PLA compared with neat PLA. Although the diffusion coefficient of water vapor for PCL is higher than PLA, PCL is more hydrophobic than PLA. In fact, high hydrophobicity of PCL is resulted from its low solubility coefficient that is expressed by the solubility parameter. In general, semi –crystal polymers are characterized by relatively lower solubility parameter compared with the amorphous polymers. Hence, it was reported in the literature that the solubility parameters of PLA and PCL are 22.7 and 20.8 J/cm^3 respectively [110]. Accordingly, since the difference in the solubility parameters between the two polymers is insignificant, the difference in WVTR between neat PLA and neat PCL-PLA was also small. Furthermore, the immiscibility of the two polymers led to reduce the free volume and diffusion path available for water diffusion, which consequently reduced WVTR. Distribution of PCL crystalline particles within PLA matrix hindered water vapor diffusion and hence reduced its permeability [111]. However, most of the hydrocarbon-based polymers that contain methyl or ethyl groups, such as PLA and PCL, are characterized by low chain flexibility and low WVTR due to the methyl and ethyl groups steric effect. Therefore, the different in WVTR between PLA and PCL/PLA was not significant.

WVTR increased for porous PCL-PLA membranes when NaCl percentage increased with regardless the to the crystallinity. This result indicated that water vapor transferring through the pores was more predominant than transferring through polymer matrix due the PCL hydrophobicity as discussed previously.

4.6. Water absorption test

4.6.1. Water absorption test for neat and porous PLA films

Water absorption and weight loss percentages were investigated in order to determine the stability of the food packaging against degradation after exposing to water. Water adsorption and weight loss percentages are strongly depended on the porosity and the surface area. Therefore, effect of NaCl percentage on these major parameters was investigated for porous PLA.

Samples name	Weight loss (%)	Water absorption (%)
Neat PLA	0.5	0.6
PL-N50	14.8	31.1
PL-N70	16.2	35.3
PL-N100	19.2	42.5

Table 17: Water Absorption and weight loss for neat and porous PLA films with different NaCl percentages

Significant increasing in water absorption was observed for porous PLA membranes compared with the neat PLA. Indeed, water absorption percentage of neat PLA was 0.59%, while it increased for samples PL-N50 to reach 31.07%. Thus, this result indicated high capability of the porous film to uptake water and to hold it within its porous cavities. This ability was resulted from the high porosity that was confirmed by the previous characterization methods. To explain, high porosity enhanced water absorption because of the availability of high surface area and free volume. The same result was reported in the literature through studying the water absorption of porous PLA scaffold, which was developed by using the same technique [112].

Although the reduction in permeability of for samples PL-N70 and PL-N100, higher water absorption percentages was observed compared with sample PLA-N50. In fact, samples PL-N70 and PL-N100 showed water absorption percentages of 35.31 % and 42.48% respectively. This result observed because of the increasing of surface area and pore volume associated with increasing in NaCl percentage as confirmed by the BET analysis. The same result was demonstrated before by Nasri et al. during studying the effect of NaCl concentration as a porogenic agent on the water uptake of PLA scaffold [113].

Moreover, formation of water clusters whiten PLA matrix is also an acceptable explanation for the observed increasing in water absorption percentage in samples PL-N70 and PL-N100. Indeed, clusters formation is an important phenomenon that affects water absorption in the amorphous polymers. To clarify, clustering is an ordered structure of PLA-water binary system that is stabilized by the hydrogen bonds between water molecules. Thus, combination of these clusters leads to form hetero-phase regions with a sized ranged between 1 and 2µm [19]. In fact, this phenomenon is enhanced with high NaCl percentage. This enchantment was resulted from the interaction between the solvated cations and the adjacent ions of NaCl residuals within the plyometric matrix after salting-out [98]. Consequentially, this interaction stimulus formation of crosslinking between lactide chains in PLA. Such crosslinking reinforced water absorption. In fact, this explanation also interpreted incomplete extraction of NaCl that occurred in samples PL-N70 and PL-N100. To explain, some of water molecules involved in leaching out step were stabilized within the polymer matrix instead of being removed with NaCl particles. Therefore, amount of dissociated NaCl remained with PLA matrix and decreased the permeability.

Moreover, high weight loss of porous PLA membranes compared with neat PLA was resulted from the effect of NaCl and porosity on PLA degradation. As shown in table 17, samples PL-N50, PL-N70 and PL-N100 showed weight loss of 14.08 %, 16.2% and 19.2% respectively compared with 0.47 % for neat PLA. The mechanism of PLA degradation is the heterogeneous erosion mechanism. To clarify, this mechanism occurs with a fast rate in the core part rather than the surface and it takes place only in the amorphous range. In fact, hydrolysis degradation by this mechanism includes cleavage of ester group in PLA that leads to formation of lactic acid oligomers. Thus, the existence of these oligomers within the plyometric matrix increases carboxylic group content. Consequentially, presence of high amount of carboxylic groups enhances and accelerates the degradation rate through the autocatalysis hydrolysis for ester group. Hence, the induced hydrolysis leads to breaking in some parts of the plyometric chains. These broken molecules diffuse out of the bulk material and lead to the resulted weight loss [114]. This mechanism is enhanced with the increasing in pore volumes because it facilitates high water diffusion and hydrolysis. Therefore, it was observed in this study that the weight loss percentage increased when NaCl percentage increased as a result of the increasing in pore volume, as proved by BET analysis.

4.6.2. Water absorption test for neat and porous PCL-PLA film

Water absorption and weight loss were investigated for porous PCL-PLA films to study the effect of porosity and the nature of the polymer on these essential parameters.

Samples name	Weight loss (%)	Water absorption (%)
Neat PCL-PLA	0.8	0.9
PL-PC4-N50	9.0	17.8
PL-PC4-N70	12.8	26.2
PL-PC4-N100	22.1	50.7

Table 18: Water Absorption and weight loss for neat and porous PCL-PLA films with different NaCl percentages

No significant difference was observed in the water uptake for porous PCL -PLA films compared with porous PLA films. As shown in table 18, sample PL-PC4-N50, PL-PC4-N70 and PL-PC4-N100 showed water uptake percentage by 17.81 % and 28.21 % and 50 .69% respectively compared with 0.9% for neat PCL-PLA film. In fact, the observed increasing in water absorption percentage when NaCl percentage increased was resulted from increasing in porosity and volume available for diffusion. This result was confirmed by the BET analysis, which showed increasing in the surface area and pore volume when NaCl percentage increased.

Moreover, high weight loss in porous PCL-PLA films also resulted from the diffusion of the PLA and PCL degradation products out of the plyometric mercies. As shown in table 18, samples PL-PC4-N50, PL-PC4-N70 and PL-PC4-N100 showed weight loss percentage by 9%, 12.8% and 22.1% respectively compared with 0.8% for neat PCL-PLA film. However, the degradation mechanism of PCL is different form PLA because PCL is semi-crystal polymer and it is more hydrophobic than PLA. Therefore, PCL is characterized by lower degradation rate and high ability to retard water diffusion. To clarify, PCL is degraded by hydrolysis through surface erosion mechanism. This mechanism involves cleavage of the plyometric backbone form the surface only. This mechanism includes cleavage of the ester group through chain scission, which is resulted from water diffusion [114]. Indeed, PCL follows this mechanism because of the lack of interaction between the polymeric matrix and water molecules. The inadequate interaction between PCL and water molecules is resulted from the un-sufficient amorphous region. Hence, PCL is able to retard the diffused water during leaching out step more than PLA. Accordingly, it can be concluded that complete leaching out of the salt form PCL-PLA blend was resulted from absence of water clusters and PCL hydrophobicity, in contrast to PLA [114, 115]. This mechanism is enhanced with

increasing in the porosity and pore volume due to the increasing water diffusions. Therefore, weight loss percentage increased when NaCl percentage increased.

4.7. Fourier-transform infrared spectroscopy (FTIR) analysis

FTIR spectra of the porous films were obtained to investigate the interaction between the blended polymers and the effect of porosity of the functional groups of the polymers

4.7.1. Fourier-transform infrared spectroscopy (FTIR) analysis for porous PLA films

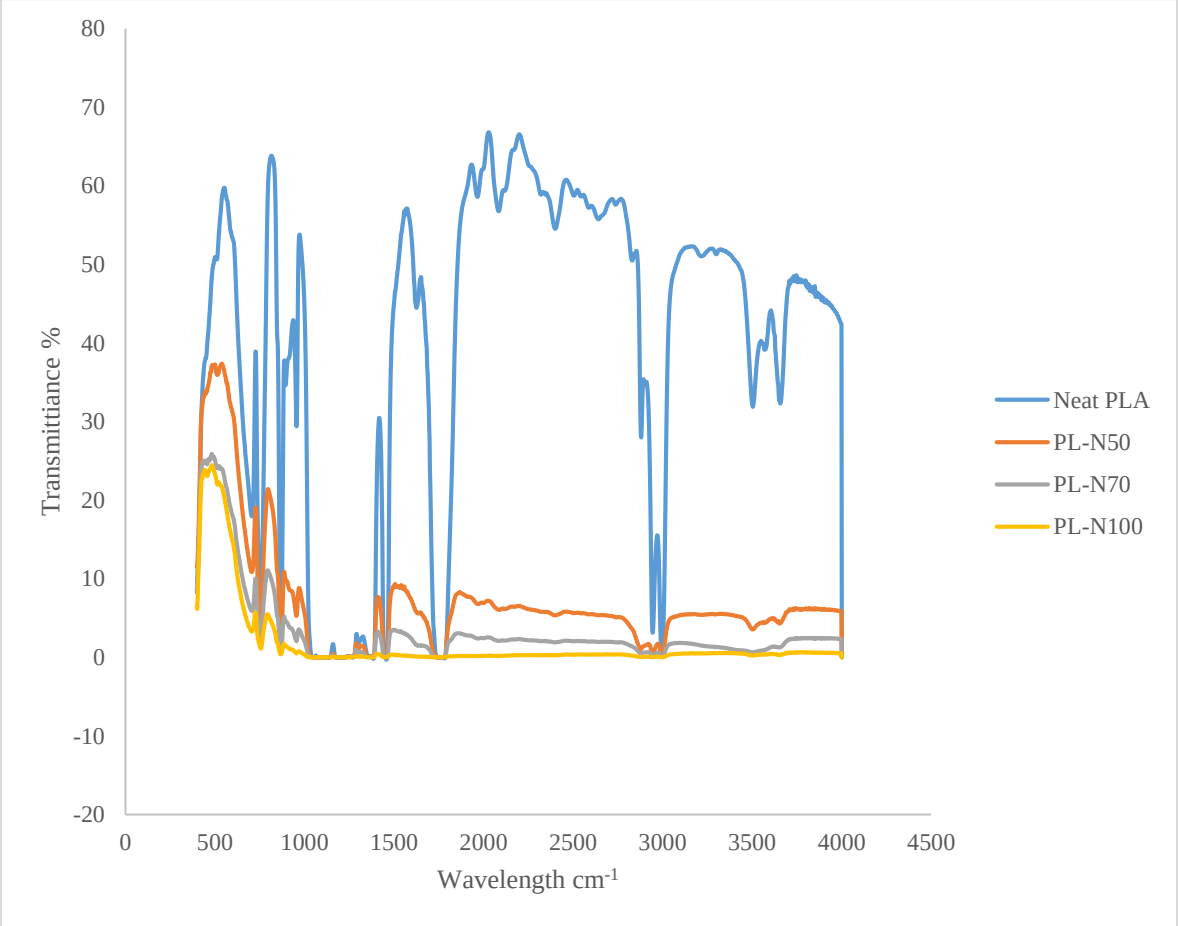

Figure 26: FTIR spectra for neat and porous PLA films.

Fourier-transform infrared spectroscopy (FTIR) spectra was used to study the effect of porosity in the functional groups of PLA and PCL. As shown figure 26, FTIR spectra for neat PLA showed sharp beaks at 3685 and 3504.6 $cm^{-1,}$ which indicated O-H vibrational stretching mode. The symmetric and asymmetric stretching vibrational modes showed at 2945.3 and 2995.9 cm^{-1} for C-H in CH_3 group respectively. The symmetric and asymmetric bending modes of $–CH_3$ showed at 1456.4 and 1366.3 cm^{-1} respectively. Stretching vibrational mode of C-O-C for the ester bond showed at 1132.5, cm^{-1} while stretching vibrational mode of C=O in the ester group showed at 1781.9 cm^{-1}. Furthermore, peaks that appeared at 956 and 894.7 cm^{-1} may represent the stretching vibration of the ester bond (O-C=O) [116, 117, 118, 119].

As shown in the FTIR spectra for the porous PLA membranes in figure 26, PEO did not form chemical bonds with the functional groups of PLA. Indeed, the same functional groups appeared in the spectra of porous PLA films without any obvious shifting in the peaks. Therefore, FTIR spectra of porous PLA films proved complete extraction of PEO because of its immiscibility and the low affinity with PLA, as discussed previously. Nevertheless, reduction in the intensities of some peaks was observed in the FTIR spectra of the porous samples. This reduction became more significant when NaCl percentage increased in samples PLA-N70 and PL-N100. Hence, it could be concluded that this change was resulted for the presence of NaCl residues within porous PLA matrices. To explain, deionized salt reacts with C-O and O-H groups in PLA, which resulted in formation of salt-oxygen bonds between the salt and PLA chains. Thus, this interaction resulted on crosslinking of lactic units within PLA matrix, which led to reduction in the intensities and broadness of some peaks in the FTIR spectra of porous PLA films. The same result and explanation were demonstrated before by Sibambo et al. during studying the effect of NaCl, as a porogenic agent, on FTIR spectra of porous PLA [98].

4.7.2. Fourier-transform infrared spectroscopy (FTIR) analysis for Porous PCL-PLA films

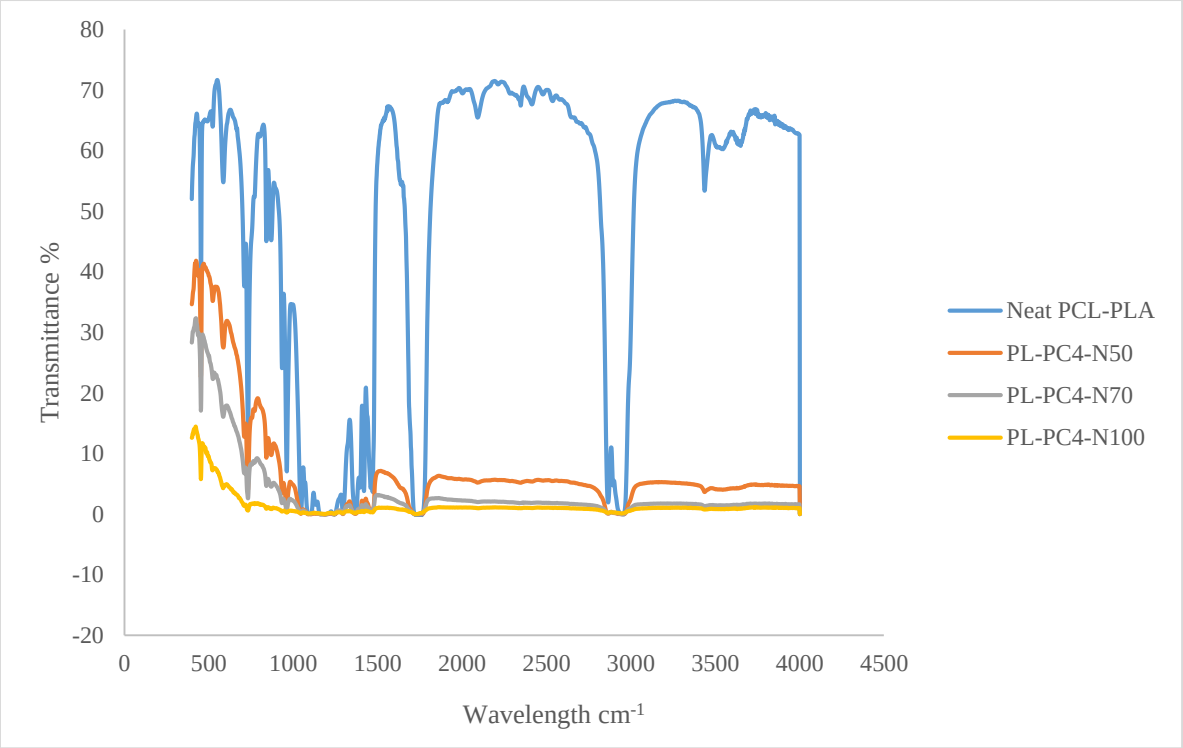

Figure 27: FTIR spectra of neat and porous PCL-PLA films.

In general, as shown in figure 27, FTIR spectra of neat PCL-PLA exhibited the same structure of neat PLA because both polymers are aliphatic polyesters with the same functional groups. Sharp intense peaks at 2956.1 and 2885.6 cm-1 indicated stretching vibrational mode of $–CH_2$ groups in PCL and PLA. Stretching vibrational mode of C=O in PCL and PLA showed at 1762.5 cm^{-1}. Sharp peaks appeared at 1193.4, 1295 and 1470 cm^{-1} indicated stretching vibrational mode of C-O in PLC and PLA while peaks at 870 and 961.9 cm^{-1} indicated the vibrational mode of C-O in PLA only. O-H vibrational stretching mode in PLA appeared at 3437. 4 cm^{-1}. Accordingly, FTIR spectra of the blend confirmed the immiscibility of the two PLA and PCL due to the lack on interaction between the functional groups of the two polymers. Furthermore, reduction in the intensities and broadness of some peaks resulted from the effect of porosity in the blend crystallinity and the effect PEO on the functional groups of PCL [120].

4.8. Brunauer–Emmett–Teller (BET)

4.8.1. Influence of PEO concentration on the BET surface area of porous PLA films

Brunauer–Emmett–Teller (BET) analysis was carried out to investigate the effect of increasing PEO percentage on the surface area and pores volume.

Sample name	BET surface area (m^2/g)	Internal pore volume (cm^3/g)
PL-N50	0.3073	$3.99*10^{-4}$
PL-PO1 N50	0.2186	$2.5 *10^{-4}$
PL-PO2 N50	0.4202	$8.9*10^{-4}$

Table19: BET surface area and total pore volume for porous PLA films with different PEO percentages.

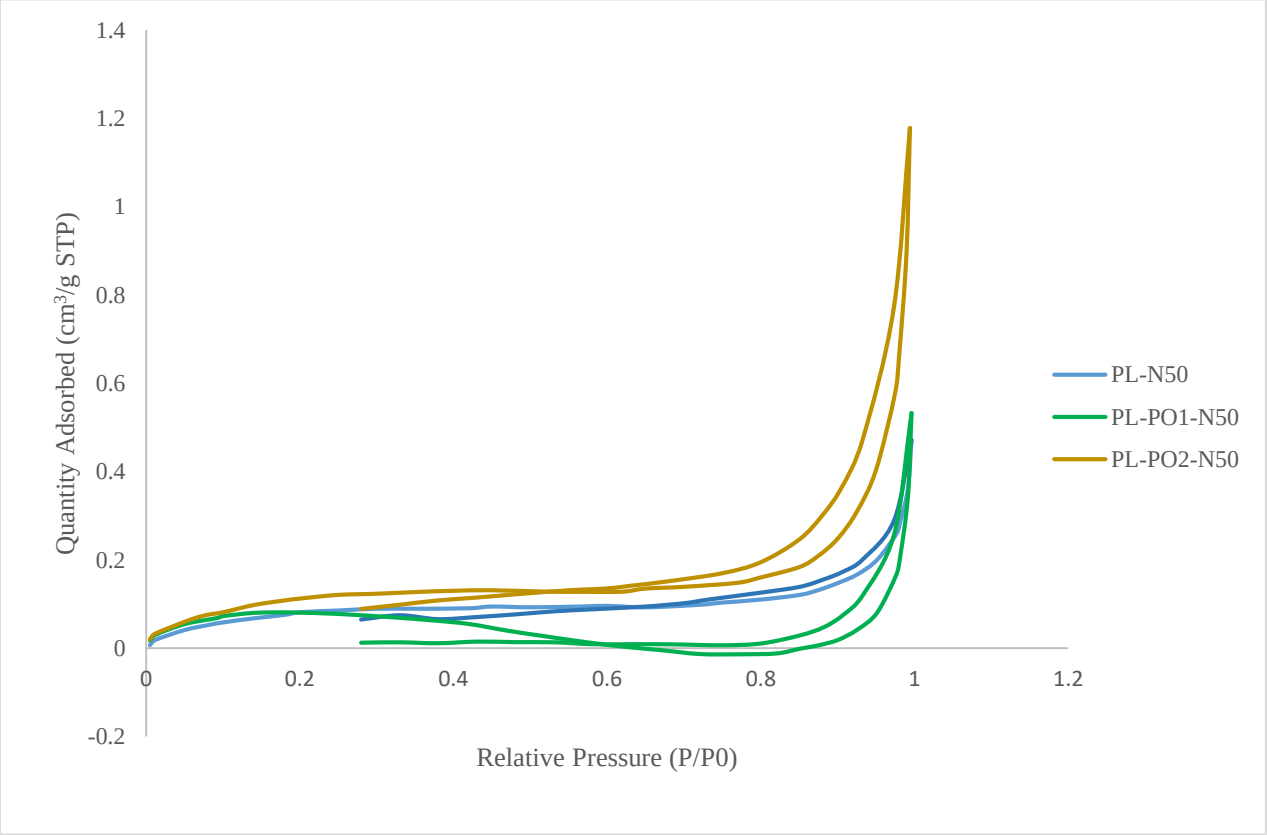

Figure 28: The hysteresis loops for porous PLA films with different PEO percentages.

As shown in figure 28, the isotherm for all the samples showed type IV. This type showed that gas condensed inside the pore after multilayers adsorption. Appearance of this type of hysteresis loop indicated the existence of pores in the nanoscale and microscale. Moreover, the hysteresis loop is classified H4, which indicted the existence of slit pores, internal voids, board sized distribution and heterogeneous porosity. In fact, BET surface area did not show obvious proportional relationship with PEO percentage. However, sample PL-PO2-N50 with 20 % PEO showed relatively high BET surface area compared with the other samples with lower PEO concentrations. To clarify, BET surface area increased because of increasing in the total pore volume, which resulted from extraction of high amount of PEO and formation of high number of microspores. Thus, increasing number of microporous led to improve the pores interconnectivity and consequently to increase in the BET surface area. Furthermore, this result might indicate that increasing in PEO concentration enhanced NaCl leaching out and consequently led to formation of high numbers of macro-pores. Indeed, increasing in BET surface and pores volume as a result of improving in interconnectivity was demonstrated before by Wang et al. In this study, it was proved that improving the interconnectivity of nano-porous carbon membrane through thermal treatment led to increase the BET surface area and the total pore volume because of the formation of three dimensional interconnected network form micro and mesopores [121].

4.8.2. Influence of Porogen Concentration on the BET Surface Area of Porous PLA Films

BET analysis was applied to porous PLA with different NaCl percentages to investigate the effect of NaCl agglomeration on the BET surface area and the pore volume.

Sample Name	BET surface area (m^2/g)	Internal pore volume (cm^3/g)
PL-N50	0.3073	$3.99*10^{-4}$
PL-N70	0.4613	$5.42*10^{-4}$
PL-N100	0.5273	$8.72*10^{-4}$

Table 20: BET surface area and total pore volume for porous PLA films with different NaCl percentages

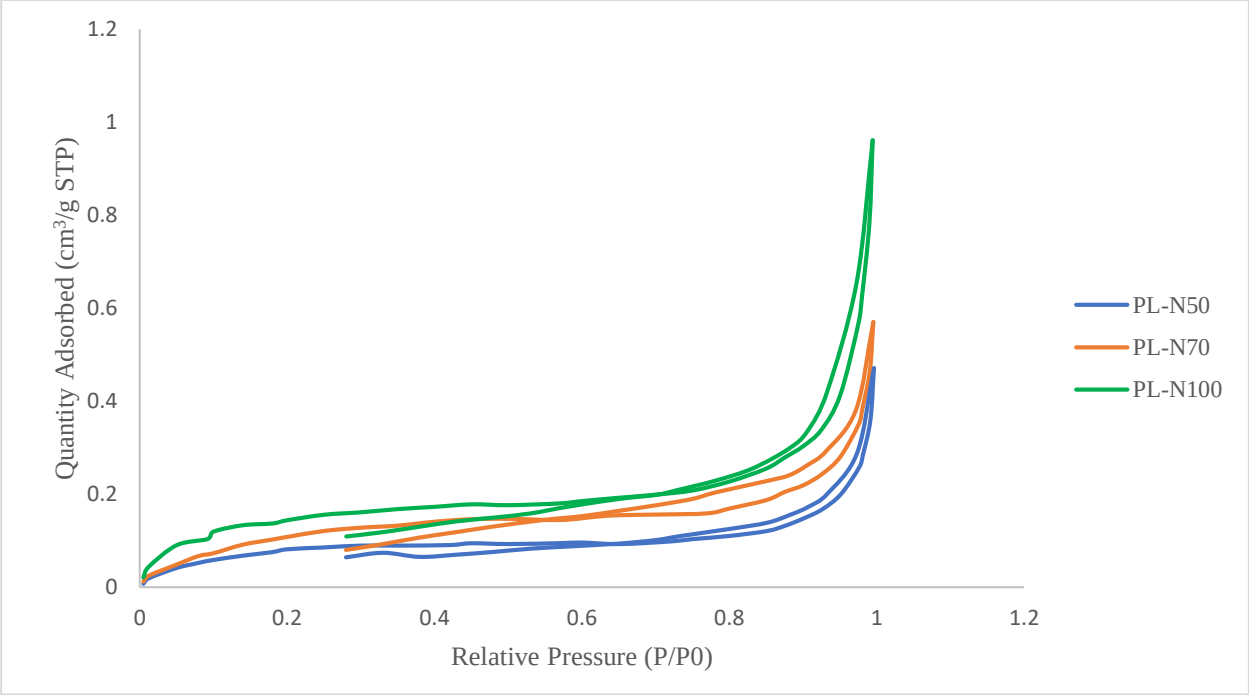

Figure 29: The hysteresis loops for porous PLA films.

As shown in figure 29, the isotherm also showed type VI, which indicted that porous PLA samples contain pores in the nanoscale and microscale. In addition, the hysteresis loop of sample PL-N50 is more likely to be classified as H3, which indicated existence of interconnected pores with uniform channels [122]. On the other hand, hysteresis loops of samples PL-N70 and PL-N100 are classified as H4, which indicated irregular porosity. This result proved formation of different sizes of pores as a result of NaCl agglomeration as discussed previously. Additionally, the irregular porosity was also resulted form incomplete leaching out of NaCl at high percentages. As shown in table 20, increasing in BET surface area and pores volume was observed in sample PL-N70 and PL-N100 compared with sample PL-N50. This result was expected because of the formation of pores with large volume, which is resulted from leaching out of agglomerated NaCl particles. Furthermore, increasing of BET surface area with increasing in NaCl was also expected due to the increasing in crystallinity, as shown in DSC results. Indeed, high crystalline structure enhances the stability of the pores and voids and prevents their collapse [123]. The result is in good agreement with the demonstrated relationship between crystallinity and BET surface area in the literature. It has been reported the crystalline porous organic polymers are characterized higher BET surface area compared with porous amorphous polymers [124].

Another possible explanation for the observed increasing in BET surface area and pore volume at high NaCl percentages is the presence of voids (dead pores). Indeed, these voids were formed in the interface between the polymer matrix and non-extracted NaCl as a result of their incompatibility [125]. The same result was demonstrated before by Takahashi et al. during studying the effect of adding silica on the BET surface area of polyether imide [126]. Nevertheless, it was demonstrated in this study that the voids resulted form addition of inorganic filler with high concentration improved the permeability of the non-porous membrane. In contrast, in this study, increasing the BET surface area was associated with reduction in permeability. This result demonstrated that gas permeability is predominant through the pores that were resulted from PEO and NaCl extraction rather than the voids, which were around NaCl particles. In fact, this result is expected because these voids are characterized by low interconnectivity. Hence, presence of these voids did not enhance the permeability. Furthermore, existence of NaCl increased the tortuosity steady state permeation path, which reduced permeability compared with sample PL-N50.

4.8.3. Influence of porogen concentration on the BET surface area of porous PCL-PLA films

BET analysis was carried out to porous PCL-PLA films to investigate the effect of NaCl percentage and the non-leached PEO on the total surface area and pore volume.

Sample Name	BET surface area (m^2/g)	Internal pore volume (cm^3/g)
PL-PC4 N50	0.4722	$1.1 *10^{-3}$
PL-PC4 N70	1.619	$2.5 *10^{-3}$
PL-PC4 N100	0.798	$1.5 *10^{-3}$

Table 21: The BET surface areas for porous PCL-PLA films with different NaCl percentages

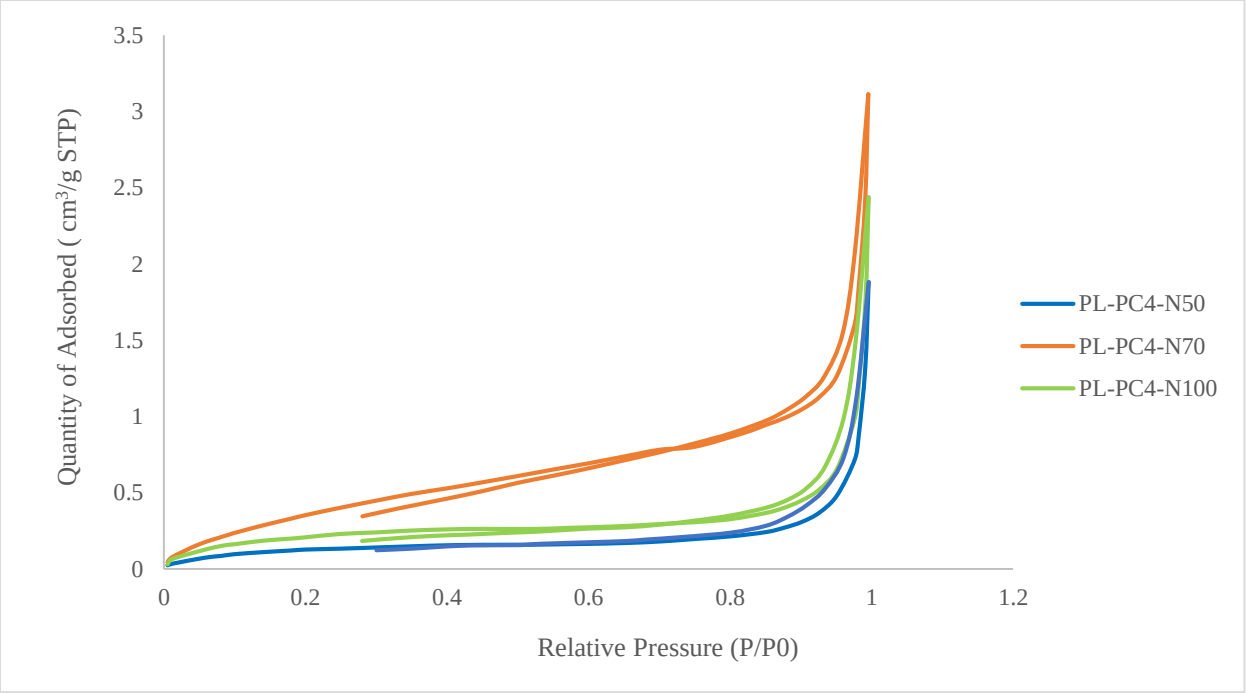

Figure 30: The hysteresis loops for porous PCL-PLA films

As shown in figure 30, the adsorption isotherms showed Type IV, which indicated that gas adsorption followed the same discussed pattern of porous PLA. The hysteresis loop of sample PL-PC4-N70 was classified as H3 while the hysteresis loop of samples PL-PC4-N50 and PL-PC4-N100 was classified as H4. As shown in table 21, BET surface areas of porous PCL-PLA films increased with increasing in NaCl percentage. This result was expected due to complete leaching out of NaCl and the associated developed porosity, which provided high free volume. However, sample PL-PC4-N70 showed the highest surface area among the other samples due to its high crystallinity degree compared with samples PL-PC4-N50 and PL-PC4-N100, as shown by the DSC results.

According to the air permeability measurement in sec 4.2, porous PCL-PLA films characterized with relatively low air permeability compared with the porous PLA films at the same PEO and NaCl concentrations. Nevertheless, BET analysis showed that the surface areas of porous PCL-PLA films were higher than the surface area of porous PLA films. Accordingly, this result indicated that the affinity of PEO to PCL hindered NaCl agglomeration and enhanced its full desperation within the blend mercies, in contrast to porous PLA films. In other words, porosity of porous PCL-PLA films developed by huge number of small pores resulted from leaching out of

well dispersed NaCl particles while porosity of porous PLA films developed by low number of relatively larger pores resulted from the leaching out of agglomerated NaCl particles. Therefore, higher BET surface areas were observed with porous PL-PLA films compared with the porous PLA films.

4.9. Antimicrobial activity of porous PLA and PCL/PLA films after coating with cinnamaldehyde

4.9.1. Influence of the polymer hydrophilicity on the antimicrobial activity of the porous films

To study the effect of trans-cinnamaldahyde concentration on the antibacterial properties of the porous films, samples PL-N50 and PL-PC4 N50, which were prepared with the same NaCl percentage, were soaked in water/ethanol mixture with different concentrations of cinnamaldahyde.

Cinnamaldahyde %	**Inhibition Zone (mm)**			
	Staph		***E.coli***	
	PL-N50	**PL-PC4-N50**	**PL-N50**	**PL-PC4-N50**
6	Not available	15	Not available	Not available
7	14.3	38	Not available	22
8	35	33	25	22

Table 22: The effect of polymer nature of the antimicrobial activities of porous PCL/PLA and PLA films with different cinnamaldahyde %. All the films contain 10% PEO and 50% NaCl

As shown in table 22, sample PL-PC4-N50 started to show antibacterial effect at lower concentration of cinnamaldahyde compared with sample PL-N50. To explain, immersion in water/ethanol mixture (soaking solution) with cinnamaldahyde concentration of 6% showed inhibition zone of 15 mm for sample PL-PC4-N50 against *Staphylococcus aureus (Staph)* while no inhibition zone showed for sample PL-N50 at the same concentration. Meanwhile, at this concentration, both of samples did not show inhibition zones against *Escherichia coli (E.coli).*

Moreover, when the concentration of cinnamaldehyde in the soaking solation increased form 6 % to 7%, the inhibition zone of sample PL-PC4-N50 against *Staph* increased to 38 mm and its antibacterial effect against *E.coli* started to appear with inhibition zone of 22 mm. At the same

concentration, the antibacterial effect of PL-N50 started to show against *Staph* with inhibition zone of 14.3 mm while no antibacterial effect showed against *E.coli*.

In addition, soaking solution with cinnamaldahyde concentration of 8% showed inhibition zones for samples PL-N50 and PL-PC4-N50 against both *Staph* and *Ecoli* . However, no significant difference was noticed between the inhibitions zones for the two samples against each strains at this concentration.

According to these results, it is obvious that the interaction between cinnamaldahyde and PL-PC4-N50 film is stronger than its interaction with PL-N50. Thus, sample PL-PC4-N50 absorbed higher amount of cinnamaldahyde from the soaking solution than sample PL-N50 at the same concentration. In fact, this result was expected because PCL is more hydrophobic than PLA as discussed previously. Therefore, cinnamaldahyde interacted with PCL in sample PL-PC4-N50.This interaction led to high loading capacity of the antimicrobial from the water-ethanol mixture within the plyometric chains and the pores in the film. The same result was proved by Patel et al. during studying the interaction between PCL-PEO diblock copolymer and cucurbitacin drug as a hydrophobic drug. In this study, it was demonstrated that increasing PCL content increased the loading capacity of the drug due to the polar interaction between the polymer and the drug [127].

In addition, existence of PEO residuals in sample PL-PC4-N50, as discussed previously, enhanced the releasing of cinnamaldehyde in the microbial suspensions. Such enchantment led to high inhibition zone at lower concentration from cinnamaldehyde compared with PL-N50. Indeed, PEO incorporated with PCL in several studies to design drug delivery system due to its hydrophilicity. Thus, PEO enhances the swelling properties of plyometric matrix and facilitates the penetration of the aqueous solution [128]. On the other hand, sample PL-N50 needed higher cinnamaldehyde concentration to show inhibition zones for both gram negative and gram positive stains. This is due to lack of hydrophilic polymer within the polymeric matrix.

In general, for the two samples, the inhibition zones for *Staph* were higher than the inhibition zones for *E.coli*. This result was expected because the structure of outer membrane for two bacteria is different. To clarify, the outer membrane of *E. coli* as a gram negative bacteria, is a thick layer of lipopolysaccharide that covers the cell wall. In fact, this structure is known by high resistance to hydrophobic antibacterial ingredient such as cinnamaldehyde. On the other hand, structure of the

outer membrane of *Staph*, as gram positive bacteria, is composed of a single peptidoglycan layer, which is lower in resistance to hydrophobic cinnamaldehyde compared with *E.coli* [129].

4.9.2. Influence of the porosity on the antimicrobial activity of the porous films

In order to study the effect of porosity on antibacterial activity, porous PLA and porous PCL-PLA films were immersed in soaking solutions with 6 %, 7 % and 8 % trans-cinnamaldehyde

Cinnamaldahyde (%)	Inhibition Zone with *Staph*(mm)					
	PL-N50	PL-N70	PL-N100	PL-PC4-N50	PL-PC4-N70	PL-PC4-N100
6	Not available			15	40	34
7	14.3	45	47	38	40	27
8	35	29	35	33	40	Not available

Table 23: Inhibition zones of porous PCL/PLA and PLA films for *Staphylococcus aureus* with different cinnamaldahyde concentrations

Cinnamaldahyde (%)	Inhibition Zone with *E.coli* (mm)					
	PL-N50	PL-N70	PL-N100	PL-PC4-N50	PL-PC4-N70	PL-PC4-N100
6	Not available			Not available	22	NA
7	Not available	24	23	22	37	19
8	25	28	24	22	22	Not available

Table 24: Inhibition zones of porous PCL/PLA and PLA films for *Esherichia coli* with different cinnamaldahyde concentrations

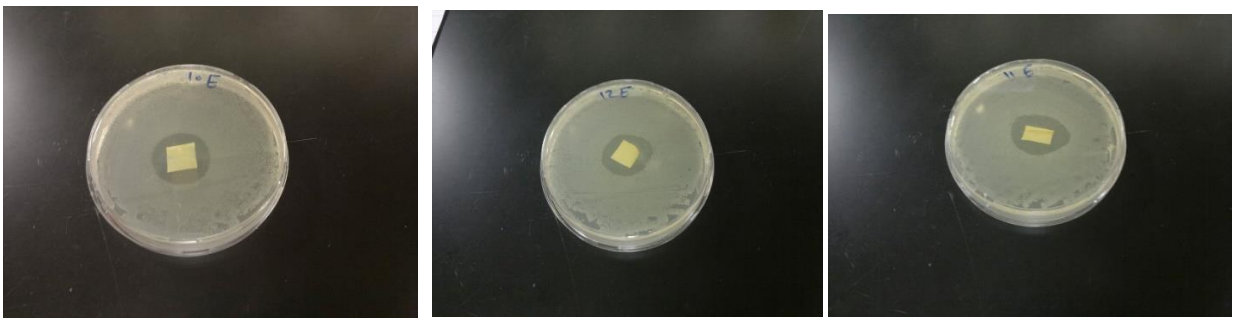

[A] [B] [C]

Figure 31: Inhabitation zones of porous PLA soaked in 8% cinnamaldahyde. against *Esherichia coli* respectively. [A] PL-N50, [B] PL-N70 and [C] PL-N100.

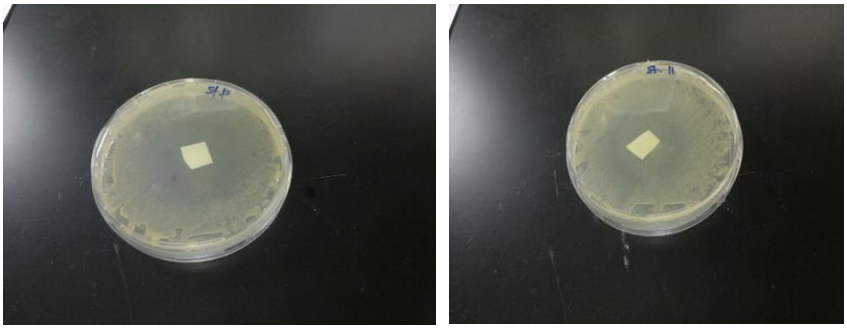

[A] [B]

Figure32: Inhabitation zones of porous PLA soaked in 8% cinnamaldahyde *Staphylococcus aureus* of porous PLA. [A] PL-N50 and [B] PL-N70.

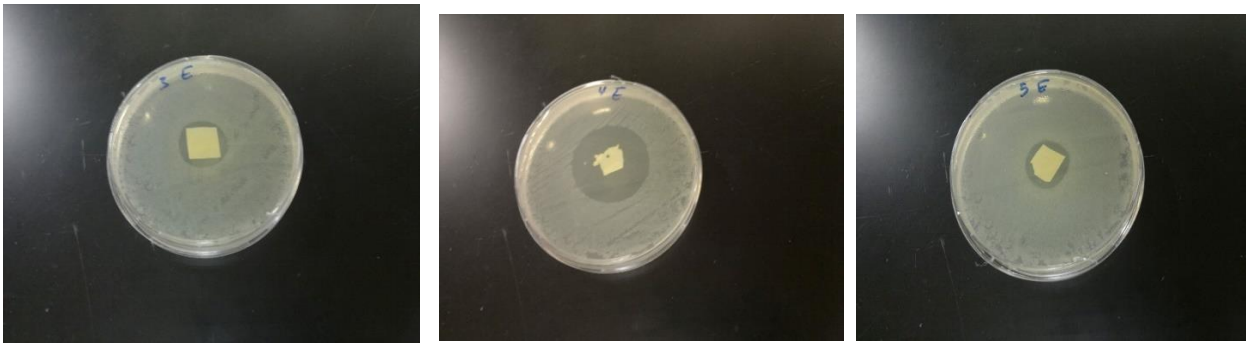

[A] **[B]** **[C]**

Figure33: Inhabitation zones of porous PCL-PLA films soaked in 7% cinnamaldahyde against *Esherichia coli.* [A] PL-PC4-N50, [B] PL-PC4-N70 and [C] PL-PC4 N100

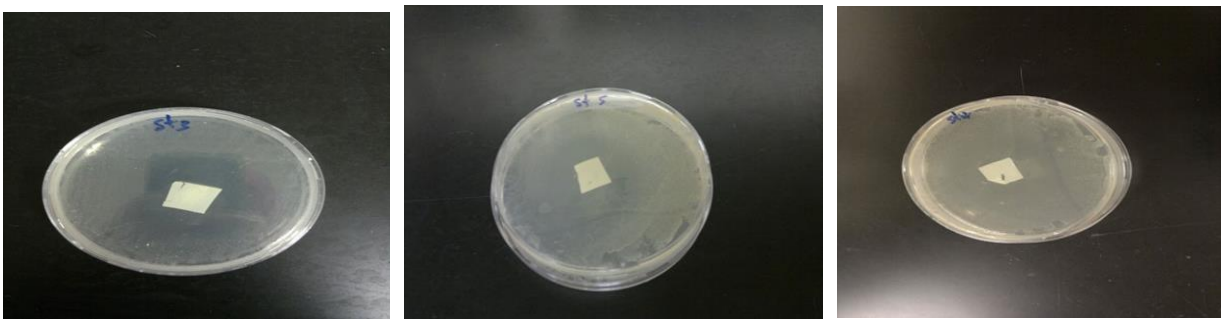

[A] **[B]** **[C]**

Figure 34: Inhabitation zones of porous PCL-PLA films soaked in 7% cinnamaldahyde against *Staphylococcus aureus.*[A] PL-PC4-N50, [B] PL-PC4-N70 and [C] PL-PC4 N100

As shown in table 23, concentration of 6% did not show antimicrobial effect for all the porous PLA samples. However, at the same concentration, inhibition zones of 40 and 34 mm showed ageist *Staphy* for samples PL-PC4-N70 and PL-PC4-N100 respectively. Indeed, the inhibition zones of these samples were higher that the inhibition zone showed for sample PL-PC4 N50 at the same cinnamaldehyde concentration. Accordingly, this result indicated that increasing in the porosity , which is associated with increasing in NaCl percentage, enhanced the antimicrobial loading capacity and consequentiality enhanced the antimicrobial activity. Nevertheless, at the same concentration, only sample PL-PC4-N70 showed inhibition zone of 22 mm against *E.coli* due to its higher surface area.

Moreover, soaking solution with cinnamaldehyde concentration of 7% showed significant increasing in the inhibition zones of samples PL-N70 and PL-N100 against *Staphy* compared with sample PL-N50. In addition, although sample PL-N50 did not show antibacterial activity against *E.coli* at this concentration, samples PL-N70 and PL-N100 showed adjacent inhibition zones against *E.coli*. Thus, this result indicated the loading capacity for cinnamaldehyde within of samples PL-N70 and PL-N100for the cinnamaldehyde form the soaking solution was higher than sample PL-N50. This result was expected because high loading capacity for samples PL-N70 and PL-N100 was resulted the increasing BET high surface area, as discussed previously.

Increasing cinnamaldehyde concentration from 7 to 8% led to develop the antimicrobial properties of sample PL-N50 against *E.coli*. In addition, the inhibition zone of sample PL-N50 against *Staph* increased compared with the lower concentration of cinnamaldehyde. However, the other porous PLA and PCL-PLA samples showed reduction or no significant change in the inhibition zones at this concentration. Furthermore, when cinnamaldehyde concentration increased from 7 to 8% in the soaking solution, no obvious proportional relationship showed between inhibition zones and NaCl percentages was observed. This result showed because the solubility and the homogenous distribution of cinnamaldehyde in the soaking solution decreased when cinnamaldehyde concentration increased because of its hydrophobic nature. This effect led un-homogeneous coating for the films with regardless to their porosity. Therfore, no obvious propational relationship was determinded between cinnmalahdye concentration and the porousity of PCL-PLA films.

5. Conclusion and Future work

The purpose of this work was to develop antimicrobial porous films from biodegradable polymers for food packaging applications. Developing porosity within the plyometric matrices was obtained by using casting/ leaching out technique. Thus, sodium chloride (NaCl) was using as a pore forming agent after recrystallized by using anti-solvent and ultrasonic techniques. In fact, the advantage of using recrystallized NaCl was producing more uniform pore size. Furthermore, polyethylene oxide (PEO) was used as hydrophilic polymer in order to facilitate leaching out of NaCl crystals from the polymer and it also was added to improve the pores interconnectivity. As a result of using two kinds of pore forming agents, the developed porous films characterized by binomial pore size distribution. Indeed, leaching out of NaCl resulted in forming macro-pores while extraction of PEO resulted in forming of micro-pores. These micro-pores act as interconnected channels between the macro-pores. However, it was proved that this porous structure was developed form the cooperative effect of both NaCl and PEO. On other words, neither NaCl nor PEO was able alone to develop high number of macro and micro pores respectively. Air permeability was used as a controlling parameter to determine the optimum NaCl and PEO concentrations. Furthermore, PCL was added to improve the mechanical properties of the porous films. Hence, the optimum PCL composition was determined based on the mechanical proprieties measurement.

Sample name	Air permeability ($cm^3/cm^2/s$)	O_2 TR ($c.c/m^2.d.atm$)	α_m	$f*m$ (Nmm^{-2})	X c (%)	BET surface area (m^2/g)	Pore volume (cm^3/g)
Neat PLA	2.06	950	1.13	27.54	19.06	NA	NA
PL-N50	5.4	4540	1.08	4.1	10.57	0.307	$3.99*10^{-4}$
PL-N70	4.7	3920	1.09	5.35	15.53	0.46	$5.42*10^{-4}$
PL-N100	3.03	3040	1.15	7.18	19.58	0.53	$8.72*10^{-4}$
PL-PC4-N50	3.07	3210	1.22	6.78	37.06	0.47	$1.1*10^{-3}$
PL-PC4-N70	3.23	4040	1.17	3.36	66.02	1.62	$2.5 * 10^{-3}$
PL-PC4-N100	4.56	4540	1.14	2.35	47.03	0.789	$1.5 * 10^{-3}$

Table 25 : Characterization results for porous PLA and porous PCL-PLA films

As shown in table 25, significant increasing in air permeability occurred in sample PL-N50 with 50% NaCl compared with neat PLA. This result proved that the developed porosity was sufficient to improve the film permeability. However, further increasing in NaCl percentage showed reduction in air permeability. The same result was confirmed by O_2TR and WVTR tests. In fact, PL-N50 showed the highest O_2TR and WVTR among all the porous samples with higher NaCl percentages. In was shown that reduction in permeability when NaCl percentages increase was resulted from agglomeration of NaCl and the associated formation of lower number of larger pores. This explanation was proved through the observed increasing in BET surface area and pore volume for samples PL-N70 and PL-N100 compared with sample PL-N50. Moreover, increasing in crystallinity degree (X_c %) when NaCl percentage increased proved the change in pores structure. Incomplete leaching out of NaCl at high concentrations in sample PL-N70 and PL-N100 might also be another possible explanation for the observed reduction in air permeability.

In attempt to improve the pores interconnectivity and porosity, PEO percentage increased from 10% to 15% and 20% in samples PL-PO1-N50 and PL-PO2-N50 respectively at the same NaCl concentration. However, reduction in air permeability was observed in these samples compared with sample PL-N50, which contains only10% PEO. Indeed, reduction in permeability was resulted from high heterogeneity in pore size distribution, which led to increase in the tortuosity of air diffusion path.

As shown in table 25, porous PLA films showed low elongation at break. Therefore, in order to improve the mechanical properties of PLA, PCL was incorporated whiten the porous PLA matrix with different concentrations. However, blending between PCL and PLA with 50% NaCl and 10% PEO showed negative effects on the overall mechanical properties when PCL percentage was below 80%. Air permeability also reduced because of the heterogeneous nature of the blend. This result was expected because of the immiscibility between the two polymer, which led to formation of phase separated systems. On the other hand, significant improvement in the mechanical properties showed for sample PL-PC4-N50, which contains 80% PCL. Nevertheless, air permeability of sample PL-PC4-N50 was slightly lower than sample PL-N50 because of incomplete extraction PEO from the blend matrix. This result proved by the observed PEO peaks in DTG-TGA thermogram of the porous PLA-PCL samples.

Increasing NaCl percentage with the PCL-PLA blend (80%, 20%) showed improving in porosity, which indicated full extraction of NaCl and formation of high amount of macrospores. The same result also proved by O_2TR and WVTR, which showed increasing when NaCl percentage increased in the blend. PL-PC4-N100, with 100 % NaCl, showed the highest air permeability, O_2TR and WVTR among the other samples with lower NaCl percentages. However, the developed porosity associated with increasing in NaCl percentage in the blend led to weaken the improved mechanical properties.

Antimicrobial effect was enhanced by coating the porous films with cinnamaldehyde. Accordingly, it was found the concentration of 7% and 8% cinnamaldehyde in soaking solution was the optimum concentrations for achieving the maximum antimicrobial effect of the coated samples . In fact, the specific optimum concentration of cinnamaldhyde is strongly dependent on the sample porosity, polymeric martial, and the strain type.

In conclusion, all the samples achieved O_2TR values within the acceptable range for breathable food packaging with different mechanical properties. Indeed, sample PL-N50 and sample PL-PC4-N50 showed the high air permeability and O_2TR values with acceptable mechanical properties. However, sample PL-N50 was characterized stiffness and low elongation at break. On the other hand, sample PL-PC4-N50 showed acceptable mechanical properties but relatively high barrier properties.

Further studies are suggested to develop porous films for food packaging applications with uniform pores sizes. Nanotechnology could be utilized through several techniques to develop films with high surface area and high permeability. Additionally, adjusting pore size and distribution to modify the atmospheric compositions inside food packaging headspace is also an interesting area that is suggested for the future work.

References

(1) Becker, B. R. Transpiration and Respiration of Fruits and Vegetables. *Food and Agriculture Organization of the United Nations*.

(2) Soltani, Mahmoud, Reza Alimardani, Hossein Mobli, and Seyed Saeid Mohtasebi. "Modified Atmosphere Packaging: A Progressive Technology for Shelf-Life Extension of Fruits and Vegetables." *Journal of Applied Packaging Research*, n.d., 28.

(3) Nasuha, S. Modified Atmosphere Packaging.

(4) Almenar, E.; Del-Valle, V.; Hernández-Muñoz, P.; Lagarón, J. M.; Catalá, R.; Gavara, R. Equilibrium Modified Atmosphere Packaging of Wild Strawberries. *J. Sci. Food Agric.* **2007**, *87* (10), 1931–1939.

(5) Gates, R. Microperforated Films for Fresh Produce Packaging. In *Modified Atmosphere Packaging for Fresh-Cut Fruits and Vegetables*; Brody, A. L., Zhuang, H., Han, J. H., Eds.; John Wiley & Sons, Inc.: Hoboken, NJ, USA, **2011**; pp 209–217.

(6) Sandhya. Modified Atmosphere Packaging of Fresh Produce: Current Status and Future Needs. *LWT - Food Sci. Technol.* **2010**, *43* (3), 381–392.

(7) *From Hand Holes to Vent Holes: What's next in Innovative Horticultural Packaging*; University Language Centre: Stellenbosch, **2011**.

(8) Ngcobo, M. E. K. Resistance to Airflow and Moisture Loss of Table Grapes Inside Multi- Scale Packaging. 260.

(9) Pathare, P. B.; Opara, U. L.; Vigneault, C.; Delele, M. A.; Al-Said, F. A.-J. Design of Packaging Vents for Cooling Fresh Horticultural Produce. *Food Bioprocess Technol.* **2012**, *5* (6), 2031–2045.

(10) Mukama, M.; Opara, U. L. Resistance to Air Flow, Cooling Characteristics and Quality of Pomegranate Fruit Inside Ventilated Packaging. 127.

(11) Berry, Tarl M., T.S. Fadiji, Thijs Defraeye, and Umezuruike Linus Opara. "The Role of Horticultural Carton Vent Hole Design on Cooling Efficiency and Compression Strength: A Multi-Parameter Approach." *Postharvest Biology and Technology* 124 (February 2017): 62–74.

(12) Hussein, Z.; Caleb, O. J.; Opara, U. L. Perforation-Mediated Modified Atmosphere Packaging of Fresh and Minimally Processed Produce—A Review. *Food Packaging. Shelf Life*. **2015**, *6*, 7–20.

(13) Wu, D.; Xu, F.; Sun, B.; Fu, R.; He, H.; Matyjaszewski, K. Design and Preparation of Porous Polymers. *Chem. Rev.* **2012**, *112* (7), 3959–4015.

(14) Mi, H.-Y.; Jing, X.; Turng, L.-S. Fabrication of Porous Synthetic Polymer Scaffolds for Tissue Engineering. *J. Cell. Plast.* **2015**, *51* (2), 165–196.

(15) Mane, S. Effect of Porogens (Type and Amount) on Polymer Porosity: A Review. *Can. Chem. Trans.* **2016**, *4* (2), 16.

(16) Tawakkal, I. S. M. A.; Cran, M. J.; Miltz, J.; Bigger, S. W. A Review of Poly(Lactic Acid)-Based Materials for Antimicrobial Packaging: Antimicrobial PLA Packaging Materials. *J. Food Sci.* **2014**, *79* (8), R1477–R1490.

(17) Ren, J. Biodegradable Poly(Lactic Acid): Synthesis, Modification, Processing and Applications; *Springer* Berlin Heidelberg: Berlin, Heidelberg, **2011**.

(18) Mistriotis, A.; Briassoulis, D.; Giannoulis, A.; D'Aquino, S. Design of Biodegradable Bio-Based Equilibrium Modified Atmosphere Packaging (EMAP) for Fresh Fruits and Vegetables by Using Micro-Perforated Poly-Lactic Acid (PLA) Films. *Postharvest Biol. Technol.* **2016**, *111*, 380–389.

(19) Siparsky, G. L.; Voorhees, K. J.; Dorgan, J. R.; Schilling, K. Water Transport in Polylactic Acid (PLA), PLA/ Polycaprolactone Copolymers, and PLA/Polyethylene Glycol Blends. 12.

(20) Yuniarto, K. Effect of Plasticizer on Oxygen Permeability of Cast Polylactic Acid (PLA) Films Determined Using Dynamic Accumulation Method. 9.

(21) Tai, H. Batch Foaming of Amorphous Poly (DL-Lactic Acid) and Poly (Lactic Acid-Co-Glycolic Acid) with Supercritical Carbon Dioxide: CO2 Solubility, Intermolecular Interaction, Rheology and Morphology. *In Rheology*; De Vicente, J., Ed.; InTech, **2012**.

(22) Conn, R. E.; Kolstad, J. J.; Borzelleca, J. F.; Dixler, D. S.; Filer, L. J.; Ladu, B. N.; Pariza, M. W. Safety Assessment of Polylactide (PLA) for Use as a Food-Contact Polymer. *Food Chem. Toxicol*. **1995**, 33 (4), 273–283.

(23) Labet, M.; Thielemans, W. Synthesis of Polycaprolactone: A Review. *Chem. Soc. Rev*. **2009**, 38 (12), 3484.

(24) Polycaprolactone :Synthesis , Properties, and Applications. *In Encyclopedia of Polymer Science and Technology*; John Wiley & Sons, Inc., Ed.; John Wiley & Sons, Inc.: Hoboken, NJ, USA, **2017**; pp 1–36.

(25) Dasari, A.; Njuguna, J. *Functional and Physical Properties of Polymer Nanocomposites*; John Wiley & Sons, **2016**

(26) Bailey, F. E. J. *Poly (Ethylene Oxide)*; Elsevier, **2012.**

(27) F.E. Bailey; J.V. Koleske. Polyethylene oxide. Academic Press. London, **1976.**

(28) Thompson, M. S.; Vadala, T. P.; Vadala, M. L.; Lin, Y.; Riffle, J. S. Synthesis and Applications of Heterobifunctional Poly (Ethylene Oxide) Oligomers. *Polymer* **2008**, 49 (2), 345–373.

(29) Herzberger, J.; Niederer, K.; Pohlit, H.; Seiwert, J.; Worm, M.; Wurm, F. R.; Frey, H. Polymerization of Ethylene Oxide, Propylene Oxide, and Other Alkylene Oxides: Synthesis, Novel Polymer Architectures, and Bioconjugation. *Chem. Rev.* **2016,** 116 (4), 2170–2243.

(30) Apicella, A.; Cappello, B.; Del Nobile, M. A.; La Rotonda, M. I.; Mensitieri, G.; Nicolais, L. Poly(Ethylene Oxide) (PEO) and Different Molecular Weight PEO Blends Monolithic Devices for Drug Release. *Biomaterials* **1993**, *14* (2), 83–90.

(31) Rardniyom, C. Development of Multi-Layer Films Containing Natural Antimicrobial Agents. 162.

(32) Atarés, L.; Chiralt, A. Essential Oils as Additives in Biodegradable Films and Coatings for Active Food Packaging. *Trends Food Sci. Technol.* **2016**, *48*, 51–62.

(33) Gill, A. O.; Holley, R. A. Mechanisms of Bactericidal Action of Cinnamaldehyde against Listeria Monocytogenes and of Eugenol against L. Monocytogenes and Lactobacillus Sakei. *Appl. Environ. Microbiol.* **2004**, *70* (10), 5750–5755.

(34) Qin, Y.; Liu, D.; Wu, Y.; Yuan, M.; Li, L.; Yang, J. Effect of PLA/PCL/Cinnamaldehyde Antimicrobial Packaging on Physicochemical and Microbial Quality of Button Mushroom (Agaricus Bisporus). *Postharvest Biol. Technol.* **2015**, *99*, 73–79.

(35) Zhang, M.; Meng, X.; Bhandari, B.; Fang, Z.; Chen, H. Recent Application of Modified Atmosphere Packaging (MAP) in Fresh and Fresh-Cut Foods. *Food Rev. Int.* **2015**, *31* (2), 172–193.

(36) Kim, D.; Seo, J. A Review: Breathable Films for Packaging Applications. *Trends Food Sci. Technol.* **2018**, *76*, 15–27.

(37) Li, X.; Jiang, Y.; Li, W.; Tang, Y.; Yun, J. Effects of Ascorbic Acid and High Oxygen Modified Atmosphere Packaging during Storage of Fresh-Cut Eggplants. *Food Sci. Technol. Int.* **2014**, *20* (2), 99–108.

(38) Singh, S. P.; Singh, Z. Controlled and Modified Atmospheres Influence Chilling Injury, Fruit Quality and Antioxidative System of Japanese Plums (Prunus Salicina Lindell). *Int. J. Food Sci. Technol*. **2013**, 48 (2), 363–374.

(39) Kumar, K. V. P. Active Packaging Systems in Food Packaging for Enhanced Shelf Life

(40) Ghaani, M.; Cozzolino, C. A.; Castelli, G.; Farris, S. An Overview of the Intelligent Packaging Technologies in the Food Sector. *Trends Food Sci. Technol*. **2016**, 51, 1–11.

(41) Aday, M. S.; Caner, C.; Rahvalı, F. Effect of Oxygen and Carbon Dioxide Absorbers on Strawberry Quality. *Postharvest Biol. Technol*. **2011**, 62 (2), 179–187.

(42) Gates, R. Microperforated Films for Fresh Produce Packaging. In Modified Atmosphere Packaging for Fresh-Cut Fruits and Vegetables; Brody, A. L., Zhuang, H., Han, J. H., Eds.; John Wiley & Sons, Inc.: Hoboken, NJ, USA, **2011**; pp 209–217.

(43) Lucera, A.; Conte, A.; Del Nobile, M. A. Shelf Life of Ready-to-Cook Cauliflower Mixtures as Affected by Packaging Film Mass Transport Properties: Ready-to-Cook Cauliflower Mixture. *Int. J. Food Sci. Technol*. **2012**, 47 (8), 1598–1604.

(44) Li, L.; Li, X.-H.; Ban, Z.-J. A Mathematical Model of the Modified Atmosphere Packaging (MAP) System for the Gas Transmission Rate of Fruit Produce. **2010**, 8.

(45) Singh, D.; Mandal, G.; Jain, R. K. Effect of Ventilation on Shelf Life and Quality of Peaches. *Acta Hortic.* **2005**, No. 696, 519–522.

(46) Vigneault, C.; Goyette, B. Design of Plastic Container Opening to Optimize Forced –Air Precooling of Fruits and Vegetables. *Appl. Eng. Agric. 18*, 4.

(47) Lufu, R. Unpacking the Influence of Internal Packaging on Cooling Characteristics and Postharvest Quality of Pomegranate Fruit. 197.

(48) Ngcobo, M. E. K.; Delele, M. A.; Pathare, P. B.; Chen, L.; Opara, U. L.; Meyer, C. J. Moisture Loss Characteristics of Fresh Table Grapes Packed in Different Film Liners during Cold Storage. *Biosyst. Eng.* **2012**, *113* (4), 363–370.

(49) Montanez, J. C.; Rodríguez, F. A. S.; Mahajan, P. V.; Frías, J. M. Modelling the Gas Exchange Rate in Perforation-Mediated Modified Atmosphere Packaging: Effect of the External Air Movement and Tube Dimensions. *J. Food Eng.* **2010**, *97* (1), 79–86.

(50) Mahajan, P. V.; Rodrigues, F. A. S.; Leflaive, E. Analysis of Water Vapour Transmission Rate of Perforation-Mediated Modified Atmosphere Packaging (PM-MAP). *Biosyst. Eng.* **2008**, *100* (4), 555–561.

(51) Shafafi, M. Effect of Modified Atmosphere Packaging on Quality Change of Fresh Parsley Spinach and Dill. *International Conference on Environmental Science and Technology*. **2011**, *6*.

(52) Larsen, H.; Liland, K. H. Determination of O2 and CO2 Transmission Rate of Whole Packages and Single Perforations in Micro-Perforated Packages for Fruit and Vegetables. *J. Food Eng.* **2013**, *119* (2), 271–276.

(53) Allan-Wojtas, P.; Forney, C. F.; Moyls, L.; Moreau, D. L. Structure and Gas Transmission Characteristics of Microperforations in Plastic Films. *Packag. Technol. Sci.* **2008**, *21* (4), 217–229.

(54) Winotapun, C.; Kerddonfag, N.; Kumsang, P.; Hararak, B.; Chonhenchob, V.; Yamwong,T.; ChinsiriKul, W. Microperforation of Three Common Plastic Films by Laser and their Enhanced Oxygen Transmission for Fresh Produce Packaging: Microperforation of Films and Their Enhanced Oxygen Transmission Rate. *Packag. Technol. Sci.* **2015**, *28* (4), 367–383.

(55) Wu, P. C.; Jones, G.; Shelle, C.; Woelfli, B. Novel Microporous Films and Their Composites. *J. Eng. Fibers Fabr.* **2007**, *2* (1), 155892500700200.

(56) Kim, H.; Biswas, J.; Choe, S. Effects of Stearic Acid Coating on Zeolite in LDPE, LLDPE, and HDPE Composites. *Polymer* **2006**, *47* (11), 3981–3992.

(57) Shao, P.; Niu, B.; Chen, H.; Sun, P. Fabrication and Characterization of Tea Polyphenols Loaded Pullulan-CMC Electrospun Nanofiber for Fruit Preservation. *Int. J. Biol. Macromol.* **2018**, *107* (Pt B), 1908–1914.

(58) Tóth, J.; Kardos-Fodor, A.; Halász-Péterfi, S. The Formation of Fine Particles by Salting-out Precipitation. Chem. Eng. Process. *Process Intensif.* **2005**, 44 (2), 193–200.

(59) Tran, R. T.; Naseri, E.; Kolasnikov, A.; Bai, X.; Yang, J. A New Generation of Sodium Chloride Porogen for Tissue Engineering. *Biotechnol. Appl. Biochem.* **2011**, *58* (5), 335–344.

(60) Lee, J.; Ashokkumar, M.; Kentish, S. E. Influence of Mixing and Ultrasound Frequency on Antisolvent Crystallisation of Sodium Chloride. *Ultrason. Sonochem.* **2014**, *21* (1), 60–68.

(61) Takiyama, H.; Otsuhata, T.; Matsuoka, M. Morphology of NaCl Crystals in Drowning-Out Precipitation Operation. *Chem. Eng. Res. Des.* **1998**, *76* (7), 809–814.

(62) Gielen, B.; Jordens, J.; Thomassen, L.; Braeken, L.; Van Gerven, T. Agglomeration Control during Ultrasonic Crystallization of an Active Pharmaceutical Ingredient. *Crystals* **2017**, *7* (2), 40.

(63) Abbas, A.; Srour, M.; Tang, P.; Chiou, H.; Chan, H.-K.; Romagnoli, J. A. Sonocrystallisation of Sodium Chloride Particles for Inhalation. *Chem. Eng. Sci.* **2007**, *62* (9), 2445–2453.

(64) Dorati, R.; Colonna, C.; Genta, I.; Modena, T.; Conti, B. Effect of Porogen on the Physico-Chemical Properties and Degradation Performance of PLGA Scaffolds. *Polym. Degrad. Stab.* **2010**, *95* (4), 694–701.

(65) Aydin, H. M.; El Haj, A. J.; Pişkin, E.; Yang, Y. Improving Pore Interconnectivity in Polymeric Scaffolds for Tissue Engineering. *J. Tissue Eng. Regen. Med.* **2009**, *3* (6), 470–476.

(66) Wang, L.-F.; Rhim, J.-W.; Hong, S.-I. Preparation of Poly(Lactide)/Poly(Butylene Adipate-Co-Terephthalate) Blend Films Using a Solvent Casting Method and Their Food Packaging Application. *LWT - Food Sci. Technol.* **2016**, *68*, 454–461.

(67) Bhatia, A.; Gupta, R. K.; Bhattacharya, S. N.; Choi, H. J. Compatibility of Biodegradable Poly (Lactic Acid) (PLA) and Poly (Butylene Succinate) (PBS) Blends for Packaging Application. 17.

(68) Almenar, E.; Samsudin, H.; Auras, R.; Harte, B.; Rubino, M. Postharvest Shelf Life Extension of Blueberries Using a Biodegradable Package. *Food Chem.* **2008**, *110* (1), 120–127.

(69) Joseph, C. S.; Prashanth, K. V. H.; Rastogi, N. K.; Indiramma, A. R.; Reddy, S. Y.; Raghavarao, K. S. M. S. Optimum Blend of Chitosan and Poly-(ε-Caprolactone) for Fabrication of Films for Food Packaging Applications. *Food Bioprocess Technol.* **2011**, *7* (4), 1179–1185.

(70) Plackett, D. V.; Holm, V. K.; Johansen, P.; Ndoni, S.; Nielsen, P. V.; Sipilainen-Malm, T.; Södergård, A.; Verstichel, S. Characterization Ofl-Polylactide Andl-Polylactide–Polycaprolactone Co-Polymer Films for Use in Cheese-Packaging Applications. *Packag. Technol. Sci.* **2006**, *19* (1), 1–24.

(71) Rao, R. U.; Suman, K.; Rao, V. K.; Bhanukiran, K. Study of Rheological and Mechanical Properties of Biodegradable Polylactide and Polycaprolactone Blend. *Int. J. Eng. Sci. Technol.* **2011**, *3* (8), 7.

(72) Scaffaro, R.; Lopresti, F.; Botta, L.; Maio, A. Mechanical Behavior of Polylactic Acid/Polycaprolactone Porous Layered Functional Composites. *Compos. Part B Eng.* **2016**, *98*, 70–77.

(73) Chavalitpanya, K.; Phattanarudee, S. Poly(Lactic Acid)/Polycaprolactone Blends Compatibilized with Block Copolymer. *Energy Procedia.* **2013**, *34*, 542–548.

(74) Reignier, J.; Huneault, M. A. Preparation of Interconnected Poly(ε-Caprolactone) Porous Scaffolds by a Combination of Polymer and Salt Particulate Leaching. *Polymer* **2006**, *47* (13), 4703–4717.

(75) Makwana, S.; Choudhary, R.; Dogra, N.; Kohli, P.; Haddock, J. Nanoencapsulation and Immobilization of Cinnamaldehyde for Developing Antimicrobial Food Packaging Material. *LWT - Food Sci. Technol.* **2014**, *57* (2), 470–476.

(76) Qin, Y.; Yang, J.; Xue, J. Characterization of Antimicrobial Poly (Lactic Acid) /Poly (Trimethylene Carbonate) Films with Cinnamaldehyde. *J. Mater. Sci.* **2015**, *50* (3), 1150–1158.

(77) Qin, Y.; Liu, D.; Wu, Y.; Yuan, M.; Li, L.; Yang, J. Effect of PLA/PCL/Cinnamaldehyde Antimicrobial Packaging on Physicochemical and Microbial Quality of Button Mushroom (Agaricus Bisporus). *Postharvest Biol. Technol.* **2015**, *99*, 73–79.

(78) Cui, Z.; Nelson, B.; Peng, Y.; Li, K.; Pilla, S.; Li, W.-J.; Turng, L.-S.; Shen, C. Fabrication and Characterization of Injection Molded Poly (ε-Caprolactone) and Poly (ε-Caprolactone)/Hydroxyapatite Scaffolds for Tissue Engineering. *Mater. Sci. Eng. C.* **2012**, *32* (6), 1674–1681.

(79) Ezzati, P.; Ghasemi, I.; Karrabi, M.; Azizi, H.; Fortelny, I. Preparation of Porous PLLA/PCL Blend by a Combination of PEO Phase and NaCl Particulate Leaching in PLLA/PCL/PEO/NaCl Blend. *Iran. Polym. J.* **2014**, *23* (10), 757–766.

(80) Lin, Y.S., and A.J. Burggraaf. "Experimental Studies on Pore Size Change of Porous Ceramic Membranes after Modification." *Journal of Membrane Science* 79, no. 1 (April 26, 1993): 65–82.

(81) Ahmad, S.; Azad, A. K.; Loughlin, K. F. A Study of Permeability and Tortuosity of Concrete. 9.

(82) De Sales, J. A.; Patrício, P. S. O.; Machado, J. C.; Silva, G. G.; Windmöller, D. Systematic Investigation of the Effects of Temperature and Pressure on Gas Transport through Polyurethane/Poly(Methylmethacrylate) Phase-Separated Blends. *J. Membr. Sci.* **2008**, *310* (1–2), 129–140.

(83) S,Thomas. Y,Grohens. P, Jyotishkuma. *Polymer Characterization*; Characterization of Polymer Blends: Miscibility, Morphology and Interfaces; Ed.; Wiley-VCH Verlag Gmbh & Co. KGaA , **2014**; Vol. 1; p 441.

(84) Cai, Q.; Bei, J.; Wang, S. In Vitro Study on the Drug Release Behavior from Polylactide-Based Blend Matrices. *Polym. Adv. Technol.* **2002**, *13* (7), 534–540.

(85) Processing and Finishing of Polymeric Materials. *Polymer processing*.Wiley: Hoboken ,**2011**; vol 1; P 1006

(86) Sawalha, Hassan, Karin Schroën, and Remko Boom. "Mechanical Properties and Porosity of Polylactide for Biomedical Applications." *Journal of Applied Polymer Science* 107, no. 1 (January 5, **2008**): 82–93.

.

(87) Riddle, K. W.; Mooney, D. J. Role of Poly(Lactide-Co-Glycolide) Particle Size on Gas-Foamed Scaffolds. J. Biomater. Sci. Polym. Ed. **2004**, 15 (12), 1561–1570.

(88) Buzimov, A Y, S N Kulkov, W Eckl, S Pappert, L A Gömze, E Kurovics, I. Kocserha, and R. Géber. "Effect of Mechanical Treatment on Properties of Zeolites with Chabazite Structure." *Journal of Physics: Conference Series* 790 (January **2017**): 012004.

(89) Roberson, D; Rocha, C; Piñon, M. Evaluation of 3D Printable Sustainable Composites.

(90) Takayama, Tetsuo, and Mitsugu Todo. "Improvement of Impact Fracture Properties of PLA/PCL Polymer Blend Due to LTI Addition." *Journal of Materials Science* 41, no. 15 (August **2006**): 4989–92.

(91) Wachirahuttapong, S.; Thongpin, C.; Sombatsompop, N. Effect of PCL and Compatibility Contents on the Morphology, Crystallization and Mechanical Properties of PLA/PCL Blends. *Energy Procedia* **2016**, 89, 198–206.

(92) Semba, T.; Kitagawa, K.; Ishiaku, U. S.; Hamada, H. The Effect of Crosslinking on the Mechanical Properties of Polylactic Acid/Polycaprolactone Blends. *J. Appl. Polym. Sci.* **2006**, *101* (3), 1816–1825.

(93) Gupta, B.; Patra, S.; Ray, A. R. Preparation of Porous Polycaprolactone Tubular Matrix by Salt Leaching Process. *J. Appl. Polym. Sci.* **2012**, *126* (5), 1505–1510.

(94) Sun, M.; Downes, S. Physicochemical Characterisation of Novel Ultra-Thin Biodegradable Scaffolds for Peripheral Nerve Repair. *J. Mater. Sci. Mater. Med.* **2009**, *20* (5), 1181–1192.

(95) Huang, R.; Zhu, X.; Tu, H.; Wan, A. The Crystallization Behavior of Porous Poly(Lactic Acid) Prepared by Modified Solvent Casting/Particulate Leaching Technique for Potential Use of Tissue Engineering Scaffold. Mater. *Lett*. **2014**, 136, 126–129.

(96) Shin, Kyusoon, Euntaek Woo, Young Gyu Jeong, Chulkyu Kim, June Huh, and Kwang-Woo Kim. "Crystalline Structures, Melting, and Crystallization of Linear Polyethylene in Cylindrical Nanopores." *Macromolecules* 40, no. 18 (September **2007**): 6617–23.

(97) Yu, F.; Liu, T.; Zhao, X.; Yu, X.; Lu, A.; Wang, J. Effects of Talc on the Mechanical and Thermal Properties of Polylactide. J. *Appl. Polym. Sci*. **2012**, 125 (S2), E99–E109.

(98) Sibambo, S. R.; Pillay, V.; Choonara, Y. E.; Penny, C. A Novel Salted-out and Subsequently Crosslinked Poly(Lactic-Co-Glycolic Acid) Polymeric Scaffold Applied to Monolithic Drug Delivery. J. *Bioact. Compat. Polym*. **2008**, 23 (2), 132–153.

(99) Huang, An, Yongchao Jiang, Brett Napiwocki, Haoyang Mi, Xiangfang Peng, and Lih-Sheng Turng. "Fabrication of Poly(ε-Caprolactone) Tissue Engineering Scaffolds with Fibrillated and Interconnected Pores Utilizing Microcellular Injection Molding and Polymer Leaching." *RSC Advances* 7, no. 69 (**2017**): 43432–44.

(100) Yin, G.; Zhang, L.; Zhou, Z.; Li, Q. Preparation and Characterization of Cross-Linked PCL Porous Membranes. J. *Polym. Res*. **2016**, 23 (11).

(101) Qiu, Zhaobin, Takayuki Ikehara, and Toshio Nishi. "Miscibility and Crystallization of Poly (Ethylene Oxide) and Poly(ε-Caprolactone) Blends." *Polymer* 44, no. 10 (May **2003**): 3101–6.

(102) Kiziltay, Aysel, Angel Marcos-Fernandez, Julio San Roman, Rui A. Sousa, Rui L. Reis, Vasif Hasirci, and Nesrin Hasirci. "Poly(Ester-Urethane) Scaffolds: Effect of Structure on Properties and Osteogenic Activity of Stem Cells: Poly(Ester-Urethane) Scaffolds." *Journal of Tissue Engineering and Regenerative Medicine* 9, no. 8 (August **2015**): 930–42.

(103) Parra, D.F., J. Fusaro, F. Gaboardi, and D.S. Rosa. "Influence of Poly (Ethylene Glycol) on the Thermal, Mechanical, Morphological, Physical–Chemical and Biodegradation Properties of Poly (3-Hydroxybutyrate)." *Polymer Degradation and Stability* 91, no. 9 (September **2006**): 1954–59.

(104) Drieskens, Marjoleine, Roos Peeters, Jules Mullens, Dirk Franco, Pieter J. Lemstra, and Denka G. Hristova-Bogaerds. "Structure versus Properties Relationship of Poly(Lactic Acid). I. Effect of Crystallinity on Barrier Properties." *Journal of Polymer Science Part B: Polymer Physics* 47, no. 22 (November 15, **2009**): 2247–58.

(105) Huang, H.-D.; Ren, P.-G.; Xu, J.-Z.; Xu, L.; Zhong, G.-J.; Hsiao, B. S.; Li, Z.-M. Improved Barrier Properties of Poly(Lactic Acid) with Randomly Dispersed Graphene Oxide Nanosheets. *J. Membr*. Sci. **2014**, 464, 110–118.

(106) Courgneau, Cécile, Sandra Domenek, Régis Lebossé, Alain Guinault, Luc Avérous, and Violette Ducruet. "Effect of Crystallization on Barrier Properties of Formulated Polylactide." *Polymer International* 61, no. 2 (February **2012**): 180–89.

(107) Lucera, Annalisa, Amalia Conte, and Matteo Alessandro Del Nobile. "Shelf Life of Ready-to-Cook Cauliflower Mixtures as Affected by Packaging Film Mass Transport Properties: Ready-to-Cook Cauliflower Mixture." *International Journal of Food Science & Technology* 47, no. 8 (August **2012**): 1598–1604.

(108) Pan, X. C.; Sasanatayart, R. Effect of plastic films with different oxygen transmission rate on shelf-life of fresh-cut bok choy (Brassica rapa var. chinensis). *International Food Research Journal*. **2016**, 23, 1865-1871.

(109) Duan, Z., and N. L. Thomas. "Water Vapour Permeability of Poly(Lactic Acid): Crystallinity and the Tortuous Path Model." *Journal of Applied Physics* 115, no. 6 (February 14, **2014**): 064903.

(110) Ikada, Y.; Tsuji, H. Biodegradable Polyesters for Medical and Ecological Applications. 16.

(111) Bouakaz, Boubkeur Seddik, Abderrahmane Habi, Yves Grohens, and Isabelle Pillin. "Organomontmorillonite/Graphene-PLA/PCL Nanofilled Blends: New Strategy to Enhance the Functional Properties of PLA/PCL Blend." *Applied Clay Science* 139 (April **2017**): 81–91.

(112) Wang, Ning, Yong Ju Zang, Gui Zhi Ren, and Qi Lin Wu. "Fabrication and Properties of Porous Scaffolds of PLA-PEG Biocomposite for Bone Tissue Engineering." *Materials Science Forum* 789 (April **2014**): 130–35.

(113) Nasri-Nasrabadi, Bijan, Mohammad Mehrasa, Mohammad Rafienia, Shahin Bonakdar, Tayebeh Behzad, and Shahin Gavanji. "Porous Starch/Cellulose Nanofibers Composite Prepared by Salt Leaching Technique for Tissue Engineering." *Carbohydrate Polymers* 108 (August **2014**): 232–38.

(114) Chouzouri, G., and M. Xanthos. "Degradation of Aliphatic Polyesters in the Presence of Inorganic Fillers." *Journal of Plastic Film & Sheeting* 23, no. 1 (January **2007**): 19–36.

(115) Sandra Sánchez-González, Nazely Diban, and Ane Urtiaga. “Hydrolytic Degradation and Mechanical Stability of Poly(ε-Caprolactone)/Reduced Graphene Oxide Membranes as Scaffolds for In Vitro Neural Tissue Regeneration.” *Membranes* 8, no. 1 (March 5, **2018**): 12.

(116) Mkhabela, Vuyiswa J., and Suprakas Sinha Ray. “Fabrication of Polylactide Nanocomposite Scaffolds for Bone Tissue Engineering Applications,” 070009. Cleveland, Ohio, USA, **2015.**

(117) Lasprilla, Astrid Juliana Rincon, Guillermo Andres Rueda Martinez, Betania Hoss, Jaiver Efren Jaimes Figueroa, Andre Luiz Jardini, and Rubens Maciel. “Synthesis and Characterization of Poly (Lactic Acid) for Use in Biomedical Field,” n.d., 6.

(118) Mofokeng, J. P., A. S. Luyt, T. Tábi, and J. Kovács. “Comparison of Injection Moulded, Natural Fibre-Reinforced Composites with PP and PLA as Matrices.” *Journal of Thermoplastic Composite Materials* 25, no. 8 (December **2012**): 927–48.

(119) Fadl, Samar Mohamed Ahmed. “Development and Characterization of Biodegradable Biorenewable Polymeric Nanocomposites for Food Packaging Applications,” May 28, **2015**.

(120) Chiu, Chun-Yi, Hsien-Wei Chen, Shiao-Wei Kuo, Chih-Feng Huang, and Feng-Chin Chang. “Investigating the Effect of Miscibility on the Ionic Conductivity of LiClO 4 /PEO/PCL Ternary Blends.” *Macromolecules* 37, no. 22 (November **2004**): 8424–30.

(121) Wang, Hong, Shixiong Min, Chun Ma, Zhixiong Liu, Weiyi Zhang, Qiang Wang, Debao Li, et al. “Synthesis of Single-Crystal-like Nanoporous Carbon Membranes and Their Application in Overall Water Splitting.” *Nature Communications* 8 (January 4, **2017**): 13592.

(122) Zhang, Pengfei. “Adsorption and Desorption Isotherms,” n.d., 19.

(123) Livshin, Shulamit, and Michael S. Silverstein. “Crystallinity and Cross-Linking in Porous Polymers Synthesized from Long Side Chain Monomers through Emulsion Templating.” *Macromolecules* 41, no. 11 (June **2008**): 3930–38.

(124) Mishra, M. Encylopedia of Polymer Application CRC Press; Vol. 3; p 2121

(125) Nuhnen, Alexander, Dennis Dietrich, Simon Millan, and Christoph Janiak. “Role of Filler Porosity and Filler/Polymer Interface Volume in Metal–Organic Framework/Polymer Mixed-Matrix Membranes for Gas Separation.” *ACS Applied Materials & Interfaces* 10, no. 39 (October 3, **2018**): 33589–600.

(126) Takahashi, S., and D.R. Paul. “Gas Permeation in Poly(Ether Imide) Nanocomposite Membranes Based on Surface-Treated Silica. Part 1: Without Chemical Coupling to Matrix.” *Polymer* 47, no. 21 (October 2006): 7519–34.

(127) Patel, Sarthak K., Afsaneh Lavasanifar, and Phillip Choi. “Roles of Nonpolar and Polar Intermolecular Interactions in the Improvement of the Drug Loading Capacity of PEO- b -PCL with Increasing PCL Content for Two Hydrophobic Cucurbitacin Drugs.” *Biomacromolecules* 10, no. 9 (September 14, **2009**): 2584–91.

(128) Ma, Lulu, Li Deng, and Jianming Chen. “Applications of Poly(Ethylene Oxide) in Controlled Release Tablet Systems: A Review.” *Drug Development and Industrial Pharmacy*, June 12, **2014.**

(129) Raeisi, Mojtaba, Hossein Tajik, Arman Yarahmadi, and Sirvan Sanginabadi. “Antimicrobial Effect of Cinnamon Essential Oil Against Escherichia Coli and Staphylococcus Aureus.” *Health Scope* 4, no. 4 (November 25, **2015**).